Forschungszentrum Karlsruhe
in der Helmholtz-Gemeinschaft
Wissenschaftliche Berichte
FZKA 6793

RelB in Secondary Lymphoid Organ Development: Differential Regulation by Lymphotoxin and Tumor Necrosis Factor Signaling Pathways*

Z. Buket YILMAZ

Institut für Toxikologie und Genetik

*Von der Fakultät für Chemie und Biowissenschaften
der Universität Karlsruhe (TH)
genehmigte Dissertation

Forschungszentrum Karlsruhe GmbH, Karlsruhe
2002

Impressum der Print-Ausgabe:

Als Manuskript gedruckt

Forschungszentrum Karlsruhe GmbH
Postfach 3640, 76021 Karlsruhe

Mitglied der Hermann von Helmholtz-Gemeinschaft
Deutscher Forschungszentren (HGF)

ISSN 0947-8620

RelB in Secondary Lymphoid Organ Development: Differential Regulation by Lymphotoxin and Tumor Necrosis Factor Signaling Pathways

Zur Erlangung des akademischen Grades eines

Doktors der Naturwissenschaften

an der Fakultät für Chemie und Biowissenschaften

der Universität Karlsruhe (TH)

genehmigte

DISSERTATION

von

Z. Buket YILMAZ

aus Ankara, TÜRKEI

2002

Dekan: Prof. Dr. Manfred Metzler

1. **Gutachter:** PD Dr. Falk Weih
2. **Gutachter:** Prof. Dr. Margot Zöller

Tag der mündlichen Prüfung: 23.10.2002

RelB in Secondary Lymphoid Organ Development: Differential Regulation by Lymphotoxin and Tumor Necrosis Factor Signaling Pathways

Abstract

Primary lymphoid organs are the major sites of lymphopoiesis where lymphocytes proliferate and mature into functional but naive cells. Secondary lymphoid organs are sites where these lymphocytes encounter antigens and elicit immune responses. RelB is a member of the Rel/NF-κB family of inducible dimeric transcription factors. RelB is abundantly expressed in secondary lymphoid organs, such as spleen, lymph nodes and Peyer's patches (PP). RelB-deficient mice have improper spleen structure and lack organizing centers for PPs, defects that can not be restored by the adoptive transfer of wild-type bone marrow cells. The work presented here revealed a significant reduction in expression of the homing chemokines B lymphocyte chemoattractant (BLC) and secondary lymphoid organ chemokine (SLC) in RelB-deficient spleen, suggesting a role for RelB in proper expression of chemokines by splenic stromal cells. Moreover, interleukin-7 (IL-7)-induced expression of lymphotoxin (LT) in intestinal cells - a crucial step in early PP development - was not impaired in RelB-deficient embryos, suggesting functional hematopoietic inducers and a defect in LTβ receptor (LTβR) expressing stromal responders. Activation of LTβR signaling in fibroblasts resulted in the specific induction of p52-RelB heterodimers, while tumor necrosis factor (TNF) induced classical p50-RelA NF-κB complexes. LTβR-induced RelB nuclear translocation and DNA binding of p52-RelB heterodimers required the degradation of the inhibitory p52 precursor, p100, which was dependent on the IκB kinase (IKK) complex subunit IKKα, but not on IKKβ or IKKγ. In contrast to LTβR signaling, TNFR signaling increased p100 and RelB levels both in cytoplasm and nucleus and RelB was bound to p100 in both compartments. Despite the abundant presence of RelB in the nucleus, RelB DNA-binding was almost undetectable in TNF treated fibroblasts. Forced expression of p50 and p52 could not rescue the lack of DNA binding. In contrast, RelB DNA-binding significantly increased in cells lacking the C-terminus of p100, but not of p105, strongly suggesting that it is the specific inhibitory function of the C-terminal domain of p100, rather than the lack of the heterodimerization partner, which prevents RelB DNA-binding in TNF-stimulated fibroblasts. Thus, RelB and p52 in stromal cells could function in the proper development of the spleen by regulating the expression of chemokines such as BLC. Furthermore, generation of p52-RelB heterodimers by the LTβR pathway involving p100 degradation, appears to be a critical step in the formation of PP anlage.

RelB in der Entwicklung sekundärer lymphoider Organe: Differentielle Regulation durch die Lymphotoxin und Tumor-Nekrose-Faktor Signalübertragungswege

Zusammenfassung

Primäre lymphoide Organe sind Orte an denen Lymphozyten zu funktionellen aber naiven Zellen heranreifen, während in sekundären lymphoiden Organen diese Lymphozyten auf Antigene treffen und Immunantworten auslösen. RelB ist ein Mitglied der Rel/NF-κB Familie induzierbarer dimerer Transkriptionsfaktoren. RelB ist stark exprimiert in den sekundären lymphoiden Organen Milz, Lymphknoten und Peyersche Plaques (PP). RelB-defiziente Mäuse haben eine gestörte Milzstruktur und besitzen keine PP-Anlagen. Reziproke Knochenmarktransferexperimente haben gezeigt, dass RelB in strahlungsresistenten stromalen Zellen benötigt wird und dass der Transfer von wildtyp Knochenmark in neugeborene und adulte RelB-defiziente Rezipienten die obengenannten Defekte nicht korrigieren kann. Die vorliegende Arbeit zeigt eine deutlich verminderte Expression der Chemokine BLC und SLC in der Milz RelB-defizienter Mäuse, was eine Rolle von RelB bei der Expression von sogenannten "Homing-Chemokinen" in stromalen Milzzellen nahelegt. Desweiteren war die Interleukin-7-induzierte Expression von Lymphotoxin (LT) in embryonalen Darmzellen, ein wichtiger Schritt während der fühen PP Entwicklung, nicht abhängig von RelB, was auf funktionelle hämatopoietische "Induktor-Zellen", aber defekte LT-β-Rezeptor (LTβR)-exprimierende Stromazellen in RelB-defizienten Mäusen schließen läßt. Die Aktivierung des LTβR in Fibroblasten induzierte DNA-bindende p52-RelB Heterodimere, während der Tumor-Nekrose-Faktor (TNF) "klassische" p50-RelA NF-κB Komplexe aktivierte. Die LTβR-induzierte Translokation von RelB in den Zellkern und die DNA-Bindung von p52-RelB Heterodimeren setzte die C-terminale Prozessierung des inhibitorischen p52-Vorläufermoleküls p100 voraus, ein Prozess, der von der IκB Kinase (IKK) α, nicht aber von IKKβ oder IKKγ, vermittelt wurde. Im Gegensatz zum LTβR, erhöhte die Aktivierung des TNF-Rezeptors die p100 und RelB Proteinmenge wobei RelB an p100 gebunden war. Trotz der deutlichen nukleären RelB Expression wurde keine signifikante DNA-Bindung von RelB in TNF stimulierten Fibroblasten beobachtet. Auch die Überexpression der NF-κB Untereinheiten p50 und p52 führte nicht zur Aktivierung von RelB nach TNF Behandlung. Die DNA-Bindung von RelB war in Zellen, denen lediglich p100 fehlt, allerdings deutlich erhöht. Diese Ergebnisse legen nahe, dass nicht die Abwesenheit des Heterodimerisierungspartners p52, sondern die erhöhte Produktion des inhibitorischen p100 Vorläufermoleküls die DNA-Bindung von RelB nach TNF-Induktion spezifisch blockiert. Die Aktivierung von p52-RelB Heterodimeren in stromalen Zellen über den LTβR könnte die Entwicklung und Kompartimentalisierung der Milz durch die Regulation der Expression von Chemokinen wie z.B. BLC regulieren. Darüberhinaus scheint die Induktion von p52-RelB Heterodimeren über die LTβR-induzierte Degradation von p100 ein wichtiger Schritt für die Ausbildung von PP-Anlagen während der Embryonalentwicklung zu sein.

TABLE OF CONTENTS

LIST OF FIGURES

LIST OF TABLES

ABBREVIATIONS

Ab(s)	Antibody (dies)
Ag	Antigen
aly	alympoplasia
BLC	B lymphocyte chemoattractant
BM	Bone marrow
bp	base pair
^{o}C	Degrees Celsius
cDNA	Complementary DNA
Ci	Curie
cpm	Counts per minute
DC	Dendritic cell
d.p.c	days post coitus
DMEM	Dulbecco's Modified Eagle Medium
DMSO	Dimethylsulfoxide
DNA	Deoxyribonucleic acid
DTT	Dithiothreitol
E	Embryonic day
ECL	Enhanced chemilluminescence
EDTA	Ethylenediamine-N,N-tetraacetate
EGTA	Ethylenguanidine- N,N-tetraacetate
ELC	EBV-induced molecule 1 ligand chemokine
ELISA	Enzyme linked immunoabsorbent assay
EMH	Extramedullary hematopoiesis
et al.	Lat. *et ali*, and others
FAE	Follicle associated epithelium
FCS	Fetal calf serum
FDC	Follicular DC
FL	Fetal liver
g	gram
GALT	Gut associated lymphoid tissue
GC	Germinal center
h	hour (s)

HEV	High endothelial venule
HVEM	Herpes virus entry mediator
HRP	Horseradish peroxidase
ICAM-1	Intercellular adhesion molecule-1
IFR	Interfollicular region
Ig	Immunoglobulin
IL	Interleukin
IL-7Rα	IL-7 receptor α chain
IκB	Inhibitor of NF-κB
IKK	IκB kinase
IP	immunoprecipitation
kD	Kilodalton
LCMV	*L. monocytogenes*
LIGHT	homologous to lymphotoxins, exhibits inducible expression, and competes with HSV glycoprotein D for HVEM, a receptor expressed by T lymphocytes
LN	Lymph node
LP	Lamina propria
LPS	Lipopolysaccharide
LT	Lymphotoxin
LTβR	LTβ receptor
MAdCAM-1	Mucosal adressin cell adhesion molecule-1
MAP3K	Mitogen activated protein kinase kinase kinase
MEF	Mouse embryonic fibroblast
M	Molar
m	milli-(10^{-3})
mAb	monoclonal Ab
mg	milligram
MHC	Major histocompatibility complex
min	minute (s)
ml	milliliter
mM	millimolar
MOPS	4-morpholinepropanesulfonic acid

mRNA	Messenger RNA
MZ	Marginal zone
μ	micro-(10^{-6})
μg	microgram
μl	microliter
μM	micromolar
n	nano-(10^{-9})
NEMO	NF-κB essential modulator (IKKγ)
NES	Nuclear export signal
NF-κB	Nuclear factor kappa B
ng	nanogram
NIK	NF-κB inducing kinase
NLS	Nuclear localization signal
OD	Optical density
O/N	Overnight
PAGE	Polyacrylmide gel electrophoresis
PALS	Periarteriolar lymphatic sheath
PBS	Phosphate buffered saline
PCR	Polymerase chain reaction
P0	day of birth
PFA	Paraformaldehyde
PNA	Peanut hemagglutinin
PP	Peyer's Patch
PVDF	Polyvinylidenedifluoride
RHD	Rel homology domain
RNA	Ribonucleic acid
RP	Red pulp
RT	Room temperature
rpm	rotation per minute
RT-PCR	Reverse transcriptase PCR
SCF	Stem cell factor
SDS	Sodium-lauryl-sulphate
SED	Subepithelial dome

sIgA	secretory IgA
SLC	Secondary lymphoid tissue chemokine
SRBC	Sheep red blood cells
TBE	Tris-boric acid-EDTA
TEMED	N,N,N',N' tetramethylene-diamine
TNF	Tumor necrosis factor
TNFR	TNF receptor
TRAF	TNFR associated factor
U	Unit (s)
UV	Ultra-violet light
V	Volt
VCAM-1	Vascular cell adhesion molecule-1
v/v	volume per volume
WCE	Whole cell extract
WP	White pulp
w/v	weight per volume

1 INTRODUCTION

1.1 Rel/NF-κB FAMILY OF TRANSCRIPTION FACTORS

NF-κB was first discovered in 1986 as a constitutive nuclear transcription factor in mature B cells which is bound to an element in the kappa immunoglobulin light-chain enhancer, hence the name nuclear factor κB (NF-κB). NF-κB was shown to contain two subunits with molecular weights of 50 kD (p50) and 65 kD (p65), and to be present not only in B cells but in most cell types in an inactive cytoplasmic form bound to an inhibitory protein called IκB **(**Perkins, 2000).

NF-κB can be activated by a large variety of inducers, which include bacteria or bacterial products, viruses, inflammatory cytokines, stress conditions, mitogens, growth factors and hormones, environmental hazards and many different chemical agents. When a cell receives one of these extracellular signals, NF-κB is released from IκB inhibition, rapidly translocates to the nucleus and activates gene expression. The active NF-κB transcription factor promotes the expression of over 150 target genes, the majority of which participate in the host immune response. These include genes encoding cytokines and chemokines, molecules involved in antigen presentation, such as major histocompatibility complex (MHC), cell adhesion molecules, acute phase proteins, stress response genes, cell surface receptors, regulators of apoptosis, growth factors and their modulators, early response genes, transcription factors and many others. This extensive list of target genes would easily designate NF-κB as the central mediator of immune responses (Pahl, 1999).

DNA binding and dimerization domain of the p50 subunit (p105/p50, *nfkb1* gene product) is highly homologous to the viral oncoprotein v-Rel, its cellular counterpart c-Rel and to the *Drosophila melanogaster* developmental protein Dorsal. Subsequent isolation of cDNAs for RelA (p65) and for two other highly homologous proteins, the p52 subunit (p100/p52, *nfkb2* gene product) and RelB, established the presence of the multigene Rel/NF-κB family of transcription factors (Gilmore, 1999; Perkins, 2000). All members of this family contain an approximately 300 amino acid N-terminal Rel-homology domain (RHD), which is required for DNA binding, homo- and heterodimerization, and interaction with IκB proteins. There exists also a nuclear

localization signal (NLS) within RHD (**Fig. 1.1**, and **Fig. 1.5**). Most combinations of NF-κB homo- and heterodimers can be found *in vivo* with the exception of RelB which does not form homodimers. The p50 and p52 subunits lack transactivation domains and are produced by processing of the precursor molecules p105 and p100, respectively, while c-Rel, RelB and RelA contain non-homologous transactivation domains in their C-termini and do not require proteolytic processing to generate their active forms **(**Perkins, 2000; Hatada, *et al.*, 2000).

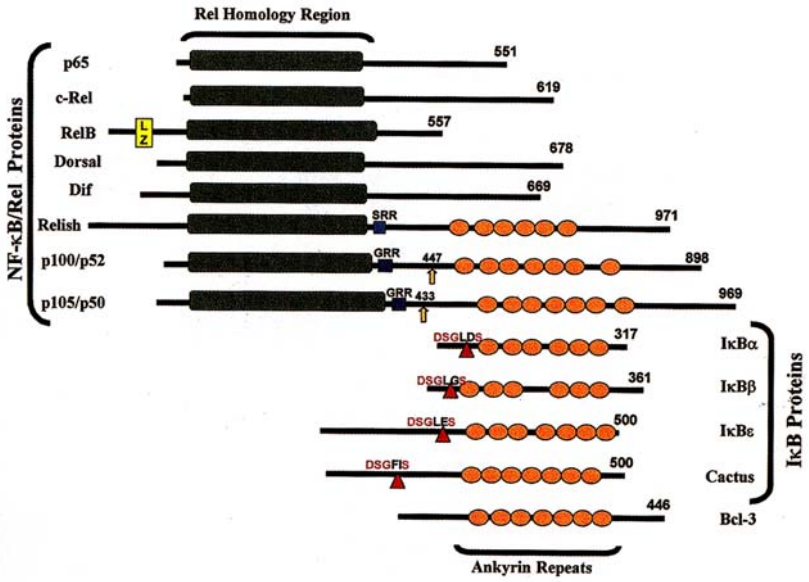

FIGURE 1.1: Family of the Rel/NF-κB and IκB proteins

Mammalian members of Rel/NF-κB and IκB proteins together with *Drosophila* homologs (Dorsal Dif, Relish, and Cactus, respectively) are schematically represented. RHD is indicated as black box. Proteolytic cleavage (arrows) of p100 and p105 gives rise to p52 and p50, respectively. Ankyrin repeats are indicated by orange circles and conserved residues located at N-termini of IκB proteins required for inducible degradation are labeled red. LZ: leucine zipper, SRR: serine rich region, GRR: glycine rich region (adapted from Karin *et al.*, 2000 b).

The activity of NF-κB is tightly regulated by interaction with IκB proteins. As the Rel/NF-κB family, IκB constitutes a family of molecules, IκBα, IκBβ, IκBγ, IκBε and Bcl-3 each with different affinities for individual Rel/NF-κB complexes. They are distinctly regulated and are expressed in a tissue specific manner. Most IκB members contain N-terminal regulatory sequences and all have either six or seven ankyrin repeats (**Fig. 1.1**), which bind to the RHD and mask the NLS of NF-κB, causing cytoplasmic retention. Ankyrin repeats are also found in the C-terminal sequences of p105 and p100 and also sequester NF-κB in the cytoplasm prior to their proteolytic processing. While

p100 and p105 precursors can bind to most of the NF-κB members *in vitro*, IκBα, IκBβ and IκBε strongly prefer dimers containing RelA or c-Rel. In contrast, Bcl-3 has a strong preference towards p50 or p52 homodimers. IκBα is the most studied and best characterized member. Only IκBα, IκBβ, and IκBε contain N-terminal regulatory sequences, which are essential for stimulus dependent degradation of IκBs, the key step in NF-κB activation. IκBs are also important in the termination of NF-κB activation by the entry of newly synthesized IκBα into the nucleus. They bind to NF-κB and enhance its dissociation from DNA, thereby causing its re-export to the cytoplasm via its nuclear export sequence (NES) (Gilmore, 1999; Heissmeyer *et al.*, 1999; Karin *et al.*, 2000).

1.1.1 The Consensus NF-κB Activation Pathway

Even though there is no full understanding or agreement about the converging point in the NF-κB activation cascade or the precise mechanisms for activation by extracellular or intracellular stimuli, there are several common features such as the rapid degradation of IκBs upon strong inducers like tumor necrosis factor (TNF) or interleukin-1 (IL-1). For IκBα, these inducible degradation steps are well characterized. The cascade is initiated by phosphorylation of serines 32 and 36 of IκBα. IκBβ (Ser19 and Ser23) and IκBε (Ser157 and Ser161) also contain two conserved serine residues in their N-terminus (see **Fig. 1.1**). Phosphorylation leads to polyubiquitination of IκBα at lysines 21 and 22 by ubiquitin ligase. Upon this modification, IκBα is targeted to rapid degradation by the 26S proteasome. Then the NLS of NF-κB is exposed which is followed by binding to karyopherins and translocation to the nucleus (**Fig. 1.2**) (Karin *et al.*, 2000). In addition, it is proposed that the precursors p105 and p100 undergo post-translational processing via the ubiquitin-proteasome system. This would not only control NF-κB activity by replenishing the cytoplasmic pool of mature p50 and p52 subunits, but also by releasing the larger subunits bound to the inhibitory precursor proteins in the cytoplasm. Moreover, NF-κB is also subject to IκB-independent levels of regulation via inducible phosphorylations of the subunits such as, p105, p100, c-Rel and RelA upon treatment with potent inducers like phorbol esters, TNF and IL-1 **(**Schmitz *et al.*, 2001; Karin *et al.*, 2000).

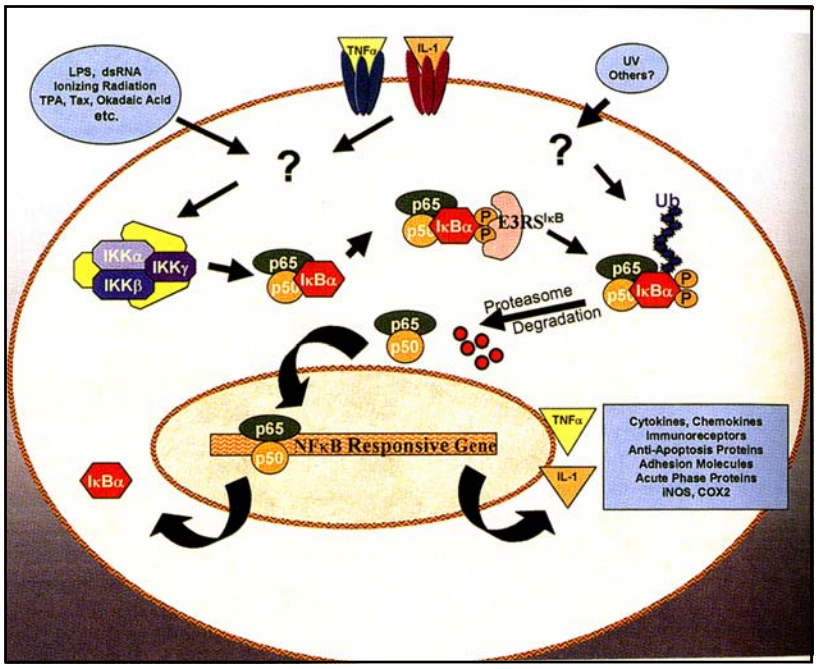

FIGURE 1.2: Schematic representation of NF-κB activation
Different stimuli activate the IKK complex, which phosphorylates IκBα followed by polyubiquitination by $E3RS^{IκB}$ resulting in rapid degradation by the 26S proteasome. This is followed by nuclear translocation of NF-κB and transcriptional regulation of its target genes including IκBα which terminates this activation in an autoregulatory loop; (adapted from Karin *et al.*, 2000 b).

Following translocation to the nucleus, NF-κB must gain access to the promoters and enhancers of the genes it regulates. The specificity and selectivity of this process is achieved by the differential activation of distinct NF-κB complexes, which can have different DNA-binding specificities. That different NF-κB subunits have distinct non-overlapping roles is supported by gene knockouts in mice where the inactivation of each member has distinct phenotypes (Attar *et al.,* 1997; Gerondakis *et al.,* 1999). Among the Rel/NF-κB members, the mechanisms of transcriptional activation have been best characterized for the RelA subunit. The transactivation domain of RelA interacts with components of the TFIID complex and the general transcription factor TFIIB. RelA also recruits histone acetyltransferase (HAT) activity to the promoter through interactions with p300 and CREB-binding protein (CBP) coactivators. In addition, RelA interacts with heterologous DNA-binding proteins such as c-Jun, CCAAT/enhancer-binding protein β (C/EBPβ) and SP1. Thus, NF-κB activity is integrated into other signaling pathways providing additional specificity to the NF-κB response. Overall, NF-κB responsive genes vary depending on the precise cellular environment and context (Perkins, 2000).

1.1.2 IκB Kinase (IKK) Complex

A protein kinase, which specifically phosphorylates the N-terminal regulatory serines of IκBs, and whose activity is greatly induced by TNF, was recently discovered. This serine specific activity, called IκB kinase (IKK), is responsive to many potent NF-κB activators in addition to TNF. IKK activity was eluted at a molecular mass of 700-900 kD, suggesting a multi component kinase complex. The identification of IKKα (IKK1) (85 kD) was followed by IKKβ (IKK2) (87 kD) (Karin, 1999; Karin *et al.*, 2000) and the third essential regulatory subunit IKKγ, also called NF-κB essential modulator (NEMO). IKKα and IKKβ are highly homologous proteins with 50% sequence identity, containing N-terminal kinase domains, leucine zipper (LZ) and helix-loop-helix (HLH) motifs. They can form homo- and heterodimers *in vitro* through their LZ motifs and recombinant forms can phosphorylate IκBα and IκBβ. Dimerization is essential for the kinase activity. The third component of the IKK complex, IKKγ, is a 48 kD protein, which is required for activation of the IKK complex by upstream components of the NF-κB cascade. IKKγ does not contain a catalytic domain (**Fig. 1.3**) (Israël, 2000).

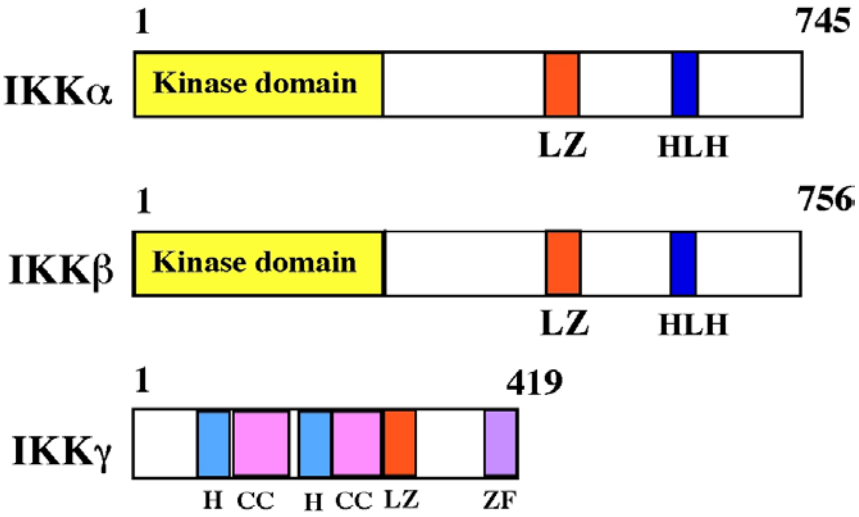

FIGURE 1.3: Putative functional and structural domains of known IKK subunits
CC, coiled coil; H, α-helix; HLH, helix-loop-helix; LZ, leucine zipper; ZF, zinc finger; adapted from (Karin *et al.*, 2000).

The stoichiometry of the known components of the IKK complex has not been precisely determined but in cells it is proposed to contain roughly equal amounts of IKKα and IKKβ and a dimer or a trimer of IKKγ. Although IKKγ appears to be the major coordinator of IKK assembly, its precise role is not yet clear. In vitro translation

experiments show an association of IKKγ with IKKβ, but not with IKKα. However, in IKKβ-deficient cells, IKKγ can be coprecipitated with IKKα even though a direct interaction is not proven (Karin *et al.*, 2000). IKKγ facilitates the association of IκBα and IκBβ with the IKK complex by interacting with the IKKβ catalytic subunit, suggesting that IKKγ not only mediates connection with upstream factors but also acts as a bridge between the IKK complex and its substrates **(**Yamamoto *et al*., 2001).

IKK activation depends on serine phosphorylations in the activation loops of the catalytic subunits. The primary target of proinflammatory signals is IKKβ rather than IKKα. Thus IKKα is not required for stimulation of IKK activity but it may contribute to the total IKK activity in the complex with IKKβ presumably by being activated by IKKβ. Once activated, IKK not only phosphorylates IκBs but also autophosphorylates its C-terminus. This alters the interaction between the C-terminal region and the kinase domain, which decreases the activity of the IKK complex (Hatada *et al.*, 2000; Karin *et al.*, 2000).

Several mitogen-activated protein kinase kinase kinases (MAP3Ks) are suggested to be inducible IKK kinases. The most potent IKK activator, when overexpressed, is NF-κB inducing kinase (NIK). NIK directly activates IKKα through phosphorylation of its activation loop. It is possible that different NF-κB inducers activate distinct IKK-Ks which activate the IKK complex by using IKKγ as a docking site depending on the cell type and the particular inducer (Karin *et al.*, 2000 a; Karin *et al.*, 2000 b).

Even though it was initially suggested that IKKα and IKKβ could be interchangeable, gene inactivation in mice, *in vitro*, and *ex vivo* experiments suggest the opposite. Inactivation of IKKβ results in a similar phenotype observed for inactivation of RelA, which is embryonic lethality at day E12.5-14.5 due to massive hepatocyte apoptosis. *IKKβ*$^{-/-}$ cells do not activate NF-κB in response to TNF or IL-1, showing that IKKα can not replace it. In contrast, IKKα-knockout mice have a different, surprising phenotype with perinatal lethality due to multiple skeletal abnormalities, limb development and keratinocyte differentiation defects. IKKα is dispensable for IKK activation by proinflammatory stimuli such as TNF, IL-1 or LPS. They result in normal IKK activation and IκBα degradation in *IKKα*$^{-/-}$ MEFs (**Fig. 1.4**). IKKγ inactivation causes death at E12.5-13 due to hepatocyte apoptosis and *IKKγ*$^{-/-}$ fibroblasts are totally

deficient in NF-κB activation in response to TNF, IL-1 and LPS (Israël, 1995; Karin *et al.*, 2000 c).

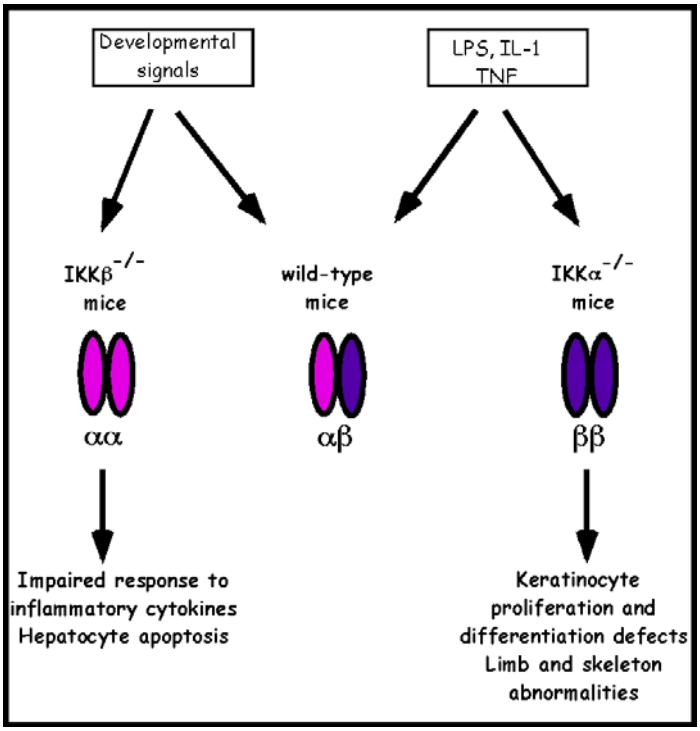

FIGURE 1.4: Functions of IKKα and IKKβ from knockout mouse phenotypes

IKKα can not compensate the lack of IKKβ subunit in NF-κB activation mediated by inflammatory cytokines but is required for transducing morphogenic signals (adapted from Hatada *et al.*, 2000).

1.1.3 RelB

RelB was originally identified as an immediate-early gene in growth factor-induced mouse fibroblasts by its striking similarity to the *c-rel* proto-oncogene. A cDNA of 2.1 kb was isolated with an open reading frame encoding a protein of 558 amino acids (60.3 kD). A unique characteristic of RelB in comparison to other Rel proteins is the region preceding the RHD, which contains a putative LZ domain and presumably provides additional protein-protein interactions (**Fig. 1.5** and **Fig. 1.1**). RelB does not form homodimers *in vitro* or *in vivo* but heterodimerizes with p50. These heterodimers transactivate transcription driven by a κB site *in vivo* (Ryseck *et al.*, 1992). The cloning of *nfkb2*, which encodes p100/p52, and the demonstration that p52-RelB heterodimers are also transcriptionally active, indicates the presence of alternative NF-κB complexes, which do not involve RelA or c-Rel (Bours *et al.*, 1992). Another unique feature of murine RelB is that both N- and C- termini are required for full transactivation.

Alterations in the LZ motif at the N-terminus of RelB decreases the transcriptional capacity, further indicating an important role of this unique region (Dobrzanski *et al.*, 1993). Similar to mouse and human, *Xenopus* homolog of mammalian RelB, XrelB, alone does not bind to κB sites efficiently while it forms transcriptionally active heterodimers with p50, but not with XrelA (Suzuki *et al.*, 1995).

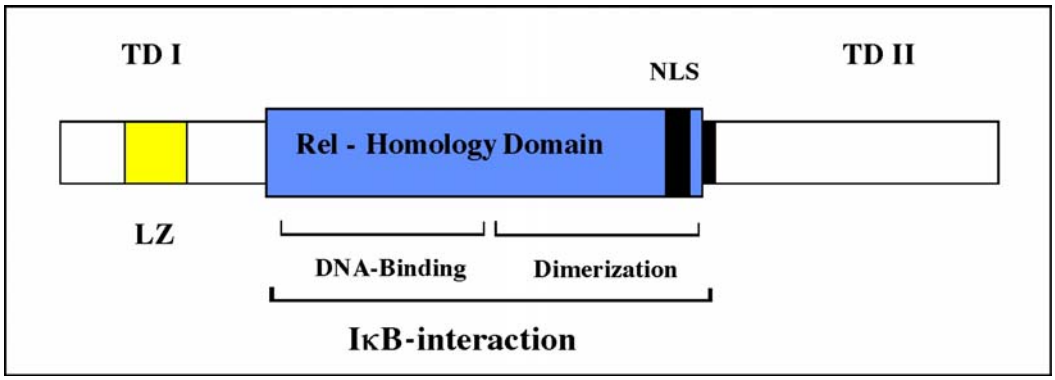

FIGURE 1.5: Structure of the mouse RelB protein

Unlike other family members, RelB has a leucine zipper (LZ) motif at its N-terminus, the exact function of which is still unclear. There are two transcriptional activation domains (TD I and II) at N- and C-termini both of which are necessary for the full activation potential of RelB. NLS: nuclear localization signal.

The expression of *relB* during mouse development shows a restricted pattern including certain regions of lymphoid organs, such as spleen, thymus, and lymph nodes. In adult animals, *relB* mRNA is detected in spleen, thymus and intestine. In thymus, *relB* transcripts are confined to the medulla and high levels of RelB is expressed in the nucleus of interdigitating dendritic cells (IDC). While in the spleen of newborn animals RelB expression is not detected, it increases later in the white pulp and periarterial lymphatic region. In lymph nodes, *relB* expression is confined to the paracortical area. While high levels of expression are detected in T cell rich areas, only low levels of expression are detected in B cell rich zones of secondary lymphoid organs. This specific spatial and temporal expression of RelB indicates an important role in these organs (Carrasco *et al.*, 1993).

The constitutive DNA-binding activity of RelB heterodimers in thymus and spleen suggests an important role in the expression of κB-regulated genes (Lernbecher *et al.*, 1994; Weih *et al.*, 1994). This constitutive activity in lymphoid organs is attributed to the decreased susceptibility of RelB complexes to IκBα inhibition in comparison to

RelA complexes or to RelB complexes in non-lymphoid settings. Alternatively, lymphoid tissue specific cofactors or posttranslational modifications of RelB may also contribute to this constitutive activity (Lernbecher *et al.*, 1994). IκBα is a weak modulator of p52-RelB complexes *in vivo* and neither IκBγ (C-terminal domain of p105) nor Bcl-3 inhibit RelB-p52 complexes. Therefore, differential interactions of NF-κB complexes with inhibitors determine constitutive nuclear and inducible cytoplasmic pools (Dobrzanski *et al.*, 1994). Overexpression of RelB in transgenic animals results increased κB-binding activity in thymocytes. Unlike in RelA-transgenic mice (Perez *et al.,* 1995), this occurs without alteration in IκBα levels, indicating differential regulation of RelA and RelB complexes and further supporting the notion of inducible and constitutive NF-κB pools in an animal model (Weih *et al.*, 1996).

As an additional regulatory mechanisms for RelB, the C-terminal domain of the precursor p100 (also called IκBδ) was shown to be a strong inhibitor of p52-RelB transcriptional activity (Dobrzanski *et al.*, 1995). In addition, RelA regulates the transcription of the *relB* gene. The delayed nuclear translocation of RelB, unlike rapid kinetics for RelA, TNF or LPS stimulation requires increased protein synthesis secondary to transcriptional induction of the *relB* gene (Bren *et al.*, 2001). RelB is degraded upon T cell receptor (TCR) or TPA/ionomycin stimulation in T cells which involves rapid phosphorylation of RelB after stimulation, an N-terminal cleavage and proteasome mediated complete degradation. This signal-induced degradation of RelB is an additional mechanism for the regulation of NF-κB activity in the lymphoid system (Marienfeld *et al.*, 2001).

1.1.4 Mice with a Targeted Disruption of RelB

Weih *et al.* generated a mutant mouse strain carrying a deletion of the fourth exon of the *relB* gene. At birth these are indistinguishable from wild-type animals. However, as this study demonstrates, Peyer's patch organogenesis is defective even at birth in these animals. Histopathological alterations are detectable in eight to ten day old mice. Analysis of lymphoid organs revealed variable thymic atrophy with reduced antigen presenting medullary dendritic cells, marked splenomegaly (twenty days of age and older) due to marked extramedullary hematopoiesis (EMH) in the red pulp with reduced splenic white pulp. Myeloid hyperplasia in the bone marrow, accompanied by decreased

number of erythroid precursors, is another consistent feature of these mice. Another striking feature of these animals is the lack of lymph nodes in adults due to lymphoid depletion (Weih *et al.*, 1995).

RelB-deficient animals show multiorgan inflammation of nonlymphoid organs, such as lung and liver. This phenotype and myeloid hyperplasia is T cell dependent (Weih *et al.*, 1996). However, *relB* disruption does not result in impaired T and B cell development as indicated by a normal distribution of CD8- and CD4-positive lymphocytes in thymus (Weih *et al.*, 1995). Furthermore, RelB-deficient mice are highly susceptible to *L. monocytogenes* infection and can not clear LCMV (Weih *et al.*, 1997). Thus, RelB-deficient animals not only have defects in lymphoid organ development but also in eliciting immune responses.

RelB-deficient mice, similar to p52-deficient mice (Poljak *et al.*, 1999), can not form germinal centers and follicular dendritic cell networks upon antigen challenge in spleen. Bone marrow chimeric animals demonstrate the requirement of RelB expression in stromal cells. RelB is also required in the hematopoietic compartment for generation of marginal zone B cells (MZB). This indicates a role for RelB for proper development of spleen microarchitacture at multiple levels (Weih *et al.*, 2001). RelB also regulates p21 protein levels and drives p21 promoter activity which suggests another role for RelB in cell cycle control, resistance to apoptosis and oncogenesis (Bren *et al.*, 2001).

Similarly, a mutation disrupting the *relB* locus by random integration of a class I MHC transgene resulted in mice with impaired antigen-presenting function and excessive production of granulocytes and macrophages, severe inflammation in lung and liver, and the lack of thymic medulla. Associated with the medullary defect, non-BM derived medullary epithelial cells (MECs) are also absent in these mice. Therefore, in addition to thymic dendritic cells, RelB is essential for the development of MECs, which determine the development of the thymic medulla (Burkly *et al.*, 1995).

1.2 SECONDARY LYMPHOID ORGANS

The cells involved in the immune response are compartmentalized into tissues and organs to function effectively. These structures are classified as either **primary** (central) or **secondary** (peripheral) lymphoid organs. Primary lymphoid organs are the major sites of lymphocyte development (lymphopoiesis). At these sites, lymphocytes differentiate from lymphoid stem cells, proliferate, and mature into functional albeit naive cells. The primary lymphoid organs for T and B lymphocytes in mammals are thymus, fetal liver and bone marrow (BM), respectively. Lymphopoiesis is followed by the migration of lymphocytes into secondary lymphoid organs which provide an environment to enable lymphocytes to interact with each other, with accessory cells, and with antigens (Ags). At these sites, naive lymphocytes encounter exogenous Ags, which results in the initiation of primary immune responses. Secondary lymphoid organs comprise lymph nodes (LNs) and spleen, Peyer's patches (PPs), tonsils and other collections of lymphocytes (Roitt *et al.*,1998).

The spleen is responsible for blood-borne Ags while LNs function in the protection of the body from Ags coming from skin or internal surfaces via the lymphatic system. The structure of the lymphatic system ensures that tissue Ags reach regional LNs, Ags in blood are trapped in the spleen, and that Ags from the gut reach PPs. Responses to Ags encountered via these routes result in antibody secretion into the circulation and local cell-mediated responses.

Equally important in generation of these responses is the migration of lymphocytes into and between secondary lymphoid tissues. Lymphocytes migrate from the blood through a specialized endothelium, so-called high endothelial venules (HEVs). Lymphocytes may also use afferent lymphatics to reach a node from tissues. Lymphocyte homing is mediated by a set of adhesion molecules expressed on endothelial cells (addressins) and their ligands (homing receptors) on lymphocytes. Adhesion is mediated by several receptors. Selectins bind to adressins on the endothelial cells, and integrins bind to the members of the Ig superfamily of molecules, such as vascular cell adhesion molecule-1 (VCAM-1) and intercellular adhesion molecule-1 (ICAM-1). PP HEVs only express mucosal adressin cell adhesion molecule-1 (MAdCAM-1) and the principal ligand for MAdCAM-1 is the integrin $\alpha_4\beta_7$ (Male *et al.,* 1996; Roitt *et al.*, 1998; Mebius *et al.,* 1998; Matheny *et al.,* 2000).

1.2.1 Spleen

The spleen is the site of generation of high-affinity antibodies in response to blood-borne Ags. The spleen can grossly be divided into red pulp (RP) and white pulp (WP) which represent the erythroid and lymphoid areas, respectively. Three major compartments can histologically be defined within WP each of which has particular characteristics:

1. ***Periarteriolar lymphatic sheath (PALS)***; consists of lymphocytes surrounding the splenic arterioles. It is called the T cell area and is also rich in a specialized antigen-presenting cell type called the IDC.
2. ***Marginal zone (MZ)***; is the site of lymphocyte entry into the spleen from the blood and contains a layer of reticular cells, macrophages and resident B cells that surrounds the PALS and follicular areas.
3. ***Primary B cell follicles***; are located in the periphery of the PALS, are also referred to as the B cell area of the WP and contain in addition to naïve and recirculating B cells, follicular dendritic cells (FDCs) which function as efficient antigen-capturing cells.

B and T lymphocytes leave the blood in the MZ; they then cross the marginal sinus and migrate to the PALS. B cells continue on to the follicles while the T cells remain within the PALS (**Fig. 1.6**). In the absence of antigenic stimulation, both B and T cells re-enter the circulation. In the presence of Ag, however, these migratory pathways considerably change. Upon immunization with T cell-dependent Ag, Ag is first localized in the IDCs of the T cell area and these Ag-specific T cells are induced to stop their migration and to proliferate within the PALS. Similarly, B cells stimulated by Ag migrate to the PALS where they also proliferate in the presence of cognate T cell help. Activated B cells either form foci of short-lived plasma cells secreting initially IgM but subsequently switching to downstream isotypes, or they migrate into the primary follicles where Ag is present on the surface of FDCs. These follicles are then transformed into a histologically defined structure termed the germinal center (GC). In these sites, affinity maturation, immunoglobulin (Ig) class switching and memory B cell generation take place. All these steps serve to expand and diversify the repertoire of the early immune response to Ags and to select high-affinity variants for the long-term maintenance of protective immunity (Hess *et al.,* 1998; Tarlinton, 1998).

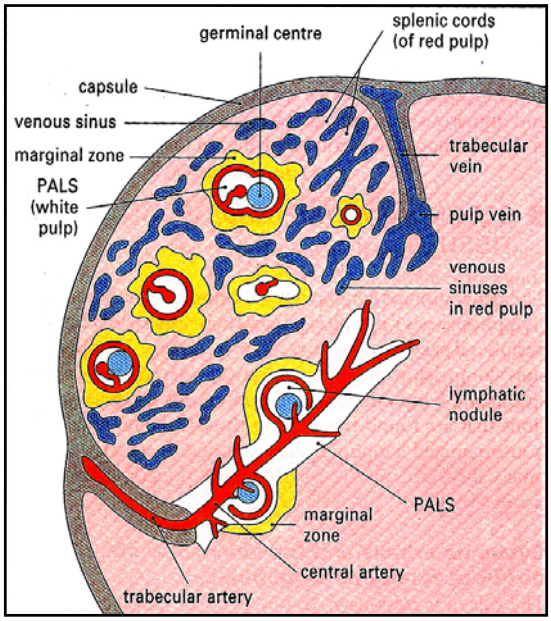

FIGURE 1.6: Schematic organization of the spleen

WP is composed of PALS and is surrounded by the MZ. The RP contains venous sinuses separated by splenic cords. Blood enters via the trabecular arteries, giving rise to central arteries some of which end in WP but most empty near or into MZ. Some arterial branches run into the RP terminating in the cords. Blood leaves the tissue through the trabecular veins (adapted from Roitt *et al.*, 1996).

RelB is expressed in PALS, GCs and MZ and RelB-deficient mice show impaired GC formation upon sheep red blood cell (SRBC) immunization. In addition, these animals lack FDC networks and have MZ formation defects as demonstrated by reciprocal BM chimeric animals (Weih *et al.*, 2001). **Table 1.1** summarizes these findings:

Adult Animals	**B6**	***relB*** $^{-/-}$	**B6 to *relB*** $^{-/-}$	***relB*** $^{-/-}$ **to B6**
GC				
PNA	+	-	-	+
FDC	+	-	-	+
MZ				
MZM	+	-	-	+
MS	+	-	-	+
MMM	+	- *	- *	+

Table 1.1: Spleen microarchitecture in adult *relB* $^{-/-}$ **animals and BM chimeras**

GCs are typically defined by PNA^{+} clusters surrounded by B cells. The plant lectin peanut agglutinin (PNA) binds to centroblasts/centrocytes in GCs. Marginal sinus (MS) is detected by MAdCAM-1 expressing marginal sinus lining stromal cells which are deficient in *relB*$^{-/-}$ mice. In addition to MZ macrophages, (MZM) metallophilic marginal macrophages (MMM) are not detected. * present but disorganized, B6: C57BL/6 wild-type mice.

RelB-deficient recipients reconstituted with wild-type BM lack GCs and FDCs, indicating that RelB expression in radioresistant stromal cells is required for the development of GCs and FDC networks in spleen. In addition, MMM cells did not form a proper MZ structure, suggesting also a requirement of RelB expression in the non-hematopoietic compartment for normal MZ formation.

1.2.2 Peyer's Patches

PPs are aggregations of lymphoid tissue in the wall of the small intestine. PPs are covered with unique epithelial cells constituting the follicle-associated epithelium (FAE). PPs act as sites where luminal Ags are transported by membranous (M) cells, components of the FAE, across the epithelium and are presented to antigen presenting cells. The description of GCs in PPs and the presence of IgA precursors ascribe to PPs a special role in the induction and dissemination of mucosal immune responses, casting PPs as secondary lymphoid organs (Griebel *et al.*, 1996). The increase both in number and size of PPs in mouse and human with aging, further indicates its function as secondary lymphoid organs (Nishikawa *et al.*, 1998).

In addition to PPs, lamina propria lymphocytes (LPL) and intraepithelial lymphocytes (IELs) are considered to form the so-called gut-associated lymphoid tissue (GALT). The lamina propria (LP) is the layer of connective tissue between the epithelium and the muscularis mucosae and contains a complex mixture of lymphoid and accessory cells, which provide an immune response. Lymphocytes interspersed through the gut epithelium are collectively called IELs. The main function of the gut is to absorb nutrients, but because of the large number of protozoa, bacteria, viruses, toxins and nutritional Ags in the gut, the organism needs a local protective system to prevent invasion, tissue damage and systemic infection. In this respect, the major function of PPs is suggested to facilitate immune reaction against antigenic stimulation (Gebert *et al.*, 1996; Adachi *et al.*, 1997).

PPs consist of definite compartments with structural elements, lymphocytes and accessory cells (**Fig. 1.7**). PPs and other sites of the GALT can be divided into three major compartments:

1. ***Lymphoid follicles*** are localized below muscularis mucosae. Proliferating B lymphocytes form GCs. Follicles are surrounded by IgM and IgD positive lymphocytes.
2. ***The interfollicular region (IFR)*** is characterized by HEVs. Lymphocytes enter the PPs from the blood via these specialized venules.
3. ***The subepithelial dome (SED)*** is the T cell zone and characterized by different lymphocytes and dendritic cells (DCs).

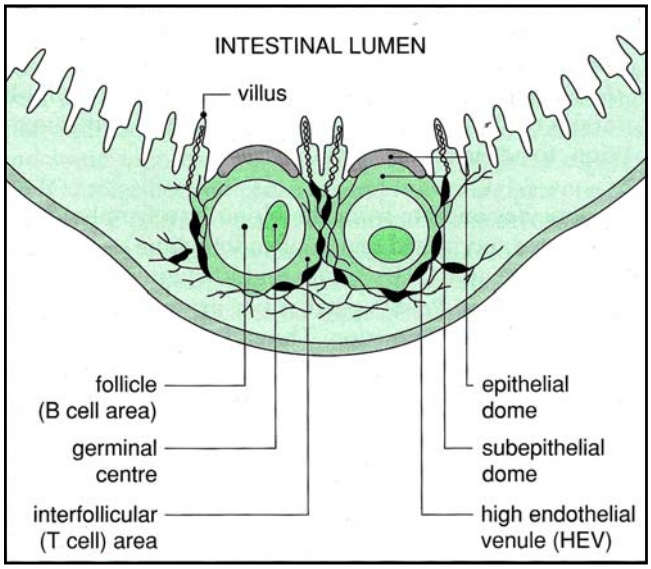

FIGURE 1.7: Schematic representation of a Peyer's patch

PPs are collections of lymphoid tissue at the intestinal wall with a specialized epithelium containing M cells which transport Ags from the gut lumen to the patch. Similar to other secondary lymphoid organs, PP is also divided into functional T and B cell areas. Lymphocytes enter the patch through HEVs (adapted from Male *et al.* 1996).

In PPs, each follicle is separated from the overlying epithelium by the SED, which is rich in T and B lymphocytes and DCs (**Fig. 1.7**). Cells in the SED interact intimately with the overlying epithelium enabling effective endocytosis, processing and presentation of Ags by M cells. The M cell pathway also transports non-pathogenic commensal bacteria and the immune responses against commensals involve T cell independent IgA production (Neutra *et al.*, 2001). IgA is the major Ig isotype in secretions and in gut fluid. In the normal gut mucosa, IgA is produced by plasma cells of the LP and then is bound to the poly-Ig receptor of enterocytes, transported to the apical membrane by endocytosis and secreted as secretory IgA (sIgA) to the gut lumen. The sIgA can agglutinate infectious microorganisms and prevent them from adhering to

and penetrating the epithelia. It also protects mucosal surfaces against inflammatory reactions by neutralizing bacterial toxins without complement activation. Since the LP harbors largely IgA-secreting plasma cells and memory T-effector cells, PPs were suggested as the sites of IgA class switching. However, recent reports indicate the dispensability of PPs and that gut LP IgA^+ cells are generated from IgM^+ B cells *in situ* by interacting with LP stromal cells. This renders PPs as the inductive sites and the LP as the effector site of GALT (Gebert *et al.*; 2001; Fagarasan *et al.,* 2001; Anderson *et al.,* 2001).

In addition to its functions in immune response, GALT functions as a site for extrathymic maturation of some T cell populations. T cell progenitor clusters are found throughout the small and large intestine, in the crypt LP. These gut cryptopatches (CP) are sites for thymus-independent development of IELs. The development of these IELs is supported by the expression of interleukin-7 (IL-7) by enterocytes (Anderson *et al.,* 2001).

The development of GALT takes place during fetal life in a sterile environment and in the absence of antigenic stimulation (Finke *et al*., 2001). Recently, a hypothetical model was described for PP organogenesis based on wholemount immunohistochemistry. Three histologically distinct steps for PP organogenesis are proposed. These include the formation of organizing centers expressing VCAM-1 and ICAM-1 in the intestine at E15.5 (step I), accumulation of blood cells expressing different surface markers to this region at E16.5-17.0 (step II), and entry of $CD3^+$ and $B220^+$ lymphocytes just before birth (step III). The IL-$7R\alpha^+CD4^+CD3^-$ cell population in the embryonic intestine is the inducer of organizing centers in PPs. This subpopulation is similar to the $CD4^+CD3^-$ cells described by Mebius *et al.,* which express lymphotoxin β (LTβ), RelB, and the chemokine receptor CXCR5. The current model for PP organogenesis consists of a yet to be described initiator cell which provides ligands for IL-$7R\alpha^+$ cells (inducers) to produce LTαβ, activating the LTβ receptor (LTβR)-positive cells (responders) to form an organizing center. The earliest marker is VCAM-1 and ICAM-1 expression detected by wholemount immunohistochemistry of the gut (**Fig. 1.8**) (Adachi *et al.*, 1997; Mebius *et al.*, 1997; Adachi *et al.*, 1998; Nishikawa *et al.*, 1998; Yoshida *et al.*, 1999).

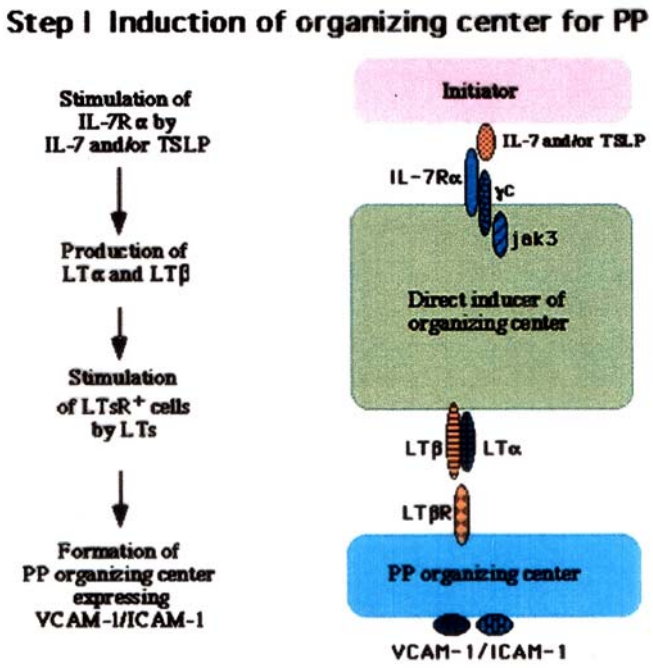

FIGURE 1.8: Early events during PP organogenesis

LTα and LTβ are produced by IL-7Rα$^+$ inducer cells in a IL-7 signaling dependent manner. LTβR expressing responder cells express adhesion molecules VCAM-1 and ICAM-1, which is the earliest marker for developing PPs. This is followed by the establishment of vascular system and mature lymphocyte homing (adapted from Yoshida *et al.*, 1999).

LTβR expressing intestinal cells and the connection between the developmental steps were recently further characterized. VCAM-1$^+$ICAM-1$^+$ (V^+I^+) cells are of mesenchymal origin, which are activated by lymphoid cells through LTβR to express not only adhesion molecules but also chemokines, such as B lymphocyte chemoattractant (BLC) and EBV-induced molecule 1 ligand chemokine (ELC). Since lymphoid cells of the embryonic intestine express chemokine receptors CXCR5 and CCR7 for BLC and ELC, respectively they are recruited along the chemokine gradient produced by non-lymphoid cells. Overall, the PP developmental program is mediated by mutual interaction between mesenchymal and lymphoid cells at certain time window in the embryonic intestine (see also **Fig. 1.10**). In this network of events, open questions are what the initial event for PP induction is and how the position of the future patch is determined. The identification of the ligand producer for IL-7Rα$^+$ cells will contribute significantly to the complete understanding of the early determining events (Honda *et al.*, 2001).

1.3 SIGNALS REGULATING LYMPHOID ORGAN DEVELOPMENT

Signals leading to the induction of secondary lymphoid structures are derived from cognate physiological cell-cell contacts and the interaction of soluble ligands and cytokines with their specific receptors. These interactions trigger intracellular signaling pathways that result in either the activation or the inhibition of transcription factors or cofactors (Hess *et al.*, 1998). As examples for such signaling pathways, distinct roles for TNF ligand and receptor family and chemokines in the lymphoid organogenesis were defined by gene targeting in mice.

1.3.1 Tumor Necrosis Factor (TNF) / Lymphotoxin (LT) Ligand and Receptor Families

The genes for the TNF/LT family map within the MHC on chromosome 6 in humans, and chromosome 17 in mouse. Three members of this gene family are TNF, LTα (also known as TNFβ), and LTβ. TNF is produced as a type II transmembrane protein, which is cleaved and released by TNF-converting enzyme (TACE) and which binds to the p55 TNF receptor 1 (TNFRI) or the p75 TNFRII. LTα can be secreted as a $LT\alpha_3$ homotrimer, which binds to both TNF receptors, supporting its functional similarity to TNF. LTα can also form a heterotrimer with LTβ, a type II transmembrane protein, and this $LT\alpha_1\beta_2$ molecule exclusively binds to LTβR, but not to either of the TNFRs. These observations suggest also that LTα acts to signal two distinct sets of cellular responses, one determined by its homotrimeric form binding to TNFRs and the other determined by its membrane form binding to the LTβR (**Fig. 1.9**). In addition, a new family member has recently been identified. Herpex simplex virus (HSV) 1 and 2 infect activated T lymphocytes by binding of the HSV envelope glycoprotein D to the cellular herpes virus entry mediator (HVEM). It was shown that HVEM binds to two cellular ligands, $LT\alpha_3$ and LIGHT (homologous to **l**ymphotoxins, exhibits **i**nducible expression, and competes with HSV **g**lycoprotein D for **H**VEM, a receptor expressed by **T** lymphocytes). LIGHT also binds to LTβR (Ruddle, NH., 1999). TNF is primarily produced by macrophages and T cells, and LTs by CD4 T helper 1 (Th_1) and CD8 T cells. Since these molecules are all important in lymphoid organ development, it is likely that they are produced by wider range of cells yet to be identified (Ruddle, 1999; Matsumoto, 1999).

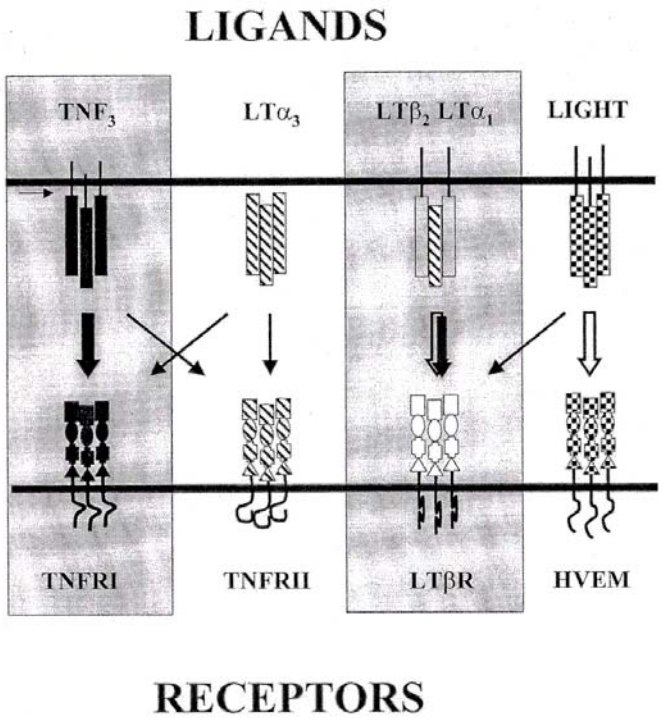

FIGURE 1.9: Complex crosstalk between TNF and LT ligands and their receptors

Ligands of the TNF superfamily form trimers and bind to trimeric receptors. Interaction of $LT\alpha_2\beta_1$ heterotrimers with TNFRI and of $LT\alpha_3$ homotrimers with HVEM, as suggested by *in vitro* studies, are not depicted in this figure. The *in vivo* significance of LIGHT-LTβR interaction remains unknown. See text for more details about HVEM and LIGHT (adapted from Shakhov, and Nedospasov, 2001).

Analyses of mice deficient for TNF/LT family members have provided detailed information about the action of LT in lymphoid organogenesis. In mice deficient for either LTα, LTβ or TNF, organized clusters of FDCs and GCs are absent in spleen. These structures are restored in LTα-deficient animals, but not in TNFR1-deficient mice, by BM transplantation, indicating that while BM derived LTα-expressing cells are required, expression of TNFRI on non BM derived cells is necessary for the establishment of these structures. Similar findings were obtained with LTβR-deficient mice, collectively leading to the conclusion that BM derived LTα, LTβ, and TNF expressing cells as well as non-BM derived TNFRI and LTβR expressing cells contribute to the organization of the lymphoid structure in spleen. TNFR2-deficient mice do not show defects in lymphoid organ development. Targeted disruption of the *tnfr1* gene blocks actions of TNF, $LT\alpha_3$ and $LT\alpha_2\beta_1$, but signaling can still occur via membrane $LT\alpha_1\beta_2$ binding to LTβR. PPs in *tnfr1*$^{-/-}$ mice are reduced in number and

they have more severe disturbance of architecture than TNF-deficient mice. Therefore, although $LT\alpha_3$ and $LT\alpha_2\beta_1$ may have a role in formation of normal PPs, they are not primary organizers of PP anlagen. However, when all membrane LT activity is disrupted, as in LTα-deficient animals, PPs do not develop and these mice also have disrupted splenic WP architecture. It seems therefore that membrane LT is vital in the organogenesis of secondary lymphoid organs, including PP. This conclusion is further strengthened by selective loss of membrane LT in LTβ-deficient mice, which also lack PPs. Taken together from the available mutant mouse phenotypes, TNF signaling through TNFRI, unlike LTαβ signaling, is not essential for lymphoid organogenesis, but rather for interactions determining the cellular and structural organization of B cell follicles in all secondary lymphoid organs (**Table 1.2**) (Ruddle, 1999; Pasparakis *et al.*, 1997).

Table 1.2: Role of TNF/LT ligands and receptors and Rel/NF-κB family members for spleen structure and PP organogenesis

Gene	*tnf*$^{-/-}$	*tnfr1*$^{-/-}$	***ltα***$^{-/-}$	***ltβ***$^{-/-}$	***ltβr***$^{-/-}$	***aly/aly***	*nfkb1*$^{-/-}$	***nfkb2***$^{-/-}$	***relB***$^{-/-}$
Spleen MZ	+[1]	+	-	-	-	-	+	-[5]	-
GC	-	-	-	-[3]	-	-	+	-	-
FDC	-	-	-	-	-	-	+	-	-
PP	-/+[2]	-/+[2]	-	-	-	-	+	-	-
VCAM-1$^+$	**NR**	**NR**	-	-	**NR**	-	+[4]	-[4]	-[4]

(adapted from Matsumoto, 1999; Weih *et al.*, 2001)

1: reduced numbers of and disorganized MZM and MMM cells
2: although PPs exist, B cell follicle and GC formation is defective
3: small numbers of PNA positive cells exist in both T- and B-cell areas
4: determined by this study
5: only MZM cells are detected
***aly/aly*:** alymphoplasia homozygous mutants, see text for details
NR: not reported

Activation of TNF/LT receptors occurs through close spatial aggregation of multiple receptors as a result of binding of the trivalent ligand, a process called receptor clustering. Cytoplasmic regions brought together in receptor-ligand complexes could therefore create a unique surface for the initiation of signaling. (Ware *et al.*, 1995). TNF and LTα are potent NF-κB activators in various cell types (Pahl, 1999). Gene targeting in mice and overexpression studies have revealed some of the components of the signal

transduction by TNF/LT family leading to NF-κB activation. Binding of TNF to TNFRI recruits adaptor proteins, such as TNFRI-associated death domain protein (TRADD), receptor interacting protein 1 (RIP1), Fas-associated death domain protein (FADD) and TNFR associated factor 2 (TRAF2). TNFRII triggering results in direct recruitment of TRAF2 followed by TRAF1. TRAF2 plays a central role in early events common to both TNFRs leading to IKK and MAPK activation. However, it is still not known what leads to the activation of IKK even though different MAP3Ks are suggested to provide the connection between TRAFs and the IKK complex (Baud *et al.*, 2001).

The cytoplasmic domain of LTβR shares little homology with the cytoplasmic domains of TNFRI or TNFRII, suggesting that activation of LTβR induces distinct cellular responses. TRAF5 was suggested to be specific activator of NF-κB through LTβR (Nakano *et al.*, 1996). Following either receptor ligation by agonistic antibody treatment, or treatment with soluble form of $LT\alpha_1\beta_2$, NF-κB is activated in a cell type specific manner in some but not all LTβR expressing cells (Mackay *et al.*, 1996). Recently, LTβR signaling regions were defined by deletion mutants. In addition to TRAF2 and TRAF5, binding of TRAF3 was also suggested. NF-κB dependent transcription downstream of LTβR is mediated by TRAF2 and TRAF5. The notion that these molecules function in the same signaling pathway is substantiated by phenotypes of TRAF2-, TRAF5- and TRAF3-deficient mice, which exhibit defects in secondary lymphoid organ development (Force *et al.*, 2000).

In addition to the gene-targeted mice described above, alymphoplasia (*aly*) mice, an autosomal recessive natural mutant strain, provide a novel and unique model for the development of lymphoid organs. Like LTα-deficient mice, *aly/aly* mice lack LNs and PPs and development of GCs, FDC clusters, and MZ formation are disturbed in spleen. The gene responsible for this mutant strain has been shown to encode NIK. Interestingly, the *aly* point mutation at the C-terminus of NIK abrogates interaction of NIK with IKKα and also with TRAFs. Taken together, LTβR signaling mediated activation of NF-κB through NIK is important in secondary lymphoid organ development (Matsumoto, 1999).

1.3.2 Chemokines

Chemokines are small basic chemotactic proteins that mediate their effect by binding to G-protein coupled receptors expressed on target cells. Chemokine receptors are members of the seven-transmembrane-receptor family and induction of migration along a chemokine gradient (chemotaxis) is signaled by members of the pertussis toxin (PTX)-sensitive Gαi subfamily of heterotrimeric G proteins. Different tissues produce different repertoires of inflammatory chemokines to attract appropriate subsets of effector cells into the tissue, to respond to a particular pathogen or tissue damage. In addition to promoting cell migration, chemokines are active in inducing integrin activation and transcription of cytokines (Cyster, 1999; Ansel *et al.*, 2001).

Recent studies identified several chemokines that are expressed constitutively in lymphoid tissues indicating a homeostatic role by regulating lymphocyte trafficking to or within lymphoid organs. ELC and secondary lymphoid tissue chemokine (SLC) are expressed constitutively at high levels in thymus, LNs, and other lymphoid tissues and attract lymphocytes, which bear the corresponding chemokine receptor CCR7. Mice lacking SLC or CCR7 have defects in lymphocyte homing, DC localization, primary immune responses, and morphological alterations in secondary lymphoid organs. In addition, mice lacking CXCR5, a chemokine receptor expressed in B lymphocytes, lack inguinal LNs, have a few phenotypically abnormal PPs, and show impaired formation of primary follicles and GCs. CXCR5-deficient B lymphocytes fail to migrate to B cell areas indicating the need for chemokines to direct lymphocyte homing to specific anatomical sites and to regulate the development of functional lymphoid tissues. The ligand for CXCR5 is BLC (Förster *et al.*, 1996; Baggiolini, 1998; Gunn *et al.*, 1999).

Insights into the role of chemokines in lymphoid organogenesis have recently been gained by demonstration of the requirement for the cytokine $LT\alpha_1\beta_2$, for the IL-7Rα chain and for the chemokine BLC for PP development. IL-7Rα^+CD3$^-$CD4$^+$ cells constitute the majority of cells present in PP anlage prior to colonization by B and T cells. Analysis of developing LNs revealed the presence of a similar cell type. Therefore, it is likely that organogenesis of PPs and LNs proceeds via similar mechanisms induced by common lymphoid tissue inducing cells (LTICs) (**Fig. 1.10**) (Yokota *et al.*, 1999; Sun *et al.*, 2000; Ansel *et al.*, 2001)

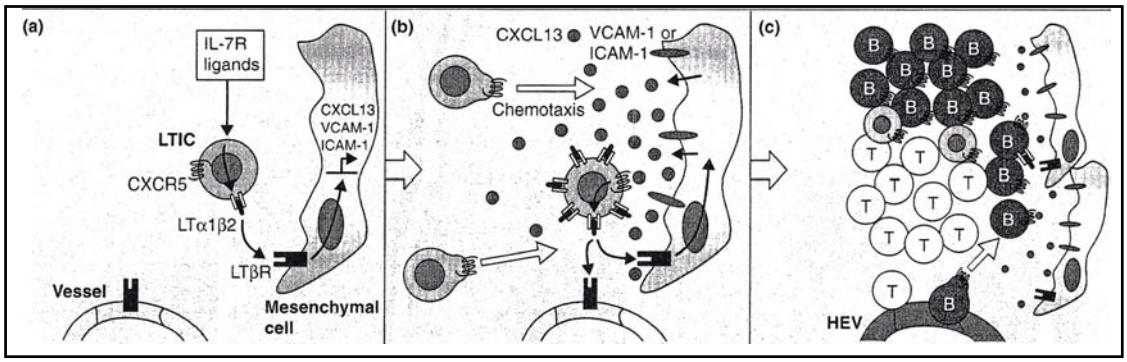

FIGURE 1.10: A proposed model for the role of chemokines in PP organogenesis
(a) IL-7R ligands stimulate surface LTαβ expression by IL-7Rα$^+$ cells and LTβR expressing mesenchymal cells respond by upregulating VCAM-1, ICAM-1 and BLC (CXCL13). **(b)** This BLC production attracts additional IL-7Rα$^+$ LTIC, expressing CXCR5 leading to further stimulation of $LT\alpha_1\beta_2$ expression. Such a positive feedback loop creates a site of high BLC and $LT\alpha_1\beta_2$ concentrations resulting in the formation of focal organ anlagen. **(c)** Finally local blood vessels differentiate into HEVs and recruit B and T cells. B cells also express CXCR5 and are important in PP organogenesis (adapted from Ansel *et al.*, 2001).

There is an inter-connected network of events involving cytokines and chemokines during lymphoid organogenesis. The expression of chemokines relevant to homing of T and B cells to the spleen, including BLC, is dependent on TNF and LT, as concluded from the analysis of TNF-, TNFRI- and LT-deficient mice (Gunn *et al.*, 1998). It is now clear that non-hematopoetic stromal cells, present in the T- and B-cell areas of the spleen and PPs, are the major sites of chemokine production which is necessary for naïve lymphocyte homing. For normal splenic structures, expression of TNFR1 and LTβR on splenic stromal cells is necessary (Tkachuk *et al.*, 1998; Endres *et al.*, 1999).

Collectively, primarily hematopoieticly derived TNF and LT are necessary for normal lymphocyte movement in all tissues, but subsequent chemokine production is a property of TNFRI- and LTβR-expressing resident stromal cells. Thus, the hematopoietic compartment initiates the signals for its own movement into the lymphoid tissues and the resident cells of the tissue direct where that movement will be by the expression of chemokines and also of adhesion molecules (Sedgwick *et al.*, 2000).

1.4 AIMS OF THE PROJECT

Adult mice with a targeted disruption of RelB have a severe phenotype in lymphoid organ development with disrupted spleen structure, lack of LNs and Peyer's patches. This study focuses on the role of RelB in the development of proper spleen architecture and in PP organogenesis.

Neither splenic defects nor lack of PPs were rescued by the adoptive transfer of BM into adult *relB*$^{-/-}$ recipients. In order to examine whether the defective development of lymphoid organs can be rescued at earlier time point, total wild-type fetal liver cells will be intrahepatically injected into newborn *relB*$^{-/-}$ mice and these animals will be analysed for spleen and PP phenotype.

Although *relB* mRNA expression was detected in mouse intestine (Carrasco et al., 1993), it is still unclear which structures and cell types express RelB. PPs will be analyzed by immunohistochemistry to identify RelB^{+} cells. Since PPs are suggested to be important for IgA production, fecal IgA levels will be determined by ELISA. To investigate the early steps of PP development, the presence and functionality of IL-7Rα^{+} inducer population and the formation of VCAM-1^{+} cell clusters in *relB*$^{-/-}$ intestine will be addressed.

TNF/LT signaling modulates chemokine expression and also involves NF-κB activation. The expression of TNF ligand/receptor family members, chemokines, and chemokine receptors will be examined in RelB-deficient spleen and intestine to investigate whether any of these genes is regulated by RelB.
LTβR signaling has a predominant role in lymphoid organogenesis. Although NF-κB activation downstream of LTβR has been reported, particular activation of RelB is unknown. Therefore, the principal aim of this work is to understand whether RelB heterodimers are activated downstream of the LTβR pathway. Non-lymphoid mouse embryonic fibroblasts, which express LTβR and TNFR, will be used as a model system to examine RelB induction. LTβR signaling will be activated in this system by agonistic antibody treatment and TNFR signaling will be induced by TNF stimulation.

2 MATERIALS AND METHODS

2.1 MATERIALS

2.1.1 Mice

Generation of *nfkb1*$^{-/-}$, *nfkb2*$^{-/-}$, *relB*$^{-/-}$, *p100*$^{-/-}$ and *p105*$^{-/-}$ mice has been previously reported (Sha *et al.*, 1995; Weih *et al.*, 1995; Ishikawa *et al.*, 1997; Caamaño *et al.*, 1998; Ishikawa *et al.*, 1998). All animals were housed and bred under the standard conditions with water and food ad libidum in the pathogen free mouse facility of the Forschungszentrum Karlsruhe, Institute of Toxicology and Genetics. For timed pregnancies, mice were mated and the noon of the day vaginal plugs were observed was accepted as 0.5 days post coitus (d.p.c).

2.1.2 Chemicals

The following list includes companies from which general chemicals used in this study were purchased:

Carl Roth GmbH + Co

E. Merck

Life Technologies

Serva Fein Biochemica GmbH & Co

Sigma Chemical Co

2.1.3 Oligonucleotides

Unless otherwise stated, all oligonucleotides were from MWG Biotech GmbH and Genset Oligos. All oligonucleotides were synthesized under standard conditions as 0.01 μM.

Below are the sequences of the oligonucleotides used in this study for RT-PCR analysis:

Chemokine and chemokine receptors:

33-BLC-52	5'-ATGAGGCTCAGCACAGCAAC-3'
278-BLC-258	5'-CCATTTGGCACGAGGATTCAC-3'
ELC atg-F	5'-GCCTCAGATTATCTGCCAT-3'
ELC atg-R	5'-AGACACAGGGCTCCTTCTGGT-3'
55-SLC-73	5'-ATGATGACTCTGAGCCTCC-3'
401-SLC-382	5'-GAGCCCTTTCCTTTCTTTCC-3'
5-CXCR5-24	5'-ACTACCCACTAACCCTGGAC-3'
514-CXCR5-493	5'-AGGTGATGTGGATGGAGAGGAG-3'
117-CCR7-138	5'-GAGAGACAAGAACCAAAAGCAC-3'
511-CCR7-490	5'-GGGAAGAATTAGGAGGAAAAGG-3'

Cytokine and cytokine receptors:

157-TNF-177	5'-ATGAGCACAGAAAGCATGATC-3'
432-TNF-412	5'-TACAGCTTGTCACTCGAATT-3'
1-LTα-20	5'-ATGACACTGCTCGGCCGTCT-3'
609-LTα-589	5'-CTACAGTGCAAAGGCTCCAAA-3'
97-LTβ-121	5'-TTGTTGGCAGTGCCTATCACTGTCC-3'
797-LTβ-774	5'-CTCGTGTACCATAACGACCCGTAC-3'
964-LIGHT-982	5'-AGACTGCTGACCTGCTTTG-3'
1425-LIGHT-1406	5'-CCCTTCTTTCCTCCCTTTCC-3'
8-IL7-29	5'-TAGCGAGCTTTCTCTGCTGCAC-3'
493-IL7-471	5'-TCTCACCACCCATAATCACTCCC-3'
1298-IL7Rα-1316	5'-CCCTCAACCATTGCCTTTC-3'
1755-IL7Rα-1736	5'-ACCCACCACTCACATCTTTC-3
274-LTβR-298	5'-TTATCGCATAGAAAACCAGACTTGC-3'
501-LTβR-482	5'-TCAAAGCCCAGCACAATGTC-3'
289-TNFRI-308	5'-GAACCTACTTGGTGAGTGAC-3'
679-TNFRI-660	5'-CACAACTTCATACACTCCTC-3'

Cell adhesion molecules and others:

324-ICAM-1-351	5’-CCGCTTCCGCTACCATCACCGTGTATTC-3’
751-ICAM-1-724	5’-GCCTTCCAGGGAGCAAAACAACTTCTGC-3’
484-VCAM-1-510	5’-CAGGAATTCAACAGACAGGAGTTTTC-3’
947-VCAM-1-921	5’-GGGGAATTCGTCAACAATAAATGGTT-3’
1072-MAdCAM-1-1093	5’-GAGGTGACCAATCTGTATGTTC-3’
1072-MAdCAM-1-1093	5’-AAAGCCCAGAAGTCAGGAG-3’
106-Actin-130	5’-AGAGGTATCCTGACCCTGAAGTACC-3’
827-Actin-803	5’-CCACCAGACAACACTGTGTTGGCAT-3’

NF-κB members:

RelA-PCR3	5’-TAGCCTTACTATCAAGTGTCTTCCTCC-3’
RelA-PCR4	5’-GTTCAGAGCTAGAAAGAGCAAGAGTCC-3’
RelB delta (Metabion)	5’-ACGCTGCTTTGGCTGCTCTGTGATG-3’
RelB gamma (Metabion)	5’-CCTCTCTTCCCTGTCACTAACGGT-3’
NFκB1 ($Ex5_{(2)}$)	5’-GCACCGTAACAGCAGGACCCAAGGACA-3’
NFκB1 (Ex8)	5’CCCGTCACACATCCTGCTGTTCTGTCCATTCT-3’
NFκB2 (p52Ex4)	5’-GCCTGGATGGCATCCCCG-3’
NFκB2 (MP50BA)	5’-CTTCTCACTGGAGGCACCT-3’
c-Rel-A	5’-TGGCTGACTGACTCACTGACTGACTGACTCGTGCCTTGC-3’
c-Rel-B	5’-CCAACTAAATCATGAGGATGAGGCTTATATGGATCATTC-3’

2.1.4 Antibodies

Antibody	*Application*	*Company*	*Dilution*
anti-VCAM-1	whole mount immunohistochemistry	Pharmingen	1:500
anti-RelB	immunoblotting / immunohistochemistry	Santa Cruz	1:500/1:200
anti-p50	immunoblotting	Santa Cruz	1:300
anti-p52	immunoblotting	Santa Cruz	1:300
anti-β actin	immunoblotting	Sigma	1:50000
KD-29-8 (anti-p100)	immunoprecipitation	in house	1:50
anti-IgA (purified)	ELISA (capture)	Pharmingen	2.5 μg/ml
anti-IgA (biotinylated)	ELISA (detection)	Pharmingen	1:200

Secondary antibodies

Antibody	*Application*	*Company*	*Dilution*
anti-mouse Ig-HRP	immunoblotting	DAKO Diagnostika	1:2000
anti-rabbit Ig-HRP	immunoblotting	DAKO Diagnostika	1:5000
anti-goat Ig-HRP	immunoblotting	DAKO Diagnostika	1:2000
streptavidin-HRP	ELISA	DAKO Diagnostika	1:2000
anti-rat Ig biotinylated	wholemount IHC	Pharmingen	1:100
anti-rabbit biotinylated	immunohistochemistry	Vector Laboratories	1:100

2.1.5 Plasmid Constructs:

pcDNAI/Amp:

Sequence information is available at Invitrogen home page (http//www.invitrogen.com/) under the vector data section.

Bluescript KS(+)-NFκB2 (p100:p52): #456

Nucleotides 259-1580 (1.3 kb) corresponding to mouse p52. Amino acids 1-443 were cloned into the BamHI site of Bluescript KS (+). This construct was used to release mouse p52 insert by NotI digestion followed by blunt end generation by T4 DNA polymerase reaction and second digestion with XhoI, in order to clone the insert into pcDNAI/Amp expression vector backbone of **#506** (see below).

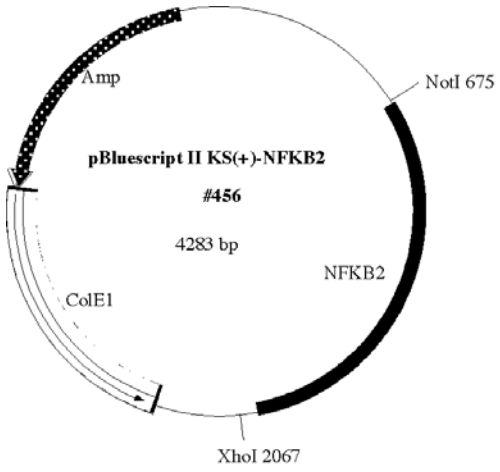

pcDNAI/Amp-NFκB1 (p105:p50): #506

Mouse p50 coding sequence (1.2 kb) has been cloned into pcDNAI/Amp XhoI/XbaI sites. This plasmid was used to release mouse p50 insert by XbaI digestion followed by blunt end generation by T4 DNA polymerase reaction and second digestion with XhoI, in order to clone the mouse p52 insert obtained from **#456** into pcDNAI/Amp expression vector backbone of **#506**.

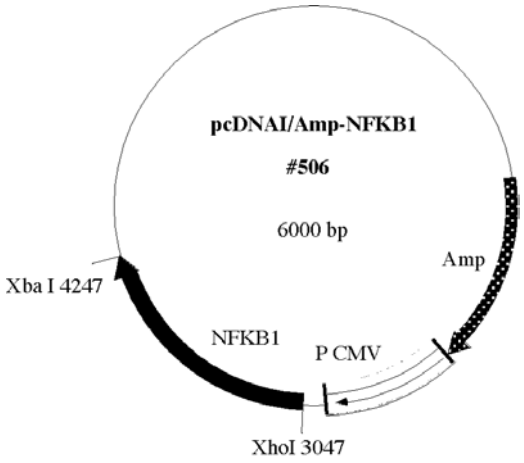

pcDNAI/Amp-mouse NFκB2 (p100:p52):

This construct was cloned by using the insert from **#456** and vector backbone from **#506**.

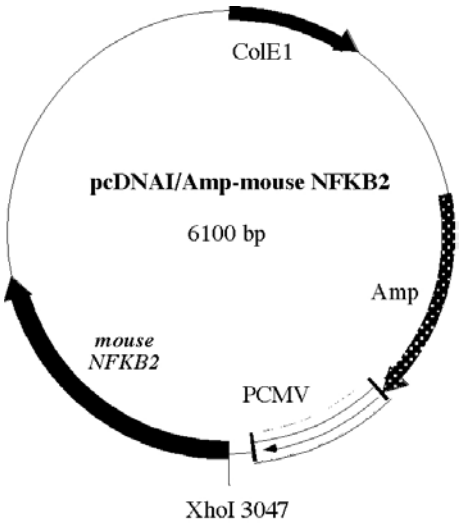

Insert and vector backbone were generated as described above and purified from agarose gels using QIAquick Spin kit (Quiagen) following manufacturer's instructions. Ligation reaction was performed using T4 DNA ligase and ligation product was electroporated into electrocompetent *E.coli* DH5α strain, plated on Ampicillin containing agar dishes. The next day colonies were picked, grown in Ampicillin containing LB medium and mini plasmid DNA preparations were done. Following a series of diagnostic restriction digestions, clones containing the correct mouse p52 insert were selected, DNA was prepared using Quiagen kit and verification was once more done by appropriate restriction digestions.

2.1.6 Cells and Cell Culture Media

IKK wild-type and IKK-deficient fibroblasts were a kind gift from Dr. Michael Karin and Dr. Peter Angel. NIH 3T3 cells were a kind gift from Dr. Susanne Weg Remers. All other primary fibroblasts were established in house.

Unless otherwise stated, all tissue culture media and PBS used to wash cells were purchased from Invitrogen GmbH together with the supplements such as Penicillin/Streptomycin and Glutamax. Trypsin was purchased from Difco Laboratories and was diluted to 0.25% in 15 mM sodium citrate and 134 mM potassium chloride, which were kept as stocks at -20^{o}C.

2.2 METHODS

2.2.1 EXTRACTION AND ANALYSIS OF RNA

2.2.1.1 RNA Isolation From Frozen Tissue Samples

Tissues were snap frozen in liquid nitrogen as soon as the animals were sacrificed. At this step, samples can be stored in Eppendorf tubes at -80^{o}C for further use. Tissues were either homogenized in 2 ml eppendorfs in 750 µl Peq GOLD RNA Pure^{TM} reagent (Peq Lab) or in 15 ml corex tubes in 3 ml RNA Pure reagent. The tip of the homogenizer (IKA Labortechnik T25 basic) was cleaned with water and 70% ethanol between samples. As soon as tissues were placed into tubes containing the reagent, homogenization was performed at highest speed.

Following homogenization, samples were left at room temperature (RT) for 5 min to ensure the complete dissociation of nucleoprotein complexes. Chloroform was added (0.2 ml / ml RNA Pure reagent), samples were vortexed vigorously for 10 sec and were centrifuged at 12000 g for 15 min at 4^{o}C. The colorless upper aqueous phase was transferred to a new tube and isopropanol was added (0.5 ml / ml RNA Pure reagent). Samples were left at RT for 5-10 min and then were centrifuged at 12000 g for 15 min at 4^{o}C. RNA forms a pellet on the side and the bottom of the tube. Supernatant was removed and pellets were washed twice with 1 ml 75% ethanol (minimum 1 ml / RNA Pure reagent). Samples were centrifuged at 7500g for 5 min at 4^{o}C, supernatants were discarded and pellets were air dried for 5-10 min. Finally the pellets were resuspended in appropriate volume of ddH_2O and were placed on a thermoshaker (Eppendorf Thermomixer 5436) for 10 min at 60^{o}C for dissolution. Samples were further used for concentration estimation and gel electrophoresis.

2.2.1.2 Extraction of Total RNA From Cells

Cells were pelleted in eppendorf tubes and homogenized in 1 ml RNA Pure reagent by vortexing till the pellet was dissolved. At this step homogenized samples can be stored at -20^{o}C. The extraction was performed as with the frozen tissue samples (see above section). When the starting material was less than 5x10^{5} cells, after the transfer of the aqueous phase to a new tube, 2 µl glycogen (20 µg) (Peq Lab) was added.

2.2.1.3 Determination of RNA Concentration and Agarose Gel Electrophoresis of RNA Samples

RNA concentration was determined spectrophotometrically (Eppendorf spectrophotometer) by taking readings at 260 nm against a blank, ddH_2O. A solution of 50 µg/ml DNA or 40 µg/ml RNA in a 1 cm quartz cuvette will give an absorbance of 1 at 260 nm. The concentrations were calculated according to absorbance values and total volume of RNA solution. Protein or phenol contamination during the extraction procedure was assessed by A_{260}/A_{280} ratio with a value of 1.7 or greater as an indication of a good purity.

The quality of RNA samples and genomic DNA contamination were assessed by agarose gel electrophoresis. Aliquots of RNA samples (minimum 0.5 µg) were mixed with RNasin (4 U/sample) and 10x gel loading buffer and were loaded on 0.8% (w/v) agarose gels prepared in 1x TAE buffer and containing ethidium bromide to a final concentration of 0.3 µg/ml for visualization of nucleic acids. Gels were observed by illumination with UV light and photographs were taken using an Eagle Eye photocamera system (Stratagene).

10x gel loading buffer: 0.25% bromophenolblue, 0.25% xylene cyanol FF, 15% Ficoll in water; kept at RT, final 1x concentration.
1x TAE buffer: 0.04 M Tris-acetate, 0.01 M EDTA

2.2.1.4 First Strand cDNA Synthesis of Total RNA Samples

First strand complementary DNA (cDNA) was synthesized from total RNA by using Superscript^{TM} II RNase H^- reverse transcriptase (Invitrogen) as described by the manufacturer. One ng-5 µg total RNA was added in an Eppendorf tube together with 1 µl oligo $(dT)_{12-18}$ (500 µg/ml) (New England Biolabs) and 1 µl 10 mM dNTP mix (Peq Lab) (10 mM each dATP, dGTP, dCTP, dTTP at neutral pH). The volume was completed to 12 µl with sterile ddH_2O. The reaction mixture was heated to 65^oC for 5 min and quickly chilled on ice. Following brief centrifugation, 4 µl 5x first-strand buffer, 2 µl 0.1 M DTT (dithiothreitol) (Invitrogen) and 1 µl RNaseOUT recombinant ribonuclease inhibitor (Promega) (40 U/µl) were added and the samples were incubated at 42^oC for 2 min. Then, 1 µl (200 U) of Superscript II was added, mixed by pipetting up and down and samples were incubated at 42^oC for 50 min. Following heat inactivation at 70^oC for 15 min, cDNA

samples were ready for amplification by PCR. The samples were diluted 5 fold (final volume 100 µl) with sterile ddH_2O before they were used as template for amplification.

2.2.1.5 Semiquantitative Reverse-Transcriptase Polymerase Chain Reaction

The reaction mix was prepared by mixing the following per reaction:

5.7 µl ddH_2O
3 µl glycerol (Calbiochem, molecular biology grade)
2 µl 10x PCR buffer (-Mg) (Invitrogen)
0.6 µl $MgCl_2$ (50 mM, Invitrogen)
1.5 µl dNTPs (2.5 mM each) (Peq Lab)
0.1 µl [α-^{32}P] dCTP (3000 Ci/mmol; 10 µCi/µl, Amersham)
1 µl sense primer (250 ng/µl for 25mer)
1 µl antisense primer (250 ng/µl for 25mer)
0.1 µl Taq polymerase (0.5 U, Invitrogen)

The above mix was distributed as 15 µl/reaction into PCR tubes and 5 µl cDNA (from 100 µl final diluted volume) was added and mixed. Optimal PCR conditions (annealing temperature (Ta), number of cycles) were established for each primer pair (see **Table 2.1**). PCR was performed with MJ Research PTC 225 thermal cycler using the following programme:

94°C 2 min
94°C 45 sec
Determined Ta 45 sec
72°C 45 sec for a total of optimised cycle number
8°C soak

For determination of the appropriate cycle number, cDNA samples (for most of the primer pairs as a positive sample, cDNA synthesized from total mouse spleen RNA was used) were either left undiluted or diluted 3 and 9 fold, respectively and reactions were amplified with different cycle numbers with increments of 3 cycles. The radiolabeled PCR products were separated by 6% polyacrylamide gels. Following electrophoresis (200-250 Volts 2-3, h), gels were dried at 80°C for 30 minutes using gel drier (Bio-Rad) and exposed using phosphoimager imaging plate (Fuji film FLA-3000). Quantifications were done using Aida software and the linear range was determined. For subsequent analyses with a particular primer pair, the determined cycle number was used and quantifications were always done as described above.

Table 2.1: Optimized Conditions For RT-PCR

Gene	Ta (^oC)	Product (bp)	Cycle number
BLC	55	246	22
ELC	60	249	21
SLC	56	347	25
CXCR5	60	510	27
CCR7	58	395	25
TNF	60	276	25
LTα	57	609	26
LTβ	60	701	24
LIGHT	56	462	23
IL-7	55	486	30
IL-7Rα	53	457	27
LTβR	60	228	25
TNFRI	56	391	25
VCAM-1	55	489	25
ICAM-1	60	428	25
MAdCAM-1	60	305	22
Actin	60	722	17
RelA	60	368	25
RelB	55	279	30
NFκB1	55	423	28
NFκB2	55	193	25
c-Rel	60	263	25

6% polyacrylamide gels: 35 ml ddH_2O, 10 ml acrylamide: bisacrylamide (30 %) (Rotiphorese), 5 ml 5x TBE, 300 µl 10% (w/v) APS, 40 µl TEMED for a final volume of 50 µl.
5x TBE: 54 g Tris base, 27.5 g boric acid, 20 ml 0.5 M EDTA (pH 8.0)

2.2.1.6 Analysis of RNA by Northern Blotting

Preparation of Radiolabeled Probes

Mouse spleen cDNA samples were used as template for PCR amplification by GAPDH, BLC, ELC and SLC primer pairs for 35-40 cycles. RT-PCR products were run at 2% agarose gels and sliced out of the gel upon visualization of products by UV. The weight of the slice was determined as miligrams and gel extraction was performed using QIAquick gel extraction kit (QIAGEN) using a microcentrifuge following the protocol supplied by the manufacturer. DNA was eluted in 30 µl elution buffer. Purified products were further

subjected to agarose gel electrophoresis and concentrations were estimated by loading 100 base pair DNA ladder marker with known concentration.

Purified RT-PCR products were labeled by Rediprime^{TM} random prime labeling system (Amersham Pharmacia Biotech) according to manufacturer's recommendations. Probes were purified by Sephadex G-50 columns (see EMSA section for detailed description). One µl of this eluate was measured using scintillation counter 1211 Minibeta (Wallac). A probe solution of 400-500 µl with 40000 cpm/µl count was used for hybridisation.

Electrophoresis of RNA Through Gels Containing Formaldehyde

Agarose gel, 1.2%, was prepared by dissolving the corresponding amount of agarose in water and the solution was cooled to 60^{o}C in a water bath. Appropriate volumes of 5x MOPS buffer (final 1x) and formaldehyde (final concentration 0.5 M) were added under a fume hood. Samples were prepared as follows:

RNA (10 µg-30 µg)	up to 15 µl
5x MOPS buffer	6 µl
Formaldehyde	3 µl
Formamide	30 µl
10x gel loading buffer	6 µl
Final volume	**60 µl**

Samples were incubated at 55^{o}C for 15 min, chilled on ice and centrifuged briefly. Before loading, 1x MOPS gel running buffer was equilibrated at 4^{o}C and the gel was pre run at 130 V for 20 min. Samples were loaded and electrophoresis was performed in the cold room at 130 V (5 V/cm) for 1 h and then the voltage was increased to 160 V for additional 4 h till bromophenol blue migrated 7-8 cm. As a reference, one sample with ethidium bromide was run and visualized by UV after the run was complete.

5x MOPS buffer: 0.1 M MOPS pH: 7.0, 40 mM sodium acetate and 5 mM EDTA pH 8.0
10x gel loading buffer: 1 mM EDTA pH 8.0, 0.25% (w/v) bromophenol blue, 0.25% (w/v) xylene cyanol, 50 % (v/v) glycerol; stable at RT for 3 months.

Transfer of RNA from Gel to Membrane

The gel was washed with DEPC-treated water on a shaker twice for 20 min each to remove formaldehyde, followed by a final wash with 20x SSPE for 20 min. The transfer set up was prepared by placing the gel upside down on a layer of 3MM Whatman paper (Bender und Hobein) prewet with transfer buffer and the membrane (Hybond-N+, Amersham) on the gel. Three sheets of prewet Whatman paper cut in the size of membrane, paper towels, glass support plate and weight were placed on top and the transfer was performed overnight (O/N). Membrane wrapped in saran wrap was placed in a UV-crosslinker (Stratagene) RNA side-up and RNA was immobilized using auto-crosslink programme. The efficiency of transfer was checked by staining the gel with ethidium bromide (0.5 µg/ml) in 20X SSPE for 10 min at RT followed by destaining with ddH_2O for 10 min and photography. In addition, the membrane was stained in 0.03% (w/v) methylene blue in 0.3 M sodium acetate, pH: 5.2, for 2 min and was destained in water for 3 times, 5 min per wash.

20x SSPE: Transfer buffer, 175.3 g NaCl, 27.6 g NaH_2PO_4, 7.4 g EDTA dissolved in 800 ml water and pH adjusted to 7.4 with NaOH.

Hybridization and Analysis

The membrane was placed RNA-side up in a hybridization tube and was prehybridized in 20 ml of hybridization buffer at 68^{o}C with rotation for 3-4 h in a hybridization oven / shaker (Amersham). The probe (purified and labeled RT-PCR product, see above) was denatured at 95^{o}C for 5 min, snap cooled on ice and appropriate amount was pipetted into the hybridization tube for 20-24 h at 65-68^{o}C. The membrane was washed 3 times, each for 10 min, under low stringency conditions at RT in hybridization oven. This was followed by 2 times each for 30 min, high stringency washes at 65^{o}C. Finally, the membrane was air dried for 1 min on a Whatman paper and autoradiography was performed with MP films (Amersham). Quantifications were performed with a Fuji film FLA-3000 fluorescent image analyzer.

Hybridization buffer: 0.5M Na_2HPO_4 pH 7.2, 7% SDS, 1 mM EDTA, 1% BSA
Low stringency wash buffer: 2x SSPE / 0.1% SDS
High stringency wash buffer: 0.2x SSPE / 0.1% SDS

2.2.2 EXTRACTION AND ANALYSIS OF PROTEINS

2.2.2.1 Whole Cell Extract (WCE) Preparation

Cells were trypsinized and pelleted by centrifugation (2000 rpm 5 min 4^{o}C) and the pellet was washed once with phosphate buffered saline (PBS). The volume of the pellet was estimated, supernatant was quickly removed and the pellet was resuspended on ice with 5-fold volume of ice cold suspension buffer. Then an equal volume (5-fold of pellet volume) of 2x SDS gel loading buffer was added as soon as possible without pipetting up and down. The concentration of loading buffer becomes 1x in the final volume. The sample was incubated at 95^{o}C for 10 min and then kept on ice. The chromosomal DNA was either sheared by sonication (full power between 30 sec and 2 min, Branson sonifier) or by repeated passages through 23 Gauge needle and 1 ml syringe. Following centrifugation at 10000 rpm for 10 min at RT, the supernatant was transferred to a new tube and kept at -80^{o}C for further use. An equal volume of samples (20-40 µl) was then loaded for SDS-PAGE analysis.

Proteinase inhibitors: One tablet in 2 ml ddH_2O gives 25x stock (Roche).
Suspension buffer: 0.01 M Tris.Cl pH 7.6, 0.1 M NaCl, 0.001 M EDTA pH 8.0, stored at RT without proteinase inhibitors and just before use inhibitor solution was added to a final concentration of 1x.
2x SDS gel loading buffer: 100 mM Tris-Cl pH 6.8, 200 mM DTT (5x dilution from 1M stock), 4% SDS (sodium dodecyl sulphate, electrophoresis grade), 0.2% bromophenol blue and 20% glycerol; this buffer is stored at RT without DTT.

2.2.2.2 Preparation of Nuclear / Cytoplasmic Fractions

Cells were trypsinized and pelleted in an Eppendorf tube. Supernatant was removed and cells were gently resuspended in 400 µl buffer A. The sample was incubated on ice for 15 min and then 25 µl 10% NP-40 was added, vortexed vigorously for 10 seconds and centrifuged at 13000 rpm for 1 min at 4^{o}C. At this step, the supernatant contains cytoplasmic RNA and proteins and pellet contains nuclei and cell debri. An aliquot of supernatant, 200-300 µl, was transferred to a new tube as **cytoplasmic** fraction. The nuclear pellet was washed once with 200 µl buffer A gently, buffer was removed and 60 µl of buffer C was added <u>without</u> resuspending. The sample was then placed on an Eppendorf shaker for 15 min at 4^{o}C to ensure vigorous mixing such that the pellet remains intact and floats around. Following centrifugation at 13000 rpm for 5 min at 4^{o}C, 50 µl of **nuclear**

fraction was recovered and protein concentration was determined. Cytoplasmic and nuclear fractions were stored at -80°C. In order to use these fractions for SDS-PAGE, appropriate amounts of protein extracts (minimum 10 µg) were taken and the volume of the samples to be analysed was brought to the same final volume by adding complete buffer C. The same final volume of 2x SDS loading buffer was then added (final 1x), samples were incubated at 95°C for 5 min and left to cool to RT before loading.

Buffer A: 10 mM HEPES pH 7.9, 10 mM KCl, 0.1 mM EDTA, 0.1 mM EGTA, 1x proteinase inhibitors and 2.5 mM DTT
Buffer C: 20 mM HEPES pH 7.9, 0.4 M NaCl, 1 mM EDTA, 25% glycerol, 1x proteinase inhibitors and 2.5 mM DTT
Both buffers were stored at 4°C without proteinase inhibitors and DTT.

2.2.2.3 Protein Concentration Determination

Protein concentration was determined by BioRad microassay procedure following the manufacturer's instructions. Bovine IgG was used as a protein standard. Several dilutions of standard were prepared (1-25 µg/ml). In dry cuvettes, 800 µl diluted standards or appropriate amount of samples (2-3 µl cytoplasmic or nuclear extract) diluted in 800 µl ddH_2O were placed. 200 µl Dye Reagent Concentrate (5x stock, BioRad) was added and gently mixed. For blanks, 800 µl ddH_2O was used. After 5 min RT incubation, OD_{595} measurement was performed and a standard curve (concentration in µg/ml versus OD_{595}) was plotted to determine the concentrations of extracted samples.

2.2.2.4 SDS-PAGE

SDS polyacrylamide gel electrophoresis (SDS-PAGE) was performed as described by Sambrook & Russel, 2001. Resolving (8%) and stacking (5%) gels were prepared as below:

	8% resolving gel		***5% stacking gel***
	9.7 ml	**ddH_2O**	6.8 ml
	8 ml	**acryl.: bisacryl. (30%)**	1.7 ml
(pH 8.8)	11.7 ml	**1 M Tris HCl (pH 6.8)**	1.3 ml
	300 µl	**10% SDS**	100 µl
	300 µl	**10% APS**	100 µl
	24 µl	**TEMED**	10 µl
	30 ml	***Final volume***	***10 ml***

Resolving gel solution was prepared and poured between 2 glass plates using the Joey casting system (Peq Lab). The glass plates were marked to provide approximately 9 cm resolving and 2 cm stacking gel. A straight boundry between resolving and stacking gels was prepared by pouring 70% ethanol. After polymerization was complete, ethanol was poured off, the surface was washed with ddH_2O and dried with Whatman paper. Then 5% stacking gel solution was poured on top and an appropriate comb was inserted. Following polymerization, comb was removed and the system was casted to P9DS apparatus (Peq Lab). Tris-glycine buffer (1x) was used as the running buffer and the gel was run until the bromophenol blue in the SDS gel loading buffer migrated out.

1x Tris-Glycine buffer: 25 mM Tris, 250 mM glycine, 0.1% SDS

2.2.2.5 Western Blotting

Transfer of Proteins from Gel to Membrane

The transfer was performed by Trans/Blot Cell transfer system (Bio-Rad). For each gel, 4 sheets of Whatman papers and one membrane were precut as the dimensions of the gel. PVDF membrane (Immobilon^{TM}-P, Millipore) was activated for 15 seconds in methanol, washed in ddH_2O for 2 min and then placed in transfer buffer for 5 min. Meanwhile the gel was removed and different bands of the loaded prestained Benchtop protein marker (Invitrogen) was recorded by placing a transparent file on the gel and marking the bands. This record was later to be used to mark the corresponding molecular weights on the autoradiogram. The gel was placed on 2 sheets of prewet Whatman papers. The membrane was placed on top of the gel, the start was cut on the edge for orientation and air bubbles were prevented by rolling over a glass pipette gently. The sandwich was completed by placing 2 extra sheets of Whatman papers and was assembled into the transfer chamber filled with transfer buffer, which was freshly prepared for each transfer. All transfers were carried out at 20 V at RT for 7 h on a magnetic stirrer to ensure continuous mixing of the buffer.

Transfer buffer: 39 mM Glycine, 48 mM Tris base, 0.037% SDS (electrophoresis grade), 20% (v:v) methanol; pH 8.3

Immunoblotting

Following transfer, membrane was placed as protein side up into a container filled with blocking solution and was blocked either for at least 1 h at RT or O/N at 4°C. Once complete, the membrane was sealed in a nylon bag and primary antibody diluted in blocking solution was added. Following 1 h RT incubation, the membrane was rinsed rapidly twice and then washed 3 times, 10 min each, with TBS-T. The membrane then was incubated similarly with appropriate horseradish peroxidase (HRP) conjugated secondary antibody for 1 h at RT. For primary and secondary antibody dilutions, see Materials / Antibodies section. Following washes as described above, chemilluminescence detection was performed by ECL Western blotting detection system (Amersham) according to the manufacturer's instructions. The exposures were performed with Hyperfilm ECL (Amersham).

10x TBS: 250 mM Tris, 1.5 M NaCl, pH adjusted to 8.0 with HCl.
TBS-T: 1x TBS in ddH_2O, 0.1% (v:v) Tween-20.
Blocking solution: 5% (w:v) nonfat dried milk (Saliter) in TBS-T.

2.2.2.6 Immunoprecipitation (IP)

Following solutions are required:

Protein-A sepharose beads: Working solution is 50% (v:v) in complete RIPA buffer. Swell 1.5 g of vial (Pharmacia, CL-4B) in 50 ml 100 mM Tris-HCl pH 7.5 for at least 1h, O/N is preferred. It is stored at 4°C. 1.5 g swells to approximately 5 ml. Alternatively, part of the vial can also be used in an appropriate volume of buffer.
RIPA buffer (without SDS): 10 mM Tris-HCl (pH 7.4), 150 mM NaCl, 1% NP-40, 1% deoxycholate, stock is kept at 4°C and working buffer is reconstituted with 25x proteinase inhibitor tablets (final 1x) before use (complete RIPA).

Wash Buffers (stocks are kept at RT)

Buffer A	**Buffer B**	**Buffer C**
10 mM Tris-HCl (pH 7.5)	10 mM Tris-HCl (pH 7.5)	10 mM Tris-HCl
150 mM NaCl	500 mM NaCl	(pH 7.5)
0.2% NP-40	0.2% NP-40	
1 mM EDTA	2 mM EDTA	

Fibroblasts were washed once with RT PBS. Plates then were placed on ice and ice-cold complete RIPA buffer (1 ml per 100 mm plate surface) was added. Cells were scraped off the plate on ice using a rubber policeman and lysate was transferred to an appropriate sized

Eppendorf tube. After centrifugation at 10000 g for 10 min at 4^{o}C, supernatant (lysate) was transferred to a new tube. The pellet at this point can be processed for SDS-PAGE (see WCE preparation) to check the efficiency of lysis. If the antigen of interest can still be detected in the pellet, alternative lysis buffers should be tried to improve the efficiency of lysis. An aliquot of lysate (50-100 µl) was taken to serve as the control before IP. All the controls were processed for SDS-PAGE by addition of appropriate volume of 2x SDS buffer and boiling (see WCE preparation). Bradford can be performed for lysate and control aliquots for concentration determination. Lysis was followed by the preclearing step by adding the appropriate preimmune serum (1:100 dilution), depending on the host antibody to be used was made in, to the lysate of 500 µl volume. Following incubation on ice for 1 h, appropriate amount of beads was added. For each antibody used, amount of beads and dilution should be adjusted by titration experiments. Generally, 50-100 µl per 0.5-1 ml of lysate solution works fine. To prepare the beads before use, depending on the number of samples, appropriate volume of beads was taken from the swollen stock solution and was pelleted by centrifugation at 10300 rpm at 4^{o}C for 20 sec. Supernatant was removed and same volume of complete RIPA buffer was added so that 50% v:v was kept. From this solution, beads were then added to the lysate and an additional 30 min incubation was performed. For this purpose, the lid of the Eppendorf tube was covered by parafilm and incubation was done in the cold room by rotation. Once complete, the sample was centrifuged at 10000 g for 15 min at 4^{o}C and the precleared lysate was transferred to a new tube. At this step, taking an aliquot of supernatant may be useful to compare the profile of pulled down non-specific proteins after the addition of preimmune serum. Minimum of 100 µg of lysate was used (volume is adjusted to 500 µl by complete RIPA) and the rest can be stored at -20^{o}C for future use. The next step was the addition of immune serum to the precleared lysate. The dilution and incubation time should be determined for each antibody used. The recommendation is to start with 1:200 dilution in a lysate volume of 500 µl and 1 hr incubation on ice. The antibody incubation can also be O/N. An important control is to include only RIPA (no lysate) to trace the performance of antibody applied and beads. This was followed by addition of beads and incubation in cold room for at least an additional hour as described above. Meanwhile, wash buffers were placed on ice. Tertiary protein A-antigen-antibody complexes were collected by centrifugation at 10000 g for 20 sec at 4^{o}C.

Beads were washed twice with 1 ml buffer A, once with 1 ml buffer B, and once with 1 ml buffer C. For each wash, centrifugation was as above for 20 sec and supernatant was removed by 1 ml syringe and 27G needle not to lose beads. Buffer was just added on top of the bead pellet and not pipetted up and down. After the last wash, all the fluid was removed and beads were resuspended in 50 µl 2x SDS gel loading buffer, incubated at 85^{o}C for 10 min, spun and either loaded on a gel (20 µl is sufficient) directly or stored at -20^{o}C for further analysis. IP samples together with controls were subjected to SDS-PAGE (8% gels) and immunoblotting was performed with the same antibody to detect the efficiency of IP. For co-immunoprecipitation experiments, immunoblotting was performed with the second antibody raised against the potential partner of interest to analyze the interaction with the immunoprecipitated antigen.

2.2.2.7 Electromobility Shift Assay (EMSA)

Preparation of Probes

Following single stranded oligonucleotides were used:

Oct-1 up: 5'-GAT CCT GTC GAA TGC AAA TCA CTA GAA A-3'
Oct-1 lo: 5'-GAT CTT TCT AGT GAT TTG CAT TCG ACT C-3'

Igκ up: 5'-GAT CCA GAG GGG ACT TTC CCA CAG GA-3'
Igκ lo: 5'-GAT CTC CTC TGG GAA AGT CCC CTC TG-3'

Annealing of Oligonucleotides

Following reaction mix was prepared:

2 µl of each single stranded oligo (100 pmol/µl)
200 µl TE (pH 7.5)
2 µl NaCl (5 M)
(1 pmol/µl oligo concentration in the final volume of 206 µl)

The reaction was incubated at 80^{o}C for 15 min and left at RT O/N.

Radioactive Labeling of the Annealed Oligonucleotides

Following reaction mix was prepared:

10 µl ddH_2O
2 µl of annealed oligo (2 pmol total)
2 µl 10x REACT 2 buffer (Invitrogen)
2 µl dNTPs (0.5 mM each without dCTP)
3 µl α^{32}P-dCTP (3000 Ci/ mmol)
1µl Klenow fragment (6.5 U, Invitrogen) as a total volume of 20 µl and was incubated at RT for 20 min.

Purification of the Probe

10 µl of blue dextran solution (0.7% (w/v) in water) was added to the labeling mix. Sephadex G-50 (Sigma) in TE buffer was used to prepare 1 ml column in 1 ml syringe the bottom of which was plugged with glass wool. Labeling mix with blue dextran was added on the column and unincorporated radioactivity was left in the column by eluting 200-400 µl blue solution (DNA complexed with blue dextran) in TE. One µl of this eluate was measured using scintillation counter 1211 Minibeta (Wallac). A total of 20000-50000 cpm per reaction was used for bandshift assay.

Bandshift Assay

Following solutions are required:

5x Binding Buffer (BB): 50 mM Tris-HCl, 250 mM NaCl, 5mM EDTA, 25% glycerol; kept at RT and before use DTT is added to a final concentration of 25 mM.
Buffer C with 1x proteinase inhibitors and 2.5 mM DTT
Unspecific competitors: Sonicated calf thymus DNA (1 µg/µl) for Igκ bandshift or dI:dC homopolymer (1 µg/µl; Sigma) for Oct-1 bandshift assays.

Rabbit Anti-Rel/NF-κB Polyclonal Antisera for EMSA
KD 57 or rabbit serum (Sigma): preimmune serum (PI)
KD 57-8: anti-p50
KD 38-2: anti-p52
KD 13-3: anti-p65 (RelA)
KD 6-8 or RR 2-8: anti-RelB
sc (N-466X) (Santa Cruz)**:** anti-c-Rel

All working solutions and binding reactions should be prepared on ice, 5x BB and buffer C were prepared on ice before setting up the binding reactions. Below are the components of a binding reaction:

5 µl **nuclear extract solution** (2-4 µg extract, volume completed to 5 µl with buffer C)
4 µl **5x BB** (final 1x)
Competitor (0.4 µg (0.4 µl/reaction) calf thymus (1/10) or 2 µg (2 µl/reaction) dI:dC (1/2) for 4 µg nuclear extract)
1 µl **antiserum** (for antibody challenge reactions only)
Oligo (2-3 µl depending on the count, 20000-50000 cpm total)
ddH_2O to complete the volume to **20 µl**

Preferentially, premixes were prepared for each oligo shift by adding 5x BB, competitor and ddH_2O the total amounts of which were determined according to the total number of reactions. Then, the mix was distributed to precooled tubes, followed by addition of appropriate volumes of buffer C and protein extract for each sample. For antibody challenge reactions, 1 µl of appropriate antiserum (see above for antisera used) was added and the reactions were incubated on ice for 10 min. The radioactively labeled probe was then added and the reactions were kept at RT for 20 min. Once complete, 2 µl 10x gel loading buffer per reaction was added and the reaction mix was loaded onto 5% gel. While the binding reactions were incubated, the wells of the gel were washed and prerun was performed at 150 V for 10 min using 0.25x TBE as running buffer. A typical run is at 150 V for 2-3 h at RT. Then the gel was dried at 80^oC for 30 min and exposure was performed using Hyperfilm MP (Amersham).

5% polyacrylamide gels: 8.3 ml acrylamide:bisacrylamide (30%), 2.5 ml 5x TBE (final 0.25x), 39.2 ml ddH_2O, total volume 50 ml.

2.2.2.8 Wholemount Immunohistochemistry (anti-VCAM-1)

Following solutions are required:
2% PFA (pH 7.4): 4% paraformaldehyde was prepared and stored at -20^oC as stocks and was diluted to 2% with PBS before use. Freeze thaw is not recommended.
PBSMT: PBS containing 2% skim milk and 0.3% Triton X-100
PBST: PBS containing 0.3% Triton X-100
PBSMT and PBST were freshly prepared before each experiment.

Digestive tract was removed from either the embryo or from the newborn mouse and was placed in a vial of 2% PFA on ice for fixation. It can be kept at 4^oC O/N but long term storage at this step is not recommended. Dehydration was performed with a series of mixtures of methanol/water (25%, 50%, 75%, 90%, and twice 100% methanol) for 15 min per step and at this point samples can be stored at -20^oC in methanol. Then, the sample was

bleached with freshly prepared hydrogen peroxide (100 µl 30% solution in 10 ml methanol) at RT for 20 min. This was followed by rehydration steps with a series of methanol/water 90%, 75%, 50%, 25% and PBS for 15 min per step at RT. Once complete, the sample was transferred into PBSMT for 40-60 min on ice with gently mixing for blocking. PBSMT was replaced with PBSMT containing primary antibody (anti-VCAM-1, 1:500 dilution) and incubated at 4^{o}C O/N. Washes were performed at RT with PBSMT for 45-60 min with 5 changes before incubation with biotinylated secondary antibody in PBSMT (biotinylated anti-rat Ig, 1:100 dilution) for 1 h at RT. If the primary antibody is biotinylated, this step is omitted. Second round of washes were performed with PBST at RT for 30 min by changing 5 times. Meanwhile, Vector ABC peroxidase standard was prepared in PBS according to manufacturer's instructions (Vector Laboratories) and was incubated on ice for at least 30 min before use. After the final wash, PBST was replaced with ABC peroxidase standard and incubated at RT for 30-45 min. Following final washes with PBST for 30 min with 5 changes at RT, DAB-$NiCl_2$ solution (Vector Laboratories) prepared according to manufacturer's instructions was added for colour reaction to develop for 15-30 min. After rapid rinse with ddH_2O, the reaction was stopped by addition of methanol. Samples were then analysed and photographed. Samples can be kept in methanol at -20^{o}C for long term storage but photography is recommended right after the experiment.

2.2.2.9 Immunohistochemistry

Immunohistochemistry was performed as described (Weih *et al.*, 2001).

2.2.2.10 Enzyme Linked Immunoabsorbent Assay (ELISA) for Determination of Fecal IgA Concentration

Preparation of Fecal Samples

Two fresh pellets per adult mouse were collected in an Eppendorf tube on ice, which can be stored at -20^{o}C till processing. Weight of feces was determined by weighing on a fine balance (100 mg was estimated as 100 µl volume). Pellets were resuspended in 4 times the estimated volume with PBS and mixed on a shaker at RT for 30 min to obtain a homogeneous suspension. Following centrifugation at 13000 rpm for 10 min at RT and the transfer of supernatant to a new tube twice, the final supernatant was stored at -20^{o}C.

ELISA

Ninetysix-well flat bottom plate (Immulon 2, Dynatech Lab.) was coated with **capture antibody** (anti-mouse IgA pure, C 10-3 Pharmingen) by adding 100 µl per well (diluted to 2.5 µg/ml in PBS). The plate was covered with plastic wrap and incubated in a humidified atmosphere O/N at 4^{o}C. Wells were emptied and washed with 200 µl/well PBS-T 4 times at RT. Blocking was performed by filling the wells with 200 µl PBS/10% FCS and incubated for at least 1 h at RT followed by 4 washes with PBST. IgA standard samples (SBA, Southern Biotechnology Associates, Inc.) were prepared by diluting in PBS/1% BSA in 2-fold serial dilutions (lowest concentration 0.781 ng/ml and highest concentration 400 ng/ml). Two wells of the plate were filled with 100 µl PBS/1% BSA as background and 100 µl of standard samples were added to the rest of 10 wells of the row in increasing concentration. Serum or fecal samples were also diluted in PBS/1% BSA. Two-fold serial dilutions can also be applied to determine the appropriate dilution for the samples. For fecal samples 1:200 or 1:400 dilutions can be recommended. Hundred µl of appropriately diluted samples were added per well, the plate was covered and incubated in a humidified atmosphere for 2 h at RT. Following 4 standard washes with PBS-T, 100 µl of **detection antibody** diluted in PBS (1:200) (anti-mouse IgA botinylated, C-10.1 Pharmingen) was added and an additional 1 h incubation at RT was performed. Following washes, 100 µl streptavidin-HRP (DAKO, 1:2000 dilution in PBS/1% BSA) antibody was added per well and incubated 1 h at RT with gentle shaking. Wells were emptied and washed 5 times with PBS-T. Meanwhile, ABTS substrate (Boehringer Mannheim GmbH) was prepared by dissolving 1 tablet (5 mg) per 5 ml of 1x ABTS buffer (diluted with ddH_2O from commercially available 10x stock). For a complete 96 well plate, 2 tablets in 10 ml of buffer would be required. Color reaction was performed by adding 100 µl per well ABTS solution and incubation at RT for 5-20 min. Color reaction was stopped by addition of 50 µl quench solution and readings were taken within 30 min at 405 nm using BioRad Microplate Reader 3550. Data analysis was performed by MPM III Microplate manager Software.

PBS-T: PBS, 0.05% Tween-20
Quench solution: 1% SDS

2.2.3 CELL CULTURE METHODS

2.2.3.1 Routine Culture of Cells and Storage

Media and Maintenance

All cells were maintained at 37°C in an incubator C200 (Labotect GmbH) in 5% CO_2 and 95% humidity. Cells were grown on appropriate sized petri plates (Greiner Labortechnik). Below are the complete media used for different cell types:

NIH 3T3: DMEM, 10% Calf serum (aseptically collected donor calf serum, Invitrogen), Penicillin (100 U/ml) / Streptomycin (100 µg/ml), Glutamax I (1x, 2 mM) (L-Alanyl-L-Glutamine) (the usage of fetal calf serum is not recommended)

Primary or established fibroblasts: DMEM, 10% fetal calf serum (Bio Whittaker), Penicillin (100 U/ml) / Streptomycin (100 µg/ml), Glutamax I (1x, 2 mM)

Starvation Medium: DMEM, **0.5%** fetal calf serum (Bio Whittaker) or 0.5% **CS** for NIH 3T3 cells, Penicillin (100 U/ml) / Streptomycin (100 µg/ml), Glutamax I (1x, 2 mM)

Transfection Medium: DMEM, 10% FCS and Glutamax I (1x, 2 mM) without Pen/Strep

Fetal/Newborn Mouse Intestine, Mesentery and Fetal Liver Cells: RPMI 1640, 10% fetal calf serum, Penicillin (100 U/ml) / Streptomycin (100 µg/ml), Glutamax I (1x, 2 mM)

Heat inactivated (at 56°C for 30 min) serum was aliquoted to 50 ml, Pen /Strep and Glutamax I (100x, 200 mM) stocks were aliquoted to 5 ml respectively and stored at -20°C. For routine complete medium preparation, one aliquot of each were used per 500 ml of plain DMEM or RPMI 1640 medium. All the media and trypsin were stored at 4°C and prewarmed to 37°C in a water bath prior to use.

For routine culture of fibroblasts, 15 cm petri plates were preferred. NIH 3T3 cells and fibroblasts were allowed to grow to 80-90% confluency for 3 days and then were splitted by trypsinization. For this procedure, 0.25% trypsin/0.5 mM EDTA solution was used. After the removal of medium, cells were washed once with PBS (-Ca/Mg, Invitrogen) and trypsin was added just enough volume to cover the cells. After incubation at 37°C for 5 min, trypsin was diluted by the addition of complete medium and cells were transferred to

appropriate falcon tubes to be pelleted by centrifugation at 1500 rpm for 5 min at RT. The pellet was then reconstituted with fresh complete medium and re-plated at desired density.

Long Term Storage

Growing cells were trypsinized, pelleted and resuspended in complete medium at a density of 2-3 million cells/ml. In a cryovial, 1 ml cell suspension, 100 µl serum (10%) and 120 µl DMSO (10%) (Fluka Chemie) were mixed. Vials were placed in a cell freezing box (Nalgene^{TM}) and left at -80^{o}C O/N for gradual freezing. Frozen cell vials then were transferred to liquid nitrogen for long term storage. Repropagation was performed by placing the vial briefly at 37^{o}C and gradually thawing the cells by the addition of complete medium. The suspension was transferred to a Falcon tube, pelleted for the removal of DMSO and was resuspended in 10 ml complete medium to be plated in 10-cm tissue culture plates.

2.2.3.2 Preparation of Mouse Embryonic Fibroblasts (MEFs)

All the primary MEFs were prepared at E15.5 or E16.5, which was determined according to the plug date of the female mouse. Head and internal organs of the embryos were removed on a petri plate. Equipment used was cleaned with PBS and 70% ethanol between processing of each embryo. The trunk of the embryo was kept in a multi well plate on ice in 1 ml PBS. If genotyping was necessary, a piece of the tail was cut and placed in an eppendorf with 200-300 µl PBND buffer. Tails were digested for at least 1 h at 55^{o}C on an Eppendorf shaker block, proteinase K was inactivated at 95^{o}C for 15 min and samples were centrifuged at full speed at RT for 5 min. For PCR genotyping 2-3 µl of supernatant was used. Following PCR, the products were analyzed by agarose gel electrophoresis (2% w/v gel) and genotypes were determined. Embryos with same genotype were pooled for processing. Embryos (one per plate) were dissected in 10 ml 0.05% trypsin (diluted from 0.25% stock with plain DMEM medium) in 10-cm dish with fine scissors. After incubation at 37^{o}C for 10 min, the solution was pipetted up and down 5 times with 20 ml glass pipette. This was repeated with 10 ml and 5 ml glass pipettes with 10 min incubations at 37^{o}C in between. Once complete, trypsinization was terminated by adding 2 ml FCS. Cell suspension and clumps were transferred into a 15-ml Falcon tube and incubated on ice to

sediment the clumps for 5-10 min. Approximately 10 ml of the supernatant was transferred into a 50-ml Falcon through 100 μm cell strainer (Falcon) leaving clumps behind. After centrifugation at 2000 rpm for 5 min at RT, the pellet was washed once with 10 ml complete medium, the suspension was transferred to a new falcon tube through the cell strainer and cells were counted using Trypan blue (Sigma) (10 μl cell suspension + 10 μl Trypan blue solution, cell number per ml was determined after counting at least 2 big squares on the hemocytometer using the following formulae: number of cells counted / number of squares x 2 (dilution factor) x 10^4). Typical yield per an embryo is 8-10 (10^6) cells. Finally, the pellet was resuspended according to the count and plated up to 10 (10^6) cells per 15 cm plate. The next day, fibroblasts adhere and non attached cells were removed by removing the medium and adding fresh medium. In 2 or 3 days, the desired confluency was reached for splitting. Primary cells prepared as described above were expanded and frozen down at 1st split for future use.

PBND buffer: PCR buffer with nonionic detergents; 50 mM KCl, 10 mM Tris-HCl pH 8.3, 2.5 mM $MgCl_2$, 0.1 mg/ml gelatin, 0.45% v/v NP-40, 0.45% v/v Tween-20, 0.1 μg/ml Proteinase K (3 μl from 10 mg/ml stock); this buffer was kept at 4°C without Proteinase K which was added before use.

2.2.3.3 Serum Starvation, Stimulation and Harvest of MEFs

Fibroblasts in this study were starved in 0.5% FCS (or CS for NIH 3T3 cells) containing DMEM medium for 24 h after reaching 80% confluency. Following stimulations were performed:

Recombinant Murine TNF: 20 ng/ml (Promokine)

Recombinant Human TNF: 20 ng/ml (Promokine)
Agonistic anti-LTβR antibody (AC.H6, pure Armenian hamster monoclonal antibody): 1 μg/ml (Biogen)
Ha 4/8 (anti-KLH Armenian hamster Ig): 1 μg/ml (Biogen); isotype matched control for AC.H6

These reagents were added into the starvation medium for appropriate time points. Cells were harvested by routine trypsinization (see media and maintenance section) using starvation medium during the procedure. Pellets were processed either for WCE, nuclear and cytoplasmic extracts and/or RNA preparation depending on the experiment.

2.2.3.4 Preparation of Single Cell Suspensions From Fetal/Newborn Intestine and Mesentery

Embryonic intestine and mesentery samples were collected at E14.5, E16.5 and E18.5 time points. Intestine was removed and opened on a Petri dish. All fat and mesentery (except E14.5 as tissue was very small for dissecting mesentery out) was removed and mesentery was collected in an Eppendorf tube with 50-100 µl PBS/2% FCS on ice. After collecting all the samples, mesentery was transferred into 50-ml Falcon tube with a magnetic stirrer and 2 ml collagenase type IV-S solution. Intestine samples were chopped into small longitudinal pieces and similar to mesentery, samples were placed into 50-ml Falcon tubes with collagenase solution and stirrer. Mesentery samples were digested for 20 min and intestine samples for 1 h at 37^{o}C (warm room) with gentle stirring. For digestion, 2 ml enzyme solution is optimal per intestine and up to 8-9 pooled mesentery samples. Once complete, couple of strokes with a 21G needle and 2 ml syringe was applied for intestine samples to dissociate cells, which are then filtered through 40 µm nylon mesh to a 15-Falcon to remove large clumps. Cells were washed with 5 ml PBS/2%FCS once for mesentery and with PBS/5% FCS twice for intestine samples, filtered through mesh and centrifuged at 1500 rpm for 5 min at 4^{o}C. Pellet was resuspended in appropriate volume of PBS/FCS and cells were counted (see above). Typical yield per mesentery was 1x10^{5}-1.5x10^{5} cells and per intestine was approximately 1x10^{6} cells. Depending on the experiment, E14.5 cells and aliquots of E16.5 and E18.5 cells were used for direct RNA extraction, and E16.5 and E18.5 cells were cultured for 24 hrs.

Collagenase type IV-S solution: Working solution is 0.5 mg/ml in PBS/2% FCS and is prepared in 2 ml Eppendorf tubes and stored at -20^{o}C as stocks, before use were thawn at 37^{o}C (Sigma).

Stimulation:

IL-7 (interleukin 7): 10 ng/ml (Pepro Tech Inc.)
SCF (stem cell factor): 100 ng/ml (from 1 µg/µl stock in 5 mM NaP buffer, pH 6.8) (Pepro Tech Inc.)

Stimulation was performed in the presence of SCF and with or without IL-7 for both mesentery and intestine cultures. After 24 h, cells were harvested by collecting the suspension cells and trypsinizing the adherent cells (0.25% trypsin) in order to pool. Cells

were pelleted by centrifugation (1500 rpm 5 min at 4°C) and pellets were processed for RNA extraction for analysis of LT-α and LT-β expression by RT-PCR.

2.2.3.5 Transient Transfection of Primary and Established Fibroblasts

Primary fibroblasts were transfected with LipofectAMINE™ 2000 reagent (LF 2000, Invitrogen) and established IKK wild-type fibroblasts were transfected with LipofectAMINE™ PLUS reagent (LF PLUS, Invitrogen) following instructions of the manufacturer. For LF 2000 method, cells were plated the day before transfection in complete medium so that they would be 90-95% confluent on the day of transfection. For 10-cm plate format, following shows the optimized conditions:

Cells plated:	$1x10^6$
DNA:	4 µg
LF 2000:	40 µl

For established fibroblasts, cells were plated the day before transfection so that they would be 50-90% confluent on the day of transfection. Following shows the optimized conditions for 6 well plate format:

Cells plated:	$3x10^5$ / well
DNA:	2 µg
LF:	12 µl
PLUS:	18 µl
Transfection volume:	1 ml

DNA was precomplexed with PLUS reagent by diluting DNA first in plain DMEM and then adding PLUS reagent and mixing in a total volume of 100 µl in an Eppendorf tube. The mix was incubated for 15 min at RT and meanwhile LF was diluted in plain DMEM in a total volume of 100 µl. Then, LF was added to DNA-PLUS mix, pipetted up and down and incubated for 15 min at RT. During this incubation, complete medium on cells was removed and cells were washed once with transfection medium. Following addition of 0.8 ml transfection medium per well, 200 µl of transfection mix was slowly added on top of the cells and incubated at 37°C for 3 h. Once complete, complete medium (with Pen/Strep) was added to bring the total volume to 3 ml and assays were performed within the next 48 h after the start of transfection.

2.2.3.6 Beta-Galactosidase Assay

Solutions:

1x PBL (passive lysis buffer): 5x stock kept at -20°C diluted in ddH_2O to give 1x working solution. 250 µl per well in 12-well plate (Promega).
Buffer B/Z: 60 mM Na_2HPO_4, 40 mM NaH_2PO_4, 10 mM KCl, 1 mM $MgCl_2$ and 50 mM β-mercaptoethanol (3.5 µl stock per cuvette, added just before use), kept at RT.
ONPG substrate: 2 mg/ml solution in Buffer B/Z, kept at 4°C.

Following transfection of cells with HS-LacZ construct, within next 48 h cells were harvested by washing twice with PBS -Ca/Mg and lysis in 1x PBL. Lysates were transferred to Eppendorf tubes, cenrifuged at RT for 5 min and supernatants were used for the assay, lysates at this step can also be kept at -20°C for further use. In a plastic cuvette, 50 µl of lysate was combined with 1 ml Buffer B/Z (β-mercaptoethanol added) and 200 µl of ONPG substrate. A blank was prepared by adding ddH_2O instead of lysate. Reactions were incubated at 37°C until yellow color develops and reaction was stopped by adding 500 µl 1M Na_2CO_3 per cuvette. Absorbance at 420 nm was measured (range is 0.05-0.9) and readings were used for normalization.

2.2.4 RECONSTITUTION EXPERIMENTS

Mice were mated in such a way that on the day RelB-deficient and control recipients were born, E14.5 embryos would be available from wild-type matings as donors. Uninjected age matched mice were used as controls. Newborn recipients were sub lethally irradiated and fetal liver cells were injected intrahepatically. Genotypes of recipients were analyzed before the injection and also peripheral blood leukocytes (PBLs) were prepared at necropsy to determine status of chimerism.

2.2.4.1 Preparation of Single Cell Suspensions From Fetal Livers

Fetuses were removed and livers were collected in 12-well plates in PBS on ice. PBS was removed and 5 ml plain PRMI medium was added. Single cell suspensions were prepared by using a 10 ml syringe and and a 23 Gauge needle by couple of strokes. This procedure was repeated with 24 Gauge, 25 Gauge and 27 Gauge needles. Cells were transferred to 15

ml tubes through nylon mesh. Following centrifugation at 1000 rpm at 4°C for 10 min, pellet was resuspended in plain RPMI medium and cells were counted.

2.2.4.2 Irradiation of Newborn Animals and Injection

Following birth, animals were clipped and then irradiated sub lethally using 500 RAD. After couple of hours of rest, meanwhile fetal liver cells were prepared, 5x 10^6 cells per pup were injected in a total volume of 10 µl intrahepatically. All injections were performed by Debra S. Weih. Animals were analysed at 2 week and 4 week time points.

2.2.4.3 *relB* Genotyping by PCR

In order to determine genotypes before injection, tail DNA was prepared by digesting the tails in 300 µl PBND buffer containing 30 µg of proteinase K at 55°C for couple of hours or O/N on Eppendorf shaking block. Samples were heated to 95°C for proteinase K inactivation and centrifuged 13000 rpm for 5 min to pellet insoluble material. For PCR reaction 2-3 µl of supernatant was used.

For chimerism analysis following injection of wild-type cells, PBL was prepared. Blood was taken via cardiac puncture into 1 ml-syringe at necropsy and was transferred into 15-ml Falcon tube with 10 ml PBSE. After centrifugation at 2000 rpm at 4°C for 5 min, pellet was vortexed and resuspended in 5 ml ACK lysis buffer for erythrocyte lysing. Following centrifugation ACK lysis step was repeated only if the pellet was still red. After washing the pellet once with 1 ml PBS and centrifugation, 200-300 µl PBND buffer including 20-30 µg proteinase K was added. Digestion and heat inactivation were performed as described for tail DNA, 2-3 µl was used for PCR reaction.

PBSE: PBS, 5 mM EDTA
Proteinase K: 10 mg/ml in 50% glycerol, stored at -20°C
ACK lysis buffer: 8.92 g NH_4Cl, 1 g $KHCO_3$, 0.32 g Na_2EDTA completed to 1 L with ddH_2O.

Primer sequences used for *relB* genotyping are as follows:

30-RelB-54	5'-CATCGACGAATACATTAAGGAGAAC-3'
412-RelB-393	5'-AAGCCCAGCAATCCTATTCC-3'
HH Neo	5'-AAATGTGTCAGTTTCATAGCCTGAAGAACG-3'

Following reaction mix was prepared per genotyping reaction:

8.1 µl ddH_2O
3 µl glycerol (Calbiochem, molecular biology grade)
2 µl 10x PCR buffer (-Mg) (Invitrogen)
0.6 µl $MgCl_2$ (50 mM, Invitrogen)
1.6 µl dNTPs (2.5 mM each) (Peq Lab)
1 µl **RelB-54 primer** (250 ng/µl for 25mer)
0.5 µl **412-RelB primer** (250 ng/µl for 25mer)
0.17 µl **HHNeo primer** (250 ng/µl for 25mer)
0.1 µl Taq polymerase (0.5 U, Invitrogen)

The above mix was distributed as 17 µl/reaction into PCR tubes and 3 µl tail or PBL DNA was added and mixed. PCR was performed with MJ Research PTC 225 thermal cycler using the following programme:

94^oC 2 min
94^oC 1 min
55^oC 1 min
72^oC 1 min for 33 cycles
8^oC soak

3 RESULTS

PART ONE

3.1 ROLE OF RelB FOR SPLEEN MICROARCHITECTURE

The observations that spleen is histologically normal at birth (P0) in *relB*$^{-/-}$ animals and that the splenic defects could not be rescued in adult animals by BM transplantation experiments (see **Table 1.1**) prompted us to reconstitute *relB*$^{-/-}$ mice at the day of birth (P0).

3.1.1 Reconstitution Experiments with Newborn Animals

Total fetal liver (FL) cells from E14.5 wild-type embryos were injected intrahepatically into sublethally irradiated *relB*$^{-/-}$ recipients at P0. Heterozygote littermates and age matched mice were used as injected and uninjected controls, respectively. The animals were sacrificed at two and four week time points for analysis. The litters were genotyped by using tail DNA. At necropsy, peripheral blood was collected via cardiac puncture and DNA extracted from leukocytes was used for *relB* genotyping by PCR (**Fig. 3.1**). Complete chimeric animals were included in the analysis group.

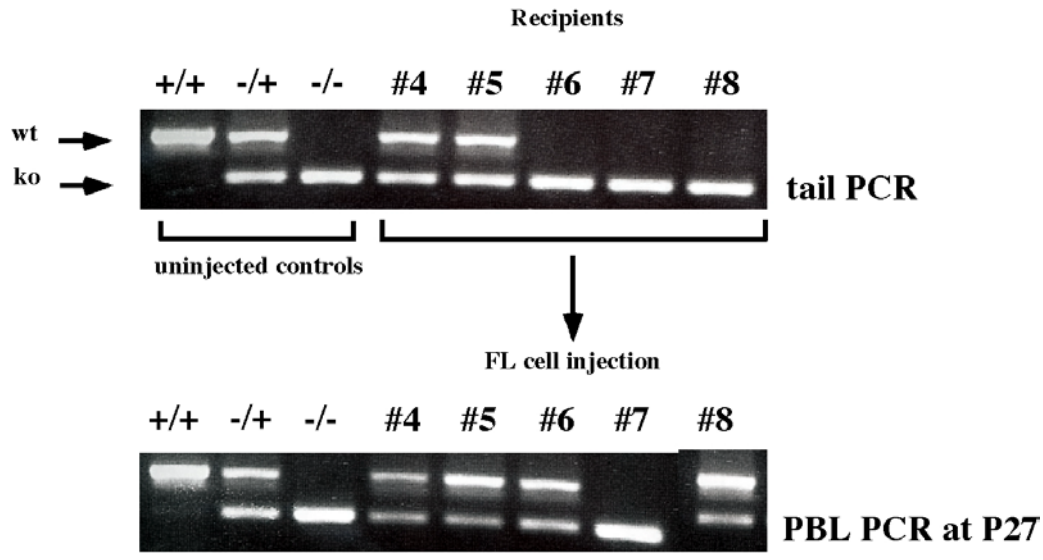

FIGURE 3.1: Chimerism analysis of reconstituted animals by *relB* PCR genotyping
Recipients were obtained by crossing *relB*$^{-/-}$ and *relB*$^{-/+}$ animals. In parallel, *relB*$^{-/+}$ intercrosses were performed for uninjected controls (first 3 lanes). Upon injection of wild-type FL cells, #6 and #8 were assessed to be chimeric due to the presence of upper wild-type band while #7 was not chimeric presumably due to failure in injection.

3.1.2 Histological and Macroscopic Examination of the Reconstituted Animals

The chimerism analysis clearly demonstrated the presence of RelB positive cells in reconstituted *relB*$^{-/-}$ mice. In order to understand whether these cells could home to the spleen, anti-RelB immunohistochemistry was performed.

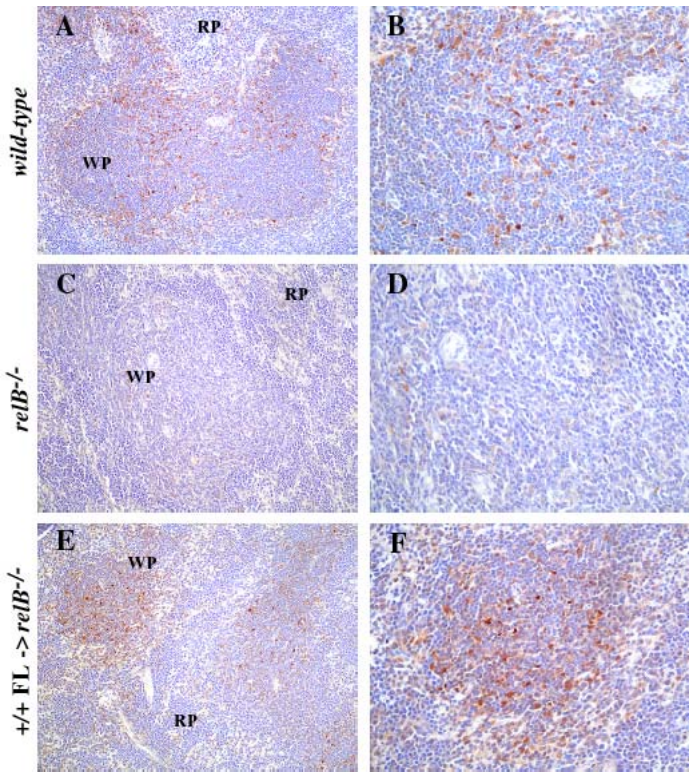

FIGURE 3.2: Immunohistochemical detection of RelB in spleen from control and reconstituted animals
Staining with anti-RelB antibody showed expression in WP of wild-type but not in *relB*$^{-/-}$ spleen (**A** and **C**, respectively). Interestingly, RelB staining (brown) was comparable to wild-type in reconstituted *relB*$^{-/-}$ splenic WP (compare **B** and **F**). Experiment was performed by Debra S. Weih. Magnification **A**, **C**, **E** 20x and **B**, **D**, **F** 40x.

As shown in **Fig. 3.2**, while *relB*$^{-/-}$ spleen sections showed no positive staining for RelB, section from the reconstituted animal clearly showed RelB expressing cells in the WP, indicating that the injected wild-type cells were not only in circulation but also could home to the secondary lymphoid organ spleen.

Spleens from these reconstituted animals were analyzed in detail using specific markers for hematopoietic and stromal cells and special microstructures. FDC-M1 was used to detect FDC networks, PNA for GC formation, MECA-367 for detection of marginal sinus lining stromal cells and MOMA-1 for marginal metallophilic macrophages (data not shown). Taken together, the results strongly suggest that RelB expression in stroma is absolutely required for the formation of an organized spleen structure.

3.1.3 RT-PCR Analysis of Spleens From NF-κB Deficient Mice

3.1.3.1 Expression Analysis of TNF Ligand / Receptor Family Members

It is known that TNF and LT signaling is important for lymphoid organ development (see **Table 1.2**). TNF and LTα are transcriptional targets of NF-κB (Pahl, 1999). In order to check whether the expression of any one of these genes was altered in NF-κB deficient spleens, semiquantitative RT-PCR analysis was performed to compare the expression profiles of TNF family members. The analysis included wild-type, *relB*$^{-/-}$, *nfkb1*$^{-/-}$, and *nfkb2*$^{-/-}$ animals (**Fig. 3.3**).

Not only the ligands, TNF, LTα, LTβ, and LIGHT, but also their receptors, TNFRI and LTβR, were expressed in spleens from all mutant mice and controls. The results showed a 40-50% reduction in mRNA levels of LTα and LTβ whereas a two-fold increase in LIGHT and LTβR mRNA levels was observed in *relB*$^{-/-}$ animals compared to wild-type controls. The expression of LTα mRNA was also reduced in *nfkb1*$^{-/-}$ and *nfkb2*$^{-/-}$ spleens but the expresion of other family members was comparable to wild-type controls. RelB is a potent transactivator in the presence of p50 or p52. These results suggest that RelB heterodimers, p50-RelB and p52-RelB, may play a role in LTα and LTβ expression in spleen.

3.1.3.2 Expression Analysis of Chemokines and Chemokine Receptors

The constitutive expression of chemokines in secondary lymphoid organs and homing of lymphocytes bearing the corresponding chemokine receptors are critical in the development of a functional organ. Given the requirement of RelB expression in stromal cells in spleen, it is likely that spleen microarchitecture defects in *relB*$^{-/-}$ animals are a result of defective lymphocyte migration due to the lack of signals in stroma mediated by RelB. SLC is expressed by stromal cells within the T cell zones and BLC is produced by follicular stromal cells in spleen. In this context, the expression profile of the chemokines, BLC, ELC, and SLC, which are constitutively expressed in lymphoid organs, and their corresponding receptors, CXCR5 and CCR7, in RelB-deficient mice was of interest. Other NF-κB-deficient mice were also included in the study. The expression of the above mentioned genes was analyzed by semiquantitative RT-PCR using total spleen RNA from adult wild-type, *nfkb1*$^{-/-}$, *nfkb2*$^{-/-}$, and *relB*$^{-/-}$ mice.

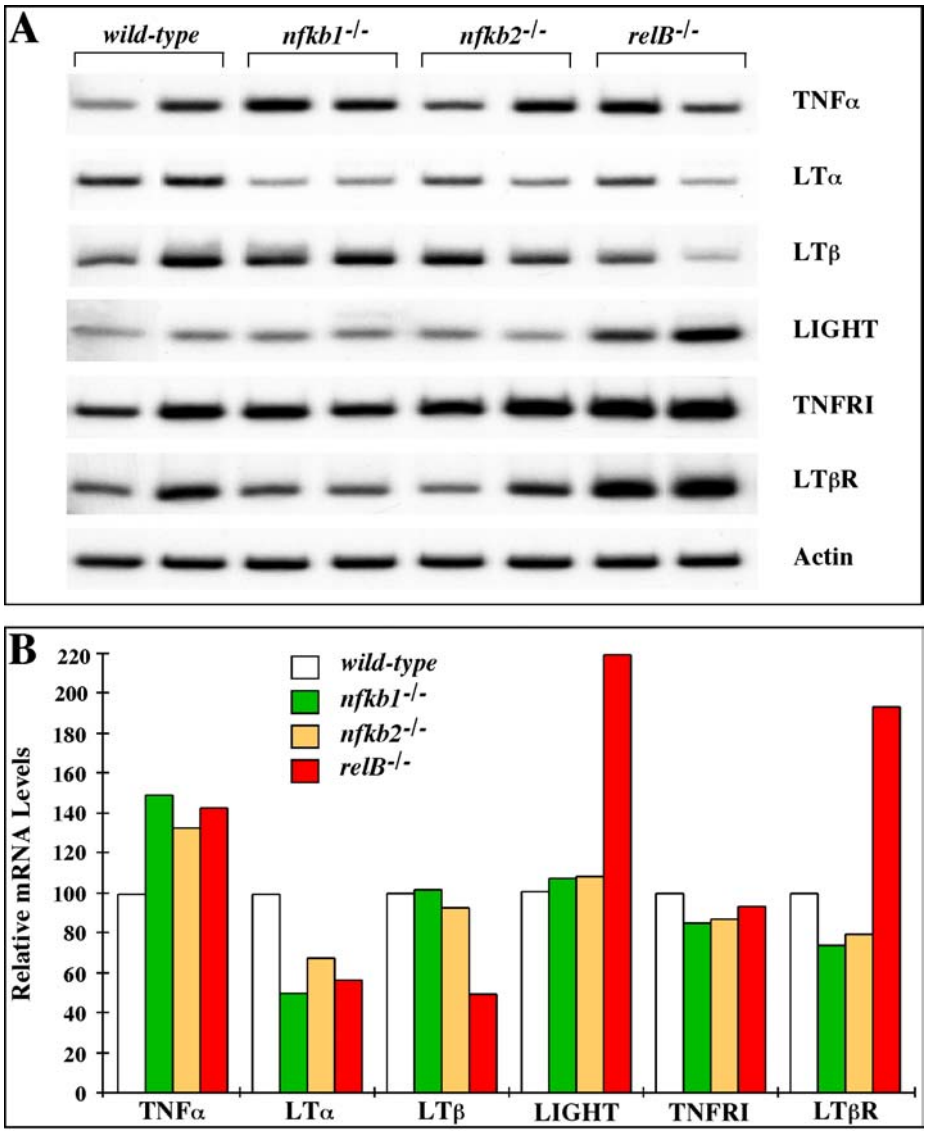

FIGURE 3.3: Expression of TNF ligand/receptor family genes in spleen from NF-κB deficient mice
Total spleen RNA from wild-type, *nfkb1*$^{-/-}$, *nfkb2*$^{-/-}$ and *relB*$^{-/-}$ mice was reverse transcribed and subject to RT-PCR analysis using specific primer pairs (**A**). β-actin expression is shown as control. (**B**) Quantification of the experiment shown in **A**. Every data point was normalized according to β-actin expression and mean values from two data points per genotype were plotted with wild-type values for each gene set to 100% of the relative expression.

The mRNA levels of all five genes were comparable between *nfkb1*$^{-/-}$ and wild-type controls. However, a significant reduction in BLC mRNA levels was detected in *relB*$^{-/-}$ mice (fifteen-fold) and also in *nfkb2*$^{-/-}$ animals (3.5-fold). ELC and SLC expression was also reduced, although to a lesser extent, in *nfkb2*$^{-/-}$ and in *relB*$^{-/-}$ animals, suggesting a

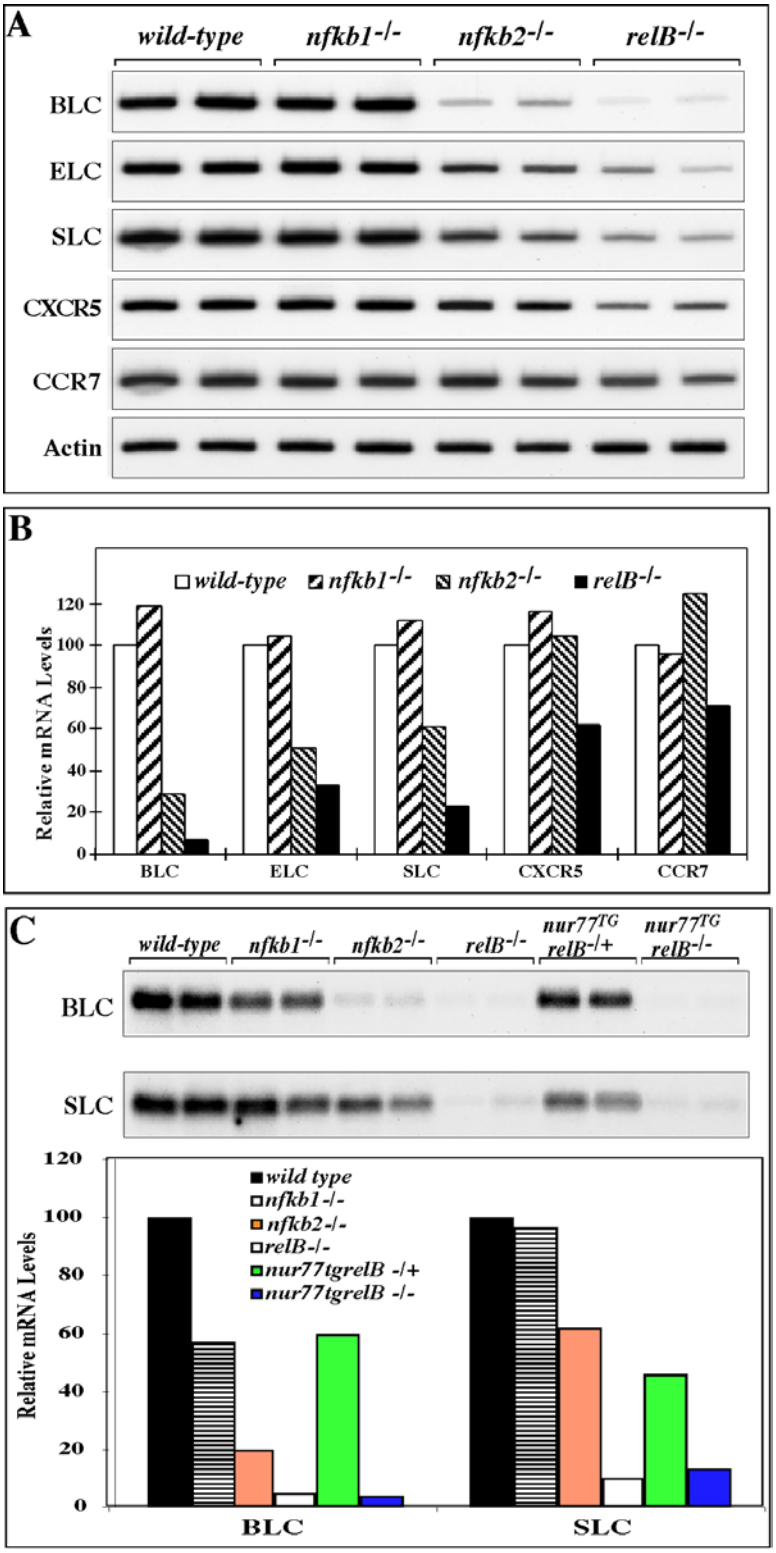

FIGURE 3.4: Expression of chemokines and chemokine receptors in NF-κB-deficient mice
(**A**) RT-PCR analysis of samples from wild-type, *nfkb1*$^{-/-}$, *nfkb2*$^{-/-}$ and *relB*$^{-/-}$ mice. β-actin expression is shown as control. (**B**) Quantification of the experiment shown in **A**. Normalization was performed as described for **Fig. 3.3**. (**C**) Northern blot analysis of BLC and SLC mRNA levels in wild-type, *nfkb1*$^{-/-}$, *nfkb2*$^{-/-}$, *relB*$^{-/-}$, *nur77*^{Tg}*relB*$^{-/+}$ and *nur77*^{Tg}*relB*$^{-/-}$ mice (top panel) and the quantification of the experiment (bottom panel). Equal loading was assessed by methylene blue staining of the membrane. The significant decrease in BLC and SLC mRNA levels persisted in *nur77* transgenic *relB*$^{-/-}$ animals.

potential regulatory role for p52-RelB heterodimers in BLC, ELC and SLC expression in spleen. The reduction in expression of BLC and SLC in *relB*$^{-/-}$ mice correlated with the requirement of RelB expression in the stroma of spleen. Expression of the chemokine receptors CXCR5 and CCR7 was only slightly affected in *relB*$^{-/-}$ mice whereas it was comparable between all other mutant mice and controls (**Fig. 3.4A**, **B**).

Since *relB*$^{-/-}$ animals have splenomegaly and disorganized lymphoid areas, the decrease in BLC and SLC levels could be a result of this structural disorganization. In order to rule out this possibility, *nur77*^{Tg} animals crossed onto a *relB*$^{-/-}$ background were analyzed. The nuclear orphan receptor Nur77 when overexpressed in thymocytes results in massive apoptosis and reduction of peripheral T cells. Multiorgan inflammation and myeloid hyperplasia in RelB-deficient mice is T cell dependent (Weih *et al.*, 1996) and these defects are markedly reduced in *nur77*^{Tg}*relB*$^{-/-}$ mice. In particular, these animals do not show splenomegaly. Northern blotting confirmed the reduced levels of BLC and SLC (twenty- and ten-fold, respectively) in *relB*$^{-/-}$ spleens (**Fig. 3.4C**). RT-PCR results for *nfkb2*$^{-/-}$ mice were also confirmed with a more significant decrease in BLC levels (five-fold) than SLC (1.6-fold). Interestingly, while *nur77* transgenic *relB* heterozygote control animals (*nur77*^{Tg}*relB*$^{-/+}$) showed a mild decrease of BLC and SLC expression (1.7-fold and two-fold, respectively), the expression in spleens of transgenic knockout animals (*nur77*^{Tg}*relB*$^{-/-}$) was more severely reduced (25 and 7.7 fold, respectively; black versus blue columns in **Fig. 3.4C**, bottom panel). These results suggest that rather than a secondary event due to splenomegaly, BLC and SLC expression by stromal cells was decreased due to the lack of RelB, thus contributing to the defective splenic microarchitecture in RelB-deficient animals.

The requirement of stromal RelB expression for BLC and SLC expression in spleen was further supported by the results of similar experiments performed using total spleen RNA from BM chimeric animals which were immunized with SRBC (**Fig. 3.5**). The results showed a partial rescue of the reduced expression of ELC in *relB*$^{-/-}$ recipients reconstituted with wild-type BM. ELC is expressed by IDCs in T cell zone of the spleen and the reduction in ELC expression is in agreement with the reduced numbers and defective distribution of DCs in *relB*$^{-/-}$ spleen.

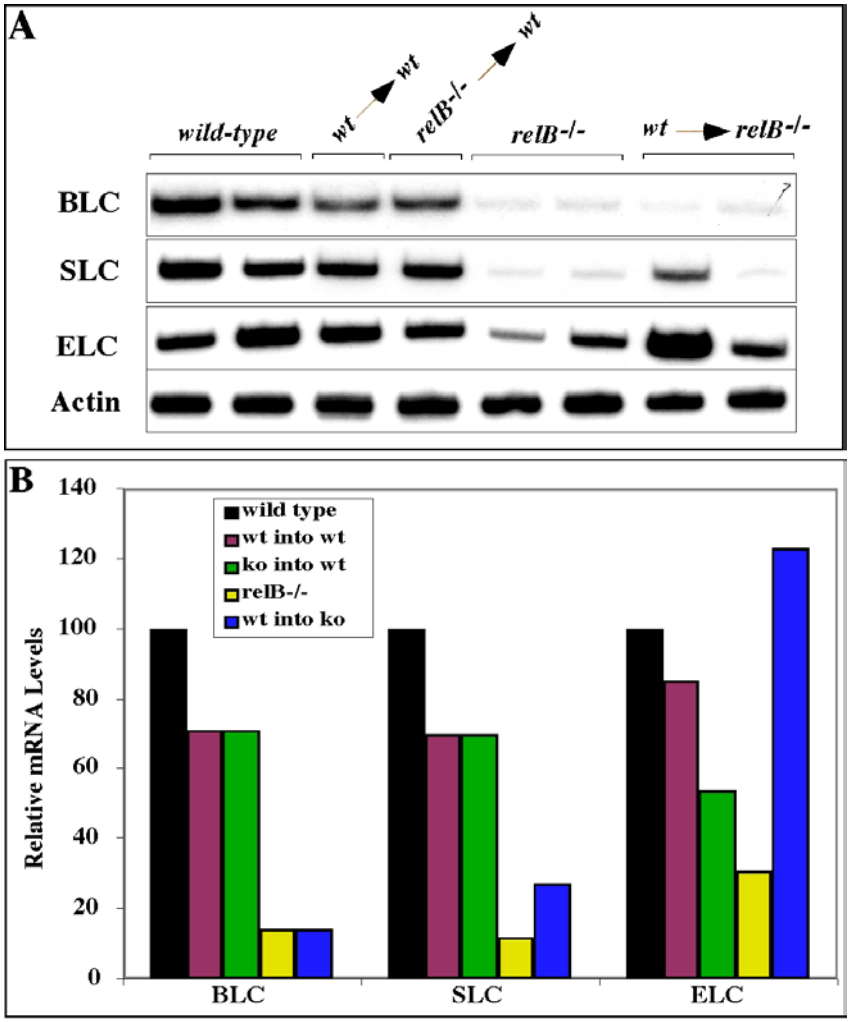

FIGURE 3.5: Expression of BLC, ELC and SLC chemokines in spleens of control and BM chimeric mice

(A) RT-PCR analysis was performed as described for **Fig. 3.3** and **Fig. 3.4**.

(B) Quantification of the experiment shown in **A**. The reduction in BLC and SLC mRNA levels persisted in RelB-deficient recipients reconstituted with wild-type BM similar to *relB*$^{-/-}$ animals (five- to seven-fold for BLC and three- to four-fold for SLC; compare black to yellow and blue bars, respectively). Reconstitution with wild-type BM cells rescued ELC expression to a certain extent as there was animal to animal variation in expression levels of chimeras (**A**, compare lanes 7 and 8).

PART TWO

3.2 ROLE OF RelB IN PEYER'S PATCH DEVELOPMENT

3.2.1 Histological and Immunohistochemical Analysis of Adult Mouse Intestine

Histological analysis in our laboratory of intestines from adult wild-type and NF-κB deficient mice revealed that while *nfkb1*$^{-/-}$ mice have PPs, although smaller in size and less in number compared to wild-type controls, serial sections of the small intestine did not show any histological evidence of PPs in *nfkb2*$^{-/-}$ and *relB*$^{-/-}$ animals, suggesting a role for p52 and RelB for PP development.

In order to analyze RelB expression in PP, immunohistochemistry was performed (**Fig. 3.6**).

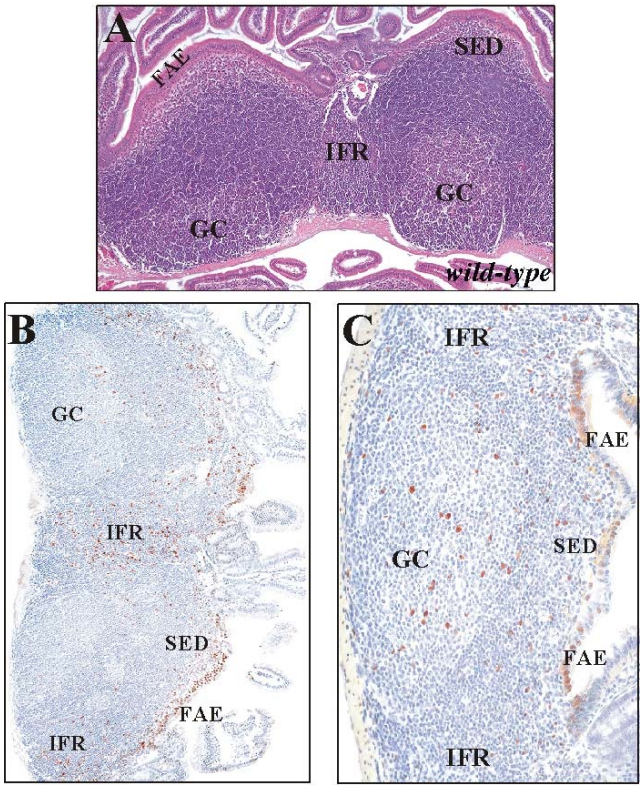

FIGURE 3.6 : RelB is expressed in stromal cells of PPs.
(**A)** Histological analysis of adult wild-type PP, sections were stained with hematoxylin and eosin. FAE, follicle-associated epithelium; SED, subepithelial dome; IFR, interfollicular region; GC, germinal center. Immunohistochemical detection of RelB in an adult wild-type PP (**B**) and from a lethally irradiated wild-type mouse reconstituted with *relB*$^{-/-}$ bone marrow (**C**). Experiment was performed by Debra S. Weih (original magnification, **A** and **B** 20x, **C** 40x).

Fully developed PPs from adult wild-type mice showed strong RelB expression in the IFR, the SED, and the FAE (**Fig. 3.6A** and **B**). Fewer $RelB^+$ cells were also observed in follicles and GCs. The analysis of mice after adoptive transfer of *relB*$^{-/-}$ BM into lethally irradiated wild-type recipients revealed that RelB in hematopoietic cells is not required for the maintenance of PP structures. While RelB expression was clearly reduced in the IFRs, $RelB^+$ cells were still detected in these chimeric PPs, in particular in the FAE close to the follicle-associated crypt (**Fig. 3.6C**). Adoptive transfer of fetal liver or wild-type BM cells failed to restore PPs in irradiated newborn or adult *relB*$^{-/-}$ mice, respectively (data not shown). These results indicate that RelB in non-hematopoietic cells is required for normal PP development.

3.2.2 Analysis of Fecal IgA Levels in NF-κB Deficient Mice

Antigenic stimulation in PP induces preferentially Ig class switching to IgA, which can be exported through the epithelial sheet. Since RelB- and p52-deficient animals lack developed PPs, fecal samples from NF-κB-deficient mice were analyzed by ELISA to determine IgA levels. As shown in **Fig. 3.7**, the concentration of IgA in fecal samples was greatly reduced in all mutant mice compared to wild-type controls with particularly low levels in *relB*$^{-/-}$ animals. Fecal IgA levels were reduced approximately 40-fold in *relB*$^{-/-}$, 20-fold in *nfkb1*$^{-/-}$, and 15-fold in *nfkb2*$^{-/-}$ mice.

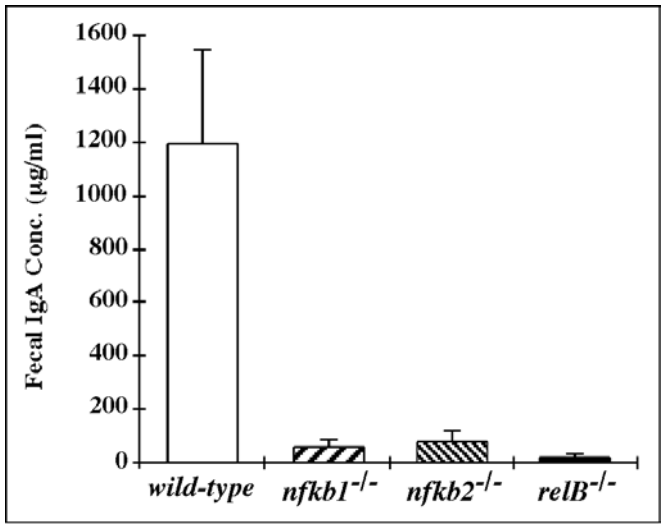

FIGURE 3.7: Fecal IgA concentration in wild-type, *nfkb1*$^{-/-}$, *nfkb2*$^{-/-}$, and *relB*$^{-/-}$ mice
Fecal samples were collected from 8-10 week old mice and analyzed by ELISA. Data represent mean values ± SEM of six to seven mice per genotype.

3.2.3 Expression of *relB* and *nfkb2* mRNA in Embryonic Intestine

RelB protein expression was demonstrated in adult PP (**Fig. 3.6**). PP development is initiated before birth and developing PPs can be detected as early as E15.5 (Adachi *et al.*, 1997). Therefore, expression of *relB* and *nfkb2* mRNA were examined in embryonic intestine. Timed pregnancies were set up and intestine tissues were collected from E14.5, E16.5 and E18.5 embryos. Mesentery was removed from all preparations with the exception of E14.5. Total RNA was obtained directly from intestine single cell suspensions and analyzed by semiquantitative RT-PCR (**Fig. 3.8**).

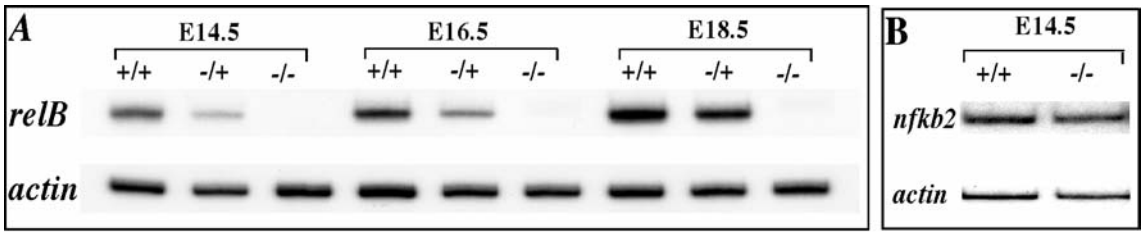

FIGURE 3.8: RT-PCR analysis of *relB* and *nfkb2* mRNA levels in intestine from wild-type (+/+), heterozygous (-/+), and RelB-deficient (-/-) embryos at E14.5, E16.5, and E18.5
Both *relB* (**A**) and *nfkb2* (**B**) were expressed in embryonic intestine as early as E14.5 and *nfkb2* expression in RelB-deficient (-/-) embryos was comparable to controls (**B**). Expression of β-actin is shown as control.

RT-PCR analysis of intestines revealed *relB* mRNA expression in wild-type E14.5 embryos with increasing levels at E16.5 and E18.5. Whereas *relB* mRNA levels were reduced in phenotypically normal heterozygous $relB^{-/+}$ embryos, no expression was detected in $relB^{-/-}$ mice (**Fig. 3.8A**). In addition, *nfkb2* mRNA expression could also be detected in wild-type E14.5 intestine and also at E16.5 and E18.5 (data not shown) and at comparable levels in $relB^{-/-}$ embryos (**Fig. 3.8B**).

3.2.4 Immunohistochemical Analysis of Embryonic Intestine

In order to analyze RelB protein expression at early embryonic stages in the intestine, wild-type E16.5 and E18.5 intestines were stained for RelB (**Fig. 3.9**). RelB was expressed significantly and specifically in developing PP but not along the intestine.

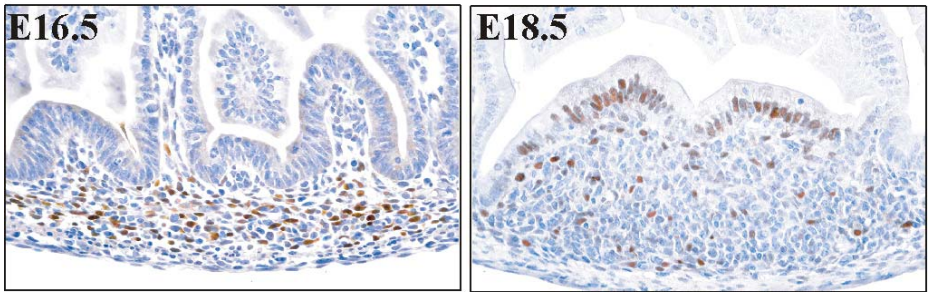

FIGURE 3.9: Immunohistochemical detection of RelB in a developing PP
RelB was detected (brown staining) in a wild-type E16.5 and E18.5 embryos. Experiment was performed by Debra S. Weih (original magnification, 40x).

3.2.5 RelB- and p52-Deficient Animals Lack VCAM-1 Positive PP Organizing Centers

IL-7Rα signaling through Jak3 in $CD3^-$ cells of the embryonic intestine is required for the production of LTαβ heterotrimers, resulting in VCAM-1 and ICAM-1 expression by LTβR-positive stromal cells (Yoshida *et al.*, 1999). The appearance of $VCAM\text{-}1^+$ PP organizing centers can be detected by whole mount immunohistochemistry at around E15.5 of mouse embryonic development and is the earliest marker for developing PPs (Adachi *et al.*, 1997). In order to examine whether these animals have a defect at an early stage of PP development, wild-type and NF-κB deficient animals were analyzed for VCAM-1 positive clusters by wholemount immunohistochemistry of intestines at P0.

Fig. 3.10 shows that $VCAM\text{-}1^+$ PP organizing centers form normally in wild-type and *nfkb1*$^{-/-}$ mice, but are absent in *nfkb2*$^{-/-}$ and *relB*$^{-/-}$ animals. Similar results were obtained for *relB*$^{-/-}$ animals at E16.5. Thus, both p52/p100 and RelB are essential for the early development of PPs, whereas the p50 subunit of NF-κB plays only a minor role in this process.

3.2.6 IL-7-induced LTα Expression in *relB*$^{-/-}$ and *nfkb2*$^{-/-}$ Embryonic Intestine

LTα and LTβ expression in embryonic intestine is exclusively mediated by IL-$7R\alpha^+CD3^-$ cells which are responsible for the induction of PP organizing centers. This signaling is IL-7 dependent and is mediated by stimulation of LTβR expressing cell, eventually leading to VCAM-1 and ICAM-1 expression at E15.5.

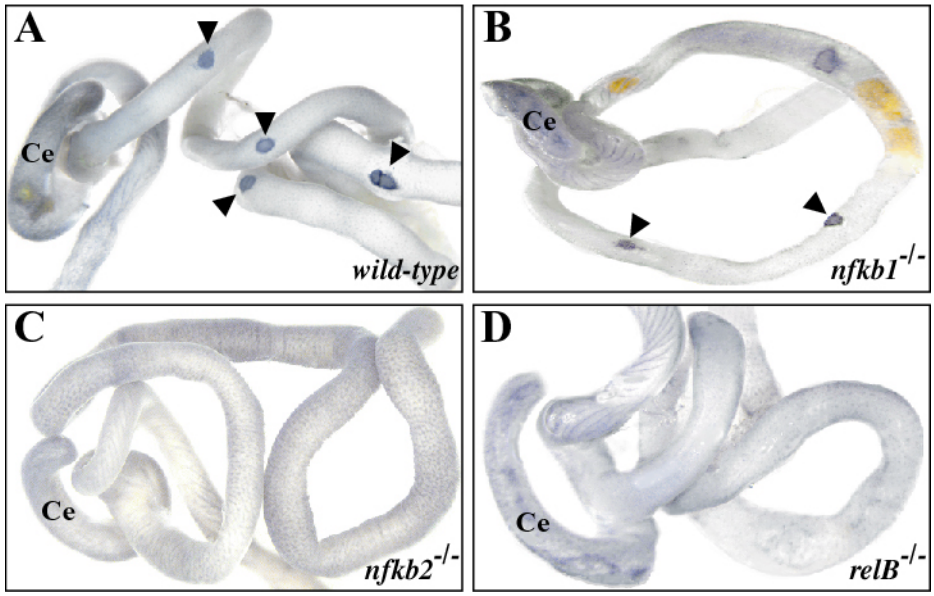

FIGURE 3.10: Lack of VCAM-1-positive cell clusters in *nfkb2*$^{-/-}$ and *relB*$^{-/-}$ mice
Whole mount immunohistochemical staining of intestines from newborn wild-type **(A)**, *nfkb1*$^{-/-}$ **(B)**, *nfkb2*$^{-/-}$ **(C)**, and *relB*$^{-/-}$ **(D)** mice with anti-VCAM-1 mAb. Arrowheads mark VCAM-1-positive spots in wild-type and *nfkb1*$^{-/-}$ mice. Experiment was performed by Debra S. Weih. Ce, cecum.

The first experiments were performed to monitor expression of ligands and receptors of this signaling cascade and compare the expression profiles in *relB*$^{-/-}$ embryonic intestine with controls. E16.5 and E18.5 intestines were collected from *relB*$^{-/-}$ embryos and heterozygote and wild-type littermates were used as controls. Total RNA was obtained both directly from intestine single cell suspensions, including also E14.5 time point without removal of mesentery, and also following culture in the absence or the presence of IL-7.

Analysis of mRNA levels at various embryonic stages did not reveal significant defects in the expression of IL-7 and the IL-7Rα chain or the LTβR and TNFRI (**Fig. 3.11A** and **B**) in *relB*$^{-/-}$ intestine compared to control littermates. Given the importance of LT signaling in PP organogenesis, LTα and LTβ expression was examined in intestinal cell cultures from *relB*$^{+/+}$ *relB*$^{-/+}$ and *relB*$^{-/-}$ E16.5 embryos. IL-7 treatment strongly upregulated LTα mRNA levels in these cultures whereas LTβ expression was only slightly induced. No significant difference however, was observed between *relB*$^{-/-}$ mice and wild-type controls (**Fig. 3.11C**). Similar results were also observed with E18.5 cultures (data not shown). These data indicate the presence of normal numbers of CD45^{+}CD3^{-}IL-7Rα^{+} cells and an intact pathway upstream of the LTβR in *relB*$^{-/-}$ embryonic intestine.

Similar to RelB-deficient animals, p52-deficient mice also lack PPs. In order to investigate whether p52-deficient intestinal cells can induce LTα expression in an IL-7 dependent manner, similar experiments were performed with E16.5 *nfkb2*$^{-/-}$ cells along with E17-18 wild-type controls. As shown in **Fig. 3.11D**, although LTβ expression was comparable to controls, IL-7 inducible LTα expression was reduced. Quantification and normalization of signals according to the corresponding actin values revealed this reduction to be four-fold. This defect may be a result of reduced numbers of CD45^{+}CD3^{-}IL-7Rα^{+} cells in p52-deficient embryonic intestine.

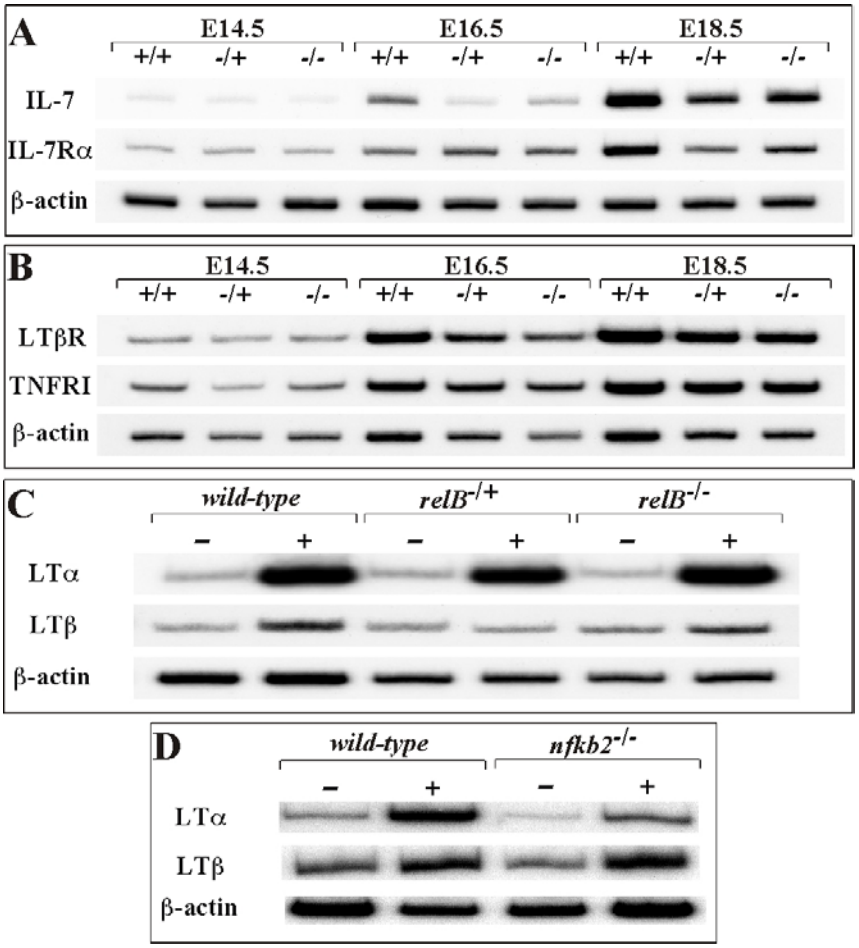

FIGURE 3.11: RT-PCR analysis of IL-7, IL-7Rα (A), LTβR and TNFRI (B), LTα, LTβ (C and D), mRNA levels in intestines from wild-type (+/+), RelB-heterozygous (-/+) and RelB- and p52-deficient (*nfkb2-/-*) embryos at E14.5, E16.5, and E18.5

IL-7-induced expression of *ltα* and *ltβ* mRNA (**C** and **D**) in intestines from *relB*$^{+/+}$, *relB*$^{-/+}$, *relB*$^{-/-}$ and *nfkb2*$^{-/-}$ E16.5 embryos. Wild-type samples in **D** are from E17-18 embryos. Intestinal cell cultures were either induced with IL-7 (+) or left untreated (-). After 24 hours, cells were harvested for RNA extraction and analyzed by RT-PCR. Expression of β-actin in **A-D** is shown as control.

3.2.7 RT-PCR Analysis of Embryonic Intestine Samples

In order to understand the defect causing the lack of PP development in *relB*$^{-/-}$ animals, the expression profile of a panel of genes was analyzed at E14.5, E16.5 and E18.5 for possible role of RelB as a transcriptional regulator. The analysis focused on monitoring the expression of LTα, LTβ, TNF, LTβR and TNFRI as TNF ligand/receptor family members, which provide signals for lymphoid organ development, MAdCAM-1, ICAM-1 and VCAM-1 as cell adhesion molecules, which are expressed in developing PP, and chemokine/chemokine receptors, which regulate cell migration into lymphoid organs. For this purpose, embryonic intestines at E14.5, E16.5 and E18.5 were collected using heterozygote and wild-type embryos as controls for all time points. The basal level of expression was analyzed by RT-PCR using total RNA samples obtained directly from corresponding intestine cells. The results for LTβR and TNFRI were shown in **Fig. 3.11,** results for the others are depicted in **Fig. 3.12**.

No significant difference was detected in mRNA levels of LTα and TNF between *relB*$^{-/-}$ and *relB*$^{-/+}$ intestine for all three time points of analysis while a slight decrease in LTβ mRNA levels was observed at E18.5 (**Fig. 3.12A**).

MAdCAM-1 and ICAM-1 expression in embryonic intestine increased significantly at E18.5, consistent with the reported increase in expression just before birth and thereafter in intestine (Hashi *et al.*, 2001). Interestingly, steady state mRNA levels of ICAM-1 and VCAM-1 were comparable between *relB*$^{-/-}$ and *relB*$^{-/+}$ intestine with the exception of a slight decrease in *relB*$^{-/-}$ intestines for VCAM-1 at E16.5 (**Fig. 3.12B**). Although VCAM-1 mRNA was detected in *relB*$^{-/-}$ intestine cells, VCAM-1 positive cell clusters did not form neither at P0 (see **Fig. 3.10D**) nor at E16.5.

BLC, ELC, SLC, CXCR5 and CCR7 expression was also detected at E16.5 intestine. CXCR5 and RelB are expressed in IL-7Rα $^{+}$CD3^{-} cell population (Mebius *et al.*, 1997). BLC is expressed by LTβR- and VCAM-1-positive cell clusters in embryonic intestine. BLC mRNA levels in *relB*$^{-/-}$ intestine were three-fold less than in *relB*$^{-/+}$ and six-fold less than in wild-type intestine at E18.5 whereas CXCR5 levels were comparable. The results depicted in **Fig. 3.12C** suggest that RelB may be required for expression of BLC at E18.5 just before birth. RelB positive intestinal cells should be identified to clarify whether the signal transduction cascade from LTβR to BLC expression requires NF-κB, particularly RelB.

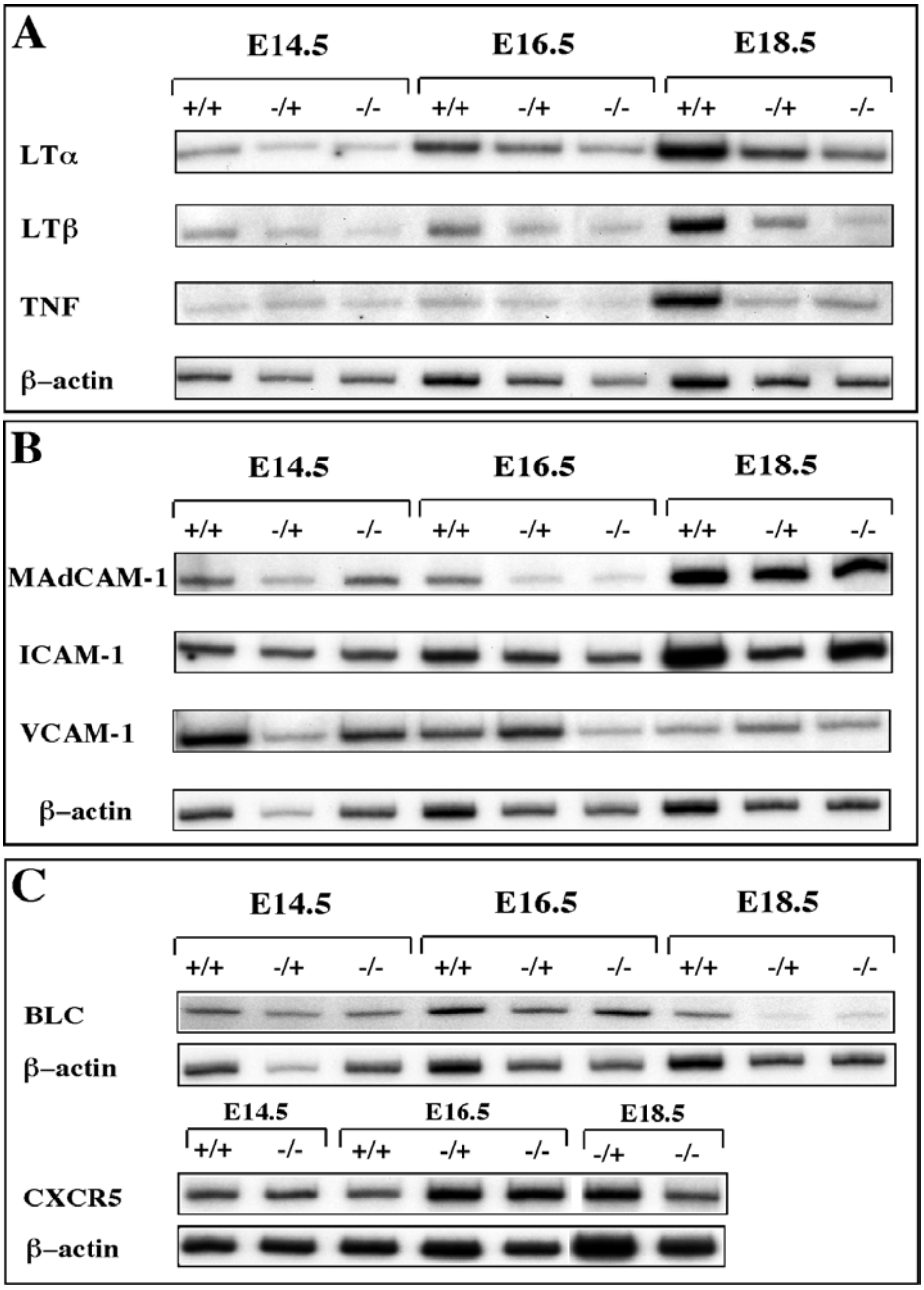

FIGURE 3.12: RT-PCR analysis in intestines from wild-type (+/+), RelB-heterozygous (-/+) and RelB-deficient (-/-) embryos at E14.5, E16.5, and E18.5
Total RNA was extracted from intestinal cell cultures, reverse transcribed and subjected to RT-PCR analysis using specific primer pairs for genes encoding cytokines LTα, LTβ and TNF (**A**), cell adhesion molecules MAdCAM-1, ICAM-1 and VCAM-1 (**B**) and chemokine BLC and its receptor CXCR-5 (**C**). For each set of experiment, corresponding β-actin expression is shown as control.

PART THREE

3.3 LTβR AND TNFR SIGNALING IN FIBROBLASTS AND REGULATION OF RelB DNA BINDING ACTIVITY

RT-PCR findings in spleen and intestine suggest that, rather than regulating transcription of genes upstream of LTβR, RelB more likely plays a role downstream of LTβR signaling. LTβR-deficient mice lack PPs (Fütterer *et al.*, 1998; Rennert *et al.*, 1998) and activation of the LTβR results in the induction of NF-κB (Mackay *et al.*, 1996; Smith *et al.*, 2001; Yin *et al.*, 2001). TNFR signaling also contributes to the full development of lymphoid organs. Both TNFRI and LTβR are expressed on stromal cells (Murphy *et al.*, 1998). In order to investigate whether RelB can be induced downstream of LTβR signaling, different primary and established mouse fibroblast lines which express both LTβR and TNFR were used. The initiation of signal transduction cascades from the receptors was achieved by treating cells with the agonistic anti-LTβR mAb, AC.H6, (Rennert *et al.*, 1998) or recombinant murine or human TNF in order to activate TNFRI and TNFRII or exclusively TNFRI, respectively. As a control for anti-LTβR mAb AC.H6, isotype matched Ha 4/8 (anti-KLH) mAb was used.

3.3.1 LTβR Signaling Induces RelB DNA Binding Activity in Quiescent NIH 3T3 Fibroblasts

A set of experiments was performed with NIH 3T3 fibroblasts. Cells were serum starved for 24 h and then induced either with TNF (T) or anti-LTβR mAb AC.H6 (AC) for 18 h. Nuclear extracts prepared from these cells were subject to EMSAs (**Fig. 3.13)**. As shown in panel **A**, both TNF treatment and LTβR triggering resulted in strong NF-κB induction. Interestingly, LTβR signaling induced a faster migrating complex (compare lanes 2 and 3,4). To identify the κB-binding complexes, supershift experiments were performed. Extracts were either treated with preimmune serum (PI) or specific antibodies (Abs) against Rel/NF-κB family members. Anti-RelB Abs removed the faster migrating complex in AC treated samples (lanes 7 and 8 and arrow). These complexes were retained in the slot (arrowhead). In order to confirm these supershift results, similar experiments were performed using wild-type and *relB*$^{-/-}$ mouse embryonic fibroblasts (MEFs) (**Fig. 3.13B**).

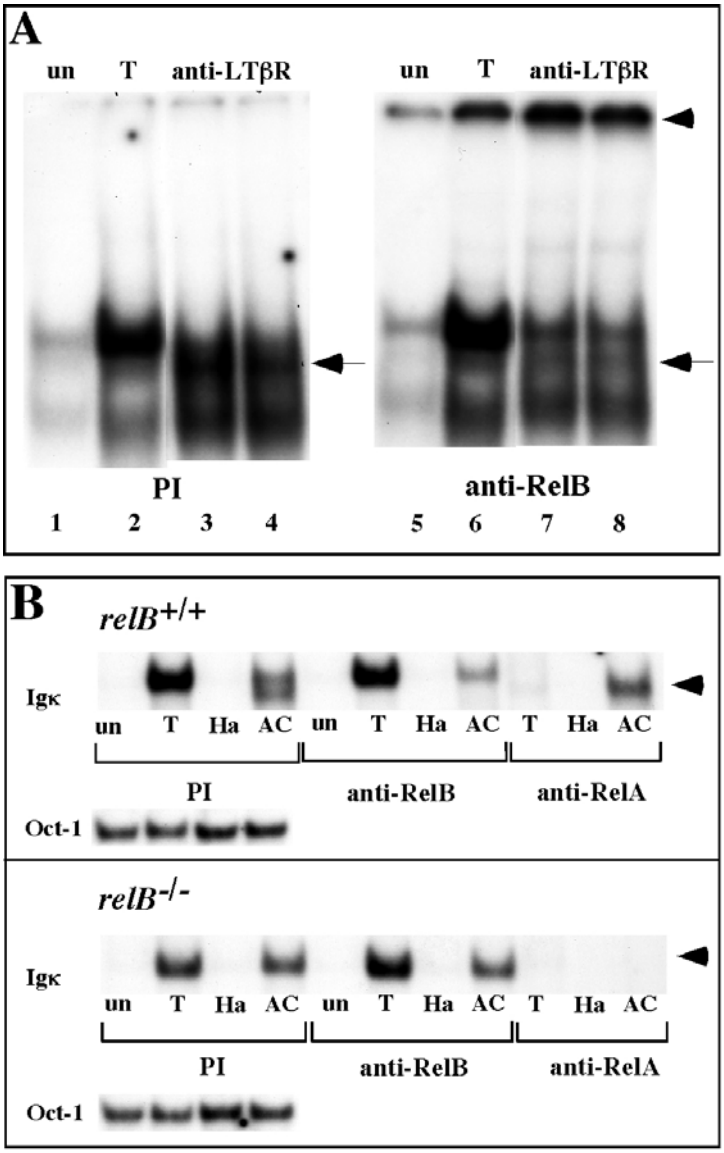

FIGURE 3.13: LTβR signaling induced DNA-binding of RelB complexes in mouse fibroblasts.
(**A**) Wild-type fibroblasts were either left untreated (un) or treated for 18 h with TNF or agonistic anti-LTβR mAb (AC.H6) and nuclear extracts were analyzed in EMSAs using an Igκ probe. Extracts were either incubated with PI (lanes 1-4) or anti-RelB Abs (lanes 5-8). (**B**) Wild-type (upper panel) and *relB*$^{-/-}$ MEFs (lower panel) were treated for 13 h with TNF or anti-LTβR mAb AC.H6 (AC). Untreated (un) or isotype mAb-treated (Ha) cultures were used as controls. Dissection of complexes in EMSAs was performed using specific Abs directed against RelA or RelB. As control for extract integrity, EMSAs performed using an Oct-1 probe are shown.

Similar to NIH 3T3 results treatment of wild-type MEFs with AC.H6 for 13 h also resulted in activation of a faster migrating complex (**B**, upper panel, PI). Anti-RelB Abs did not affect TNF-induced κB-binding but abolished the faster migrating complex in extracts from AC.H6-treated wild-type fibroblasts (arrowhead). Anti-RelA Abs, in

contrast, almost completely blocked TNF-induced κB-binding and specifically abolished slower migrating upper complex in AC.H6-treated samples (upper panel, last lane). The remaining binding was due to RelB complexes since it was not detected in extracts from *relB*$^{-/-}$ MEFs (**B**, lower panel, arrowhead) while TNF induced κB-binding was unaltered upon anti-RelB Ab treatment. Isotype matched control (Ha) treatment did not result in any unspecific effects. Thus, the conclusion is that while TNF resulted predominantly activation of RelA complexes, LTβR triggering induced not only RelA but also RelB complexes.

3.3.2 Requirement for *de novo* Protein Synthesis For Induction of RelB Downstream of LTβR

Time course experiments were performed to analyze the kinetics of RelB and RelA induction downstream of LTβR and TNFR (**Fig. 3.14**). RelA was rapidly induced upon TNF treatment (lanes 1 versus 2). LTβR signaling, however, showed slower activation kinetics (lanes 6 versus 8) with RelB being activated after 3 hours of stimulation. In order to investigate whether this activation required *de novo* protein synthesis, experiments were performed in the presence of emetin as protein synthesis inhibitor (**Fig. 3.14**, lower panel).

Inhibition of protein synthesis by emetin treatment did not change RelA activation upon both TNF and AC.H6 treatment (compare –E versus +E). Prolonged treatment of cells with TNF in the presence of emetin at 12 h time point caused massive cell death. Anti-apoptotic role for NF-κB in preventing TNF induced apoptosis has been reported for RelA-deficient MEFs (Beg *et al.*, 1995). Protein synthesis was clearly required for NF-κB to perform its anti-apoptotic function. Therefore, a 12 h TNF time point in the presence of emetin was not included in EMSA experiments. In striking contrast, RelB complexes were completely abolished in the presence of emetin (lanes 15, 16 and arrow). These results indicate that formation of RelB complexes downstream of LTβR is dependent on protein synthesis, which provides an explanation for the delayed induction kinetics. RelA, in contrast, showed a rapid *de novo*-protein-synthesis-independent response.

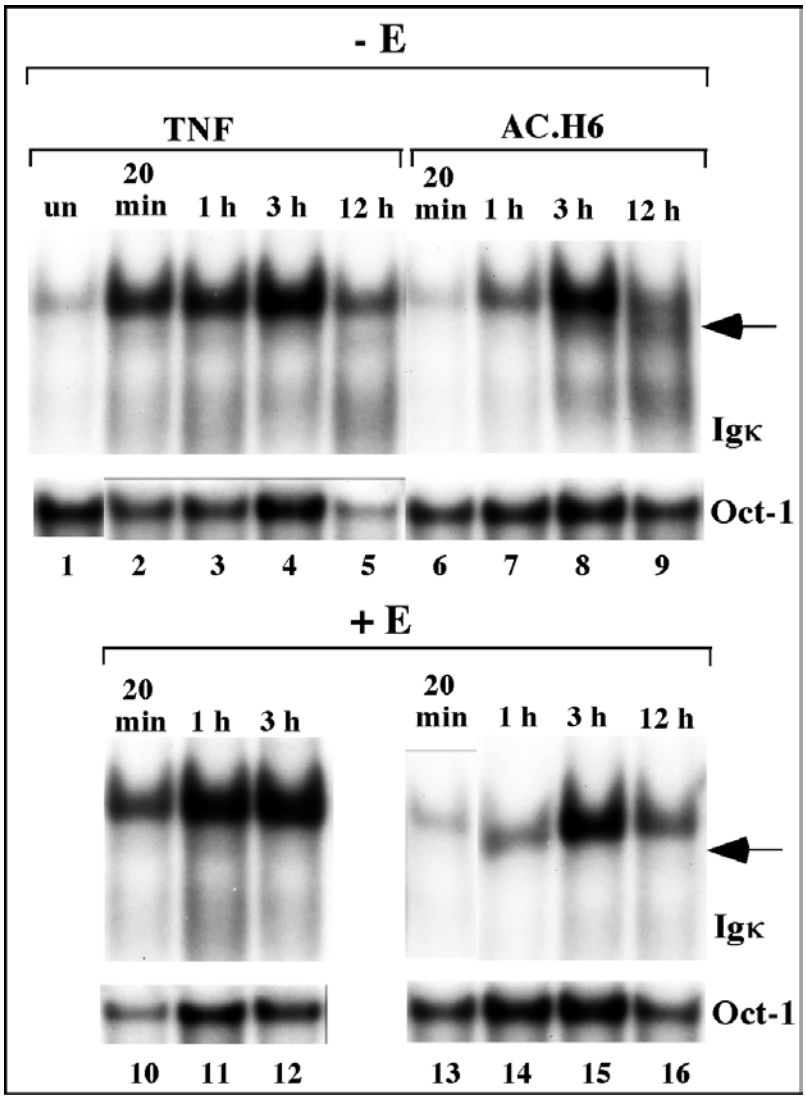

FIGURE 3.14: RelB DNA binding downstream of LTβR was induced after 3 h of stimulation and was emetin treatment sensitive.
NIH 3T3 fibroblasts were either left untreated or treated with TNF or agonistic anti-LTβR mAb, AC.H6, for the indicated time points in the absence (-E, lanes 1-9) or in the presence of 10 μg/ml emetin (+E, lanes 10-16). Cells were preincubated with emetin for 1 h. Nuclear fractions were extracted and subjected to EMSAs with Igκ and Oct-1 probes. Position of slower migrating RelB complexes upon AC.H6 treatment is denoted by an arrow.

3.3.3 Specific Activation of p52-RelB Complexes Downstream of LTβR

Similiar to NIH 3T3 and primary MEFs (**Figures 3.13** and **3.14**), in an independent fibroblast line, TNF treatment resulted in strong NF-κB induction at 1 h and was sustained. In contrast, the maximal levels of NF-κB induction by AC.H6 treatment was reached only after four to eight hours. In addition to the quantitative and kinetics differences, qualitative differences were also observed between these two signaling

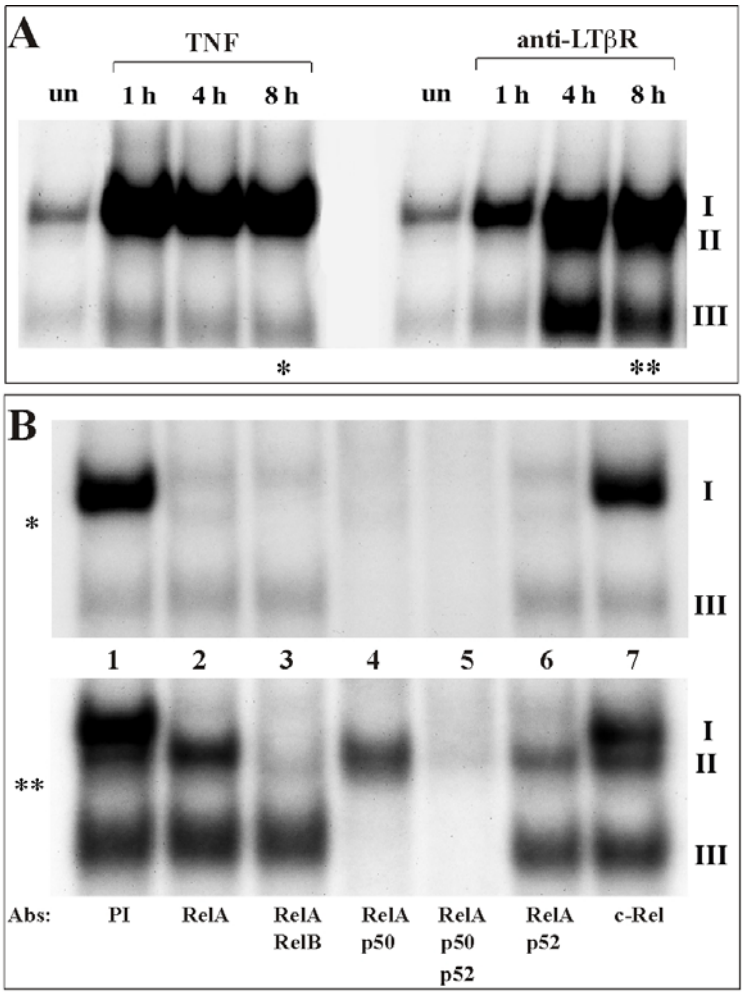

FIGURE 3.15: LTβR signaling induced specifically DNA-binding of p52-RelB complexes while TNFR activated RelA complexes.
(**A**) Wild-type fibroblasts were either left untreated (un) or treated for 1, 4, and 8 h with TNF or agonistic anti-LTβR mAb and nuclear extracts were analyzed in EMSAs using Igκ probe. (**B**) Dissection of complexes using extracts from 8 h TNF-(*) or anti-LTβR-treated (**) fibroblasts to identify nuclear complexes using following Abs: lane 1, PI; lane 2, α-RelA; lane 3, α-RelA + α-RelB; lane 4, α-RelA + α-p50; lane 5, α-RelA + α-p50 + α-p52; lane 6, α-RelA + α-p52; and lane 7, α-p52 for upper panel and α-cRel for bottom panel. **I**: RelA complexes, **II**: p52-RelB and p50-RelB complexes, **III**: p50-p50 homodimers.

pathways particularly with the appearance of complex II after LTβR triggering (**Fig. 3.15A**, right panel).

Dissection experiments were performed with 8 h stimulated samples using different Abs against different Rel/NF-κB family members. As depicted in **Fig. 3.15B**, TNF almost exclusively resulted in RelA binding (complex I) as anti-RelA Ab abolished binding almost completely (lane 2). Addition of anti-RelB Ab specifically removed the faint

bottom band (lane 3), indicating that RelB DNA binding was almost not induced upon TNF treatment. In contrast, LTβR signaling resulted only in RelA induction at 1 h (**Fig. 3.15A**) while both RelA, RelB and p50 complexes were induced at later time points (complex I, II and III). Dissection results showed that complex I consisted of RelA (**B**, bottom panel lane 2) and complex III exclusively consisted of p50 homodimers (lane 4). Complex II on the other hand, consisted predominantly of p52-RelB and also to a lesser extent, of p50-RelB complexes (lane 6). The further addition of anti-p52 Abs completely abolished binding (compare lanes 4 and 5) and LTβR signaling did not induce strong c-Rel either (lane 7). Collectively, the results observed in three independent fibroblast cell lines indicate that while TNFR activated RelA, LTβR activated both RelA and RelB.

3.3.4 LTβR Induced Activation of p52-RelB Requires IKKα and IKKβ Subunits Independent of the Regulatory Subunit IKKγ

The signals which activate NF-κB converge at the IKK complex. In order to examine which subunits of this complex are involved in LTβR mediated activation of p52-RelB, NF-κB activation in response to TNF and AC.H6 treatment was analyzed by EMSA in IKK-deficient fibroblasts (**Fig. 3.16)**. The corresponding wild-type control of this experiment has already been also shown in **Fig. 3.15** and is redepicted in **Fig. 3.16** for the ease of comparison.

While TNF induced binding of NF-κB and complex I was comparable to wild-type in IKKα-deficient fibroblasts (panel **A**), IKKα subunit was absolutely required for LTβR mediated induction of complex II. LTβR induced binding of RelA (I), was still detected albeit to a much lesser extent (**Fig. 3.16B**) in these cells. Similarly in IKKβ-deficient cells, complex II was almost completely abolished and complex I was strongly reduced (**Fig. 3.16C**). This suggests that both IKKα and IKKβ subunits are absolutely required for activation of p52-RelB and are also necessary for full RelA activation downstream of LTβR. Consistent with earlier reports, TNF mediated NF-κB activation was impaired to a greater extent in IKK-β deficient cells than in cells lacking IKKα.

Interestingly, although TNF mediated NF-κB activation was completely abolished in cells lacking the regulatory subunit IKKγ, LTβR triggering still resulted in specific induction of p52-RelB (II) and p50 homodimers (III) (**Fig. 3.16D** and **E**, lanes 4 and 5).

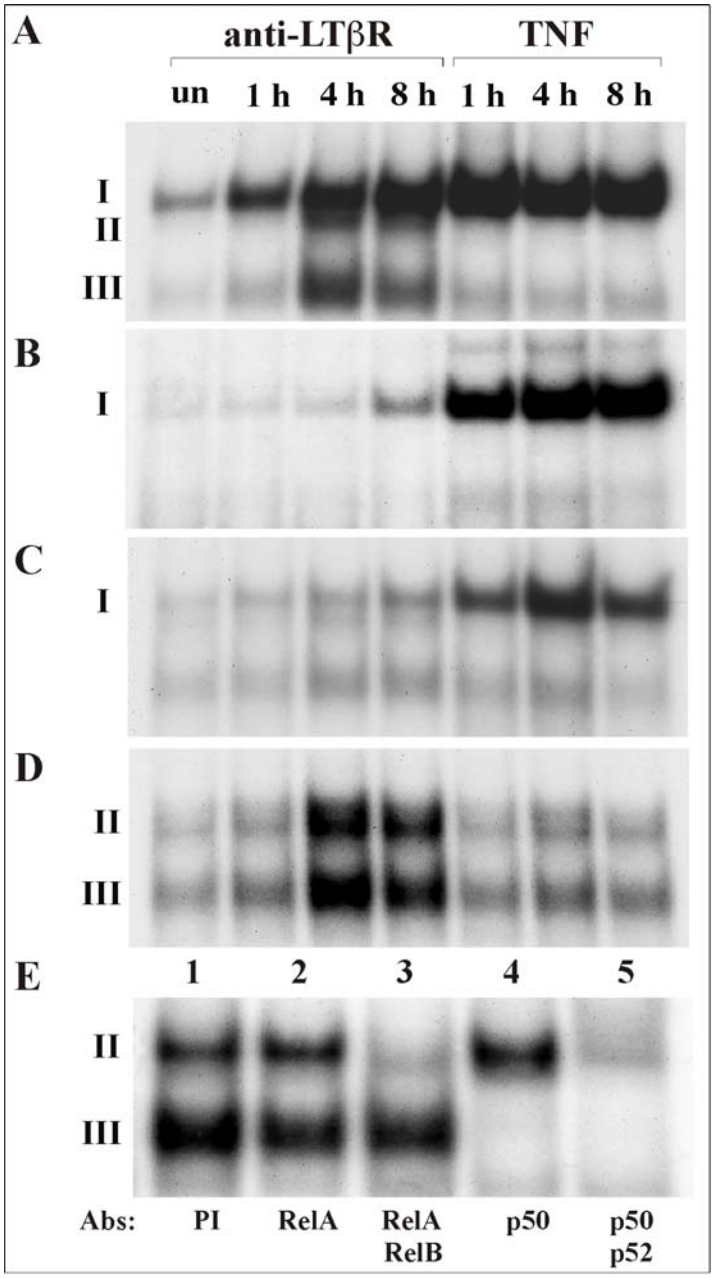

FIGURE 3.16: NF-κB activation in IKK-deficient fibroblasts upon TNFR and LTβR signaling
Wild-type (**A**) and IKKα- (**B**), IKKβ- (**C**) and IKKγ-deficient (**D, E**) fibroblasts were either left untreated (un) or treated for 1, 4, and 8 h with TNF or AC.H6 and nuclear extracts were analyzed in EMSAs using Igκ probe. LTβR signaling induced p52-RelB in an IKKα- and IKKβ-dependent manner (**B** and **C**). (**D**) LTβR activated p52-RelB independent of IKKγ. Dissection of complexes using 8 h anti-LTβR-treated IKKγ-deficient fibroblast extract using following Abs: lane 1, PI; lane 2, α-RelA; lane 3, α-RelA + α-RelB; lane 4, α-p50; lane 5, α-p50 + α-p52. **I**: RelA complexes, **II**: p52-RelB complexes, **III**: p50-p50 homodimers.

RelA activation downstream of LTβR on the other hand, was completely inhibited as shown in panel **E** (anti-RelA Ab treatment, lane 2). The binding shown in panels **D** and **E** was obtained after a longer exposure of the autoradiogram in comparison to panels **A, B** and **C** in order to visualize clearly the binding and dissection results. Quantifications revealed an approximately three-fold reduction in DNA binding of complexes II and III in IKKγ-deficient cells compared to wild-type controls. Taken together, these results show that while for LTβR mediated activation of RelA all three subunits of IKK are essential, p52-RelB activation by LTβR requires only IKKα and β subunits. TNF induces only RelA independent of IKKα.

3.3.5 LTβR but not TNFR Mediates p100 Processing in a *de novo* Protein Synthesis Dependent Manner

Upon activation of LTβR p52-RelB DNA binding complexes were formed while TNFR signaling induced negligible RelB DNA binding in three fibroblast systems used. In order to understand the mechanism underlying this qualitative and quantitative differences in NF-κB response, protein levels for p100, RelB and p52 were analyzed by immunoblotting. Since p52 is generated from its precursor p100, one mechanism could be differential processing of the precursor downstream of these signaling pathways, making p52 levels the limiting factor. Indeed, while p100 was processed upon LTβR triggering and the generated p52 was partly nuclear, consistent with the observed increase in DNA binding activity, TNFR triggering resulted in massive production and accumulation of the p100 precursor both in cytoplasm and in nucleus (**Fig. 3.17A**, compare p100 levels in TNF and AC lanes). In addition, TNFR induced total cellular RelB levels more significantly than LTβR (**Fig 3.17 A**). Interestingly, nuclear RelB levels were significantly higher in TNF stimulated fibroblasts compared to LTβR activated ones. Despite this, no significant RelB DNA binding activity was detectable upon TNF induction (see **Figures 3.13B** and **3.15B**).

In order to investigate whether p100 processing requires protein synthesis, 8 h stimulation experiment was performed in the presence of emetin as protein synthesis inhibitor. **Fig. 3.17B** clearly shows that in emetin treated wild-type fibroblasts, LTβR induced p100 processing was completely blocked (compare p100 and p52 levels on left panel, lane 2 versus lane 4) resulting in the lack of nuclear p52 (right panel). Interestingly, even though total cellular RelB levels were not significantly affected by

emetin treatment (left panel, WCE), nuclear translocation of RelB was completely impaired (right panel, nuclear RelB levels). Thus, LTβR mediated activation of p52-RelB correlates with induced p100 processing, suggesting that newly generated p52 induced nuclear translocation of RelB. All of these processes were protein synthesis dependent. These results are in agreement with the results in NIH 3T3 cells, which also suggest delayed activation of RelB and requirement of new protein synthesis (see **Fig. 3.14**).

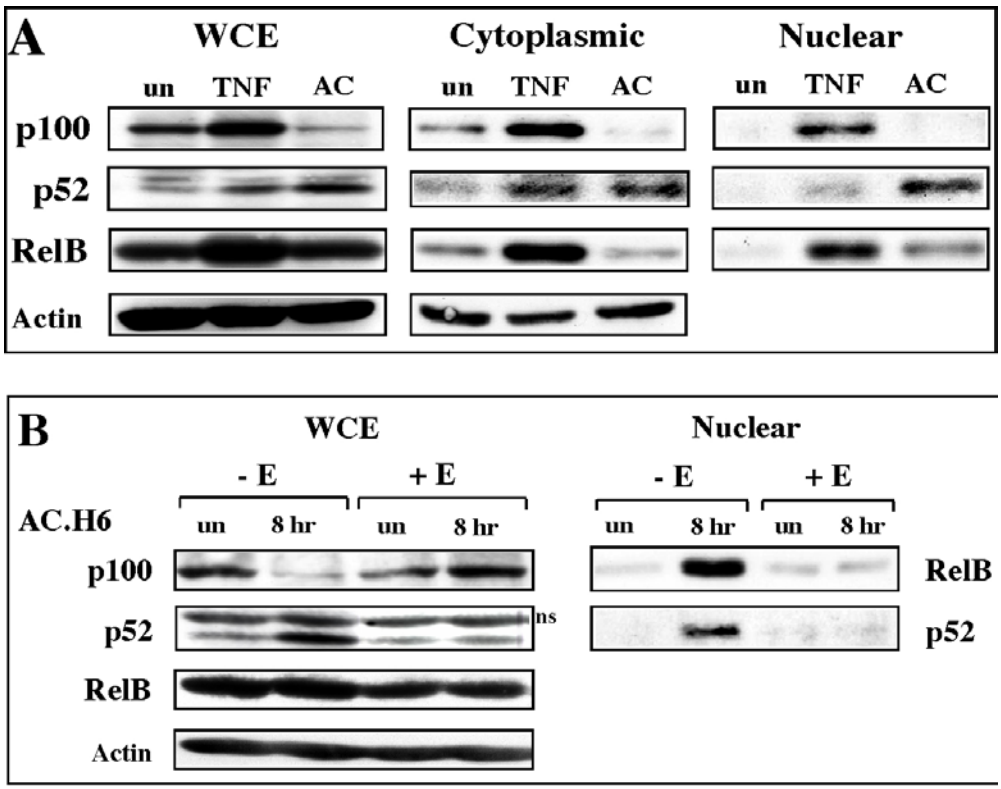

FIGURE 3.17: LTβR induces p100 processing while TNFR induces production and nuclear translocation of RelB and p100.
(A) Wild-type fibroblasts were either left untreated or stimulated with TNF or AC.H6 for 8 h, whole cell (WCE), cytoplasmic (50 μg) and nuclear extracts (25 μg) were analysed by immunoblotting for p100, p52 and RelB levels. (**B**) LTβR induced p100 processing is dependent on *de novo* protein synthesis. Wild-type fibroblasts were either left untreated or stimulated with AC.H6 for 8 h in the absence (-E) or the presence (+E) of 10 μg/ml emetin. WCEs and nuclear extracts were analysed by immunoblotting. Cytoplasmic β-actin is shown as loading control. ns: non-specific band.

3.3.6 LTβR Mediates p100 Processing Through IKKα Subunit

In the light of the results shown above and given the requirement of IKKα and IKKβ for LTβR induced p52-RelB activation, Western blot experiments were performed in a time course analysis with wild-type and IKK-deficient fibroblasts stimulated with AC.H6. In wild-type fibroblasts, p100 processing and p52 generation started at four h of stimulation and persisted (**Fig. 3.18**), which nicely correlated with the observed DNA binding of p52-RelB and nuclear accumulation of RelB. This induced processing of p100 was intact in IKKγ-deficient cells, although to a lesser extent (**Fig. 3.18**, lanes 13-16). RelB levels were also comparable to controls, which is in agreement with the detected activation of p52-RelB in these cells (see **Fig. 3.16D** and **E**). In contrast, IKKα-deficient cells showed impaired p100 processing, resulting in very low levels of p52 and also RelB (**Fig. 3.18**, lanes 5-8).

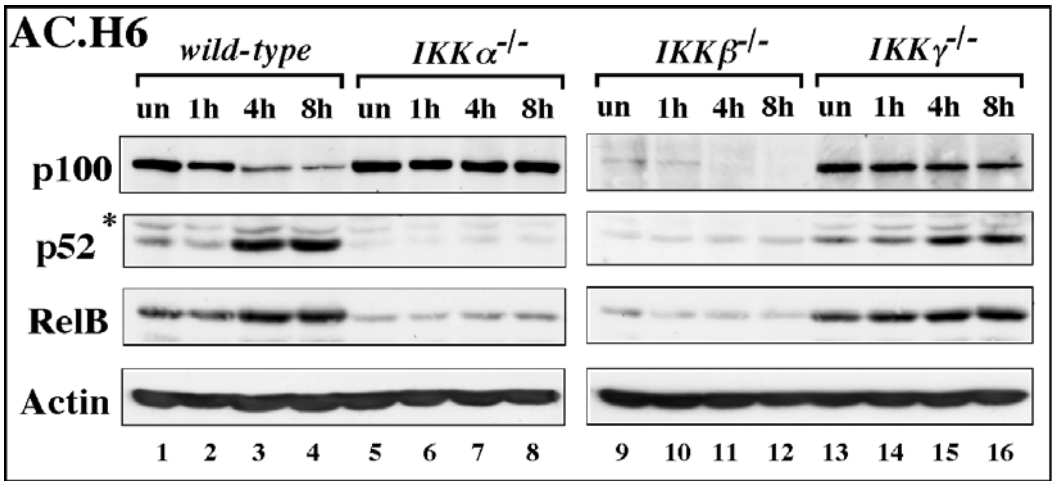

FIGURE 3.18: LTβR induces p100 processing in an IKKα dependent manner
Western blot analysis of p100, p52 and RelB protein levels in whole cell extracts of wild-type and IKK-deficient fibroblasts following stimulation with anti-LTβR mAb, AC.H6 for 1, 4, and 8 h. Cytoplasmic β-actin is shown as loading control. * non-specific band.

IKKβ subunit was essential for basal levels of the p100 precursor albeit processing was intact in cells lacking this subunit. Interestingly, RelB levels were also very low in these cells (**Fig. 3.18**, lanes 9-12). Taken together, these data suggest that LTβR mediates p100 processing through the IKKα subunit and that this process is independent of IKKβ and IKKγ. The defective p52-RelB activation in IKKα-deficient cells could not only be due to the impaired p100 processing but also to very low RelB levels. In IKKβ-deficient cells, the lack of p52-RelB induction seems to be caused by the very low basal levels of

p100 and RelB. Thus, upon LTβR signaling the IKK complex controls both p100 processing through its α subunit and RelB basal levels through its α and β subunits.

3.3.7 LTβR Induces p52-RelB Independent of RelA

In different anti-LTβR stimulated fibroblasts used in this study, p52-RelB binding was preceded by induction of RelA complexes. Recently, Bren *et al.* reported that *relB* transcription is regulated by NF-κB, particularly by RelA and RelB, possibly via identified binding sites in the promoter (Bren *et al.*, 2001). In order to understand whether RelB activation downstream of LTβR is mediated by RelA, *relA*$^{-/-}$ fibroblasts were used to analyze NF-κB activation. **Fig. 3.19A** shows that after four h of stimulation, NF-κB was activated in wild-type fibroblasts and that this induction was also detectable, albeit to a lesser extent, in RelA-deficient cells upon AC.H6 treatment. Treatment of extracts with anti-RelB Abs completely removed this binding, suggesting that RelB complexes were activated downstream of LTβR in *relA*$^{-/-}$ fibroblasts. Analysis of p100 processing and RelB protein levels in these cells by Western blotting revealed that p100 basal levels were reduced but the processing was intact (**Fig. 3.19B**), a defect similar to fibroblasts lacking IKKβ subunit (see **Fig. 3.18**). While in wild-type cells, RelB protein induction was detected at four and eight h time points, in *relA*$^{-/-}$ fibroblasts this induction was also reduced and occurred with slightly delayed kinetics. Collectively, these findings may provide an explanation for reduced levels of RelB activation in *relA*$^{-/-}$ fibroblasts downstream of LTβR.

3.3.8 Precursor p105 Processing and IκBα Regulation Downstream of LTβR in Mouse Fibroblasts

In addition to p52-RelB complexes, the activation of p50-RelB was observed to a lesser extent upon LTβR signaling (see **Fig. 3.15**). In order to investigate the mechanism of activation of different NF-κB members, p105 precursor and IκBα inhibitor levels were analysed by Western blotting in wild-type and IKK-deficient fibroblasts (**Fig. 3.20**). Similar to the p100 precursor, p105 was proteolytically processed/degraded upon LTβR triggering (**Fig. 3.20**, lanes 1-4). Although p52 levels were increased upon p100 processing, p50 levels were unchanged. p50 is cotranslationally processed from its precursor p105 and although the levels of overexpressed p105 was decreased, p50 levels were unchanged *in vivo* as shown by pulse-chase experiments, suggesting that there is

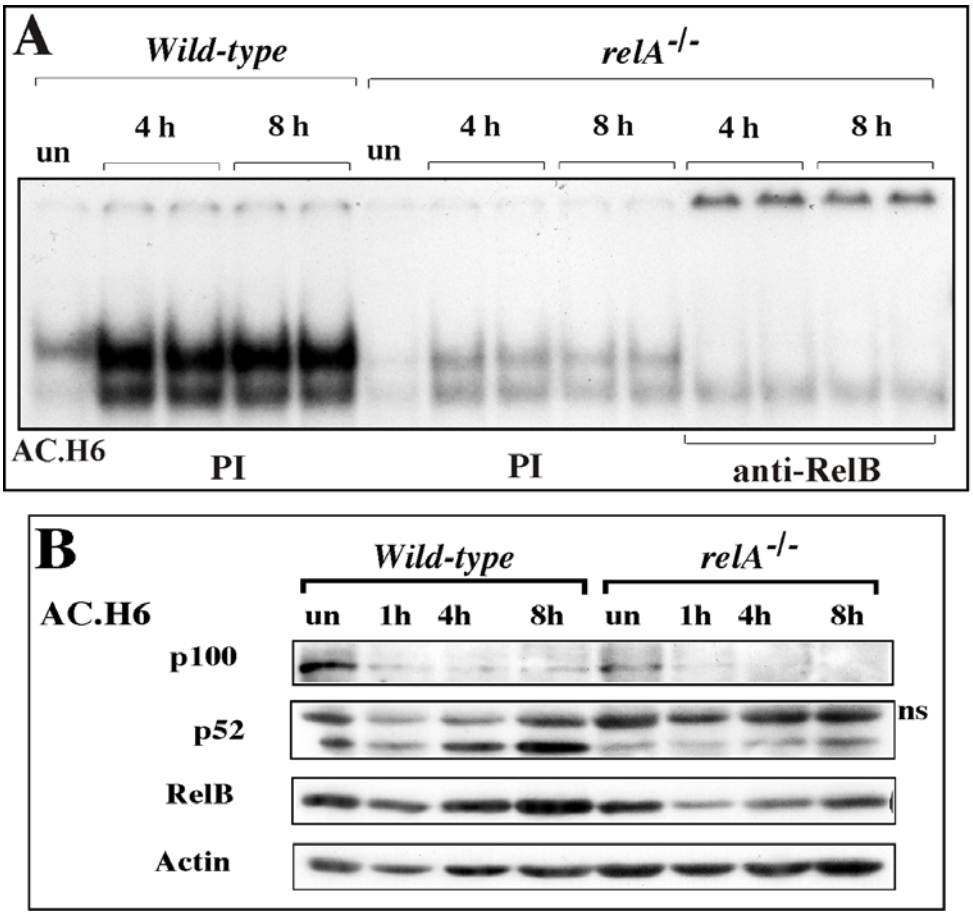

FIGURE 3.19: LTβR induces RelB complexes in *relA*$^{-/-}$ fibroblasts.
(**A**)Wild-type or RelA-deficient fibroblasts were either left untreated (un) or stimulated with AC.H6 for 4 and 8 h. Nuclear extracts were analysed by EMSA. NF-κB was still activated in RelA-deficient cells and anti-RelB Ab completely abolished this binding indicating activation of RelB complexes. (**B**) Western blot analysis of p100, p52 and RelB protein levels in whole cell extracts of wild-type and *relA*$^{-/-}$ fibroblasts following stimulation with anti-LTβR mAb, AC.H6 for 1, 4, and 8 h. Cytoplasmic β-actin is shown as loading control. ns: non-specific band.

not a classical precursor-product relationship between p105 and p50 (Lin *et al.*, 1998). In all experiments, endogenous proteins were analysed, which makes it difficult to compare these results with overexpression studies. A possible interpretation is that p105 processing functions in the canonical p50-RelA activation pathway which requires all three IKK subunits. This assumption is supported by the impaired processing in IKKα- and IKKγ-deficient fibroblasts. In IKKβ-deficient cells, p105 basal levels were significantly reduced, but the processing was intact (**Fig. 3.20A**, lanes 9-12). The *in vivo* association of the IκBα-like C-terminal portion of p105 with RelA is sufficient for its cytoplasmic retention (Mercurio *et al.*, 1993). Whether there is yet a third activation pathway downstream of LTβR signaling, which is IκBα independent but involves p105 processing, remains to be shown.

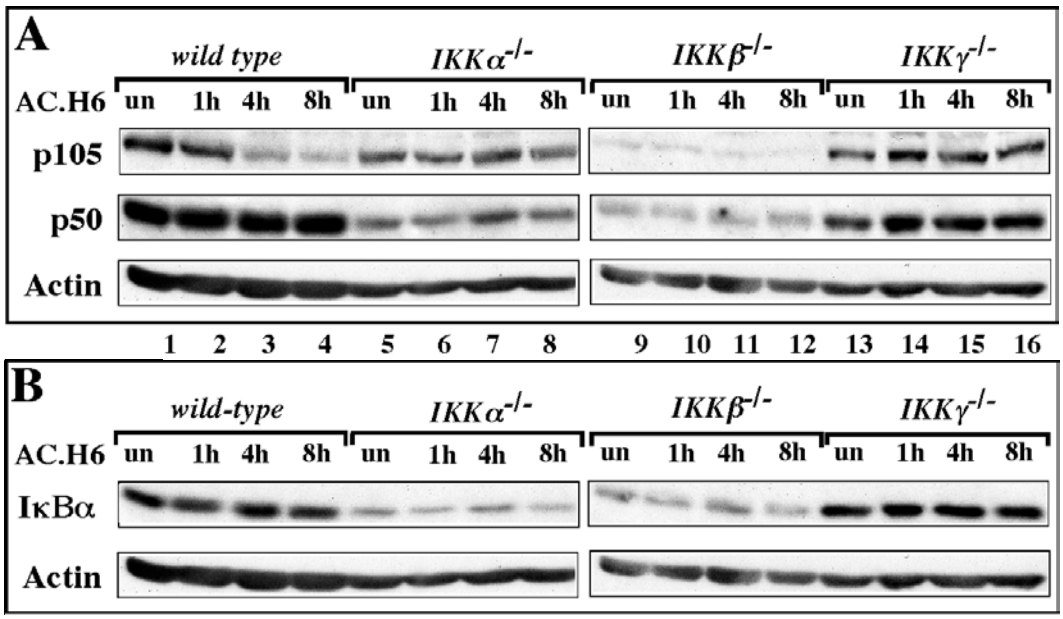

FIGURE 3.20: LTβR also induces p105 processing while IκBα is not degraded.
Western blot analysis of p105, p50 (**A**) and IκBα (**B**) protein levels in whole cell extracts of wild-type and IKK-deficient fibroblasts following stimulation with anti-LTβR mAb, AC.H6 for 1, 4, and 8 h. β-actin is shown as loading control.

In contrast to the classical p50-RelA NF-κB complexes, p52-RelB heterodimers are only poorly regulated by IκBα (Dobrzanski *et al.*, 1994; Lernbecher *et al.*, 1994). Therefore, it is unlikely that the inducible degradation of IκBα upon □□β□ triggeringaccounts for the activation of p52-RelB complexes. Indeed, at four and eight h of anti-LTβR stimulation, when the detected p52-RelB activity was maximal, IκBα levels were unchanged (**Fig. 3.20B**, lanes 1-4). IκBα levels were comparable between controls and IKKγ-deficient cells, but in IKKα- and IKKβ-deficient fibroblasts IκBα levels were significantly reduced. Taken together, these data suggest that IκBα degradation does not result in activation of RelB complexes downstream of LTβR and that IKK α and β subunits are required for normal expression levels of IκBα, p50 and also RelB (see **Fig. 3.18**).

3.3.9 RT-PCR Analysis in LTβR and TNF Stimulated Fibroblasts

The results shown so far address the kinetics as well as quantitative and qualitative differences in NF-κB activation downstream of LTβR and TNFR signaling in fibroblasts. However, the original aim was to be able to understand the defect downstream of LTβR, which leads to defective PP organogenesis in RelB-deficient animals. Since RelB was activated upon LTβR triggering, gene expression analysis was performed to detect RelB dependent differences. For this purpose, NIH 3T3 and primary wild-type and RelB-deficient fibroblasts were used to analyse expression of NF-κB members and cell adhesion molecules VCAM-1 and ICAM-1, which were implicated in PP organogenesis. Previously, *nfkb1* and *nfkb2* were reported to be NF-κB target genes along with *icam-1* and *vcam-1* (Pahl, 1999). In addition and consistent with the presented results, *relB* was reported to be transcriptionally regulated by NF-κB upon TNF treatment (Bren *et al.*, 2001). The expression pattern of the above mentioned genes and also other NF-κB family members was analysed by RT-PCR and the results of this analysis in NIH 3T3 cells are summarized in the **Table 3.1**.

Gene	Unstimulated	TNF	AC.H6
nfkb1	+	++	+
nfkb2	+	++	++
relB	+	+++	++
relA	+	++	+
c-rel	+	+++	+
icam-1	-	+++++++ **(*)**	+
vcam-1	+	++++	+++

TABLE 3.1: RT-PCR analysis in NIH 3T3 cells
Serum starved fibroblasts were either left unstimulated or stimulated with TNF or AC.H6 for 18 h. Quantification results were normalized according to the signal obtained by actin result for each sample and the foldness is depicted by the number of + signs. (*****): *icam-1* is almost exclusively responsive to TNF in this system.

Similar analyses were performed in wild-type and RelB-deficient primary fibroblasts including *nfkb2*, *ikba, icam-1* and *vcam-1* genes. In these experiments, cells were also stimulated with the isotype control Ha4/8 Ab which did not reveal any unspecific effects. Wild-type fibroblasts showed a similar expression profile as NIH 3T3 cells in response to TNF and AC.H6, with the exception of *icam-1* which was also potently activated by anti-LTβR mAb AC.H6. For all the genes analysed, *relB*$^{-/-}$ fibroblasts were comparable to control cells with respect to the basal and the induced expression levels, suggesting that none of these genes is a direct target of RelB.

Summary

Analysis of signaling events downstream of LTβR and TNFR in different fibroblast systems revealed the following findings:

- LTβR initially activates RelA and with slower kinetics also RelB, predominantly p52-RelB, while TNFR almost exclusively activates RelA, as an early and more potent response.
- LTβR mediated RelB activation requires IKKα and β subunits but is independent of the regulatory subunit IKKγ and also RelA.
- LTβR induces p100 processing through IKKα subunit which results in the activation and nuclear translocation of RelB. This process requires *de novo* protein synthesis.
- LTβR also induces p105 processing in an IKKα dependent manner while IκBα levels are unchanged. IKKβ is essential for basal levels of p100 and p105 precursors, and IKKα and IKKβ regulate RelB protein levels.

See also Discussion and **Fig. 4.1**.

PART FOUR

3.4 TNFR SIGNALING IN MOUSE FIBROBLASTS

3.4.1 Regulation of p100 and RelB Downstream of TNFR in Mouse Fibroblasts

TNFR mediated activation of NF-κB is a result of signal transduction cascade which involves TRAFs and the IKK complex. In fibroblasts, this activation involves almost exclusively RelA complexes. The comparative analysis of events downstream of LTβR and TNFR revealed interesting findings about p100 and RelB regulation. Unlike LTβR, TNFR did not induce p100 processing but rather its increased synthesis without affecting total cellular levels of p52 (**Fig. 3.21A**).

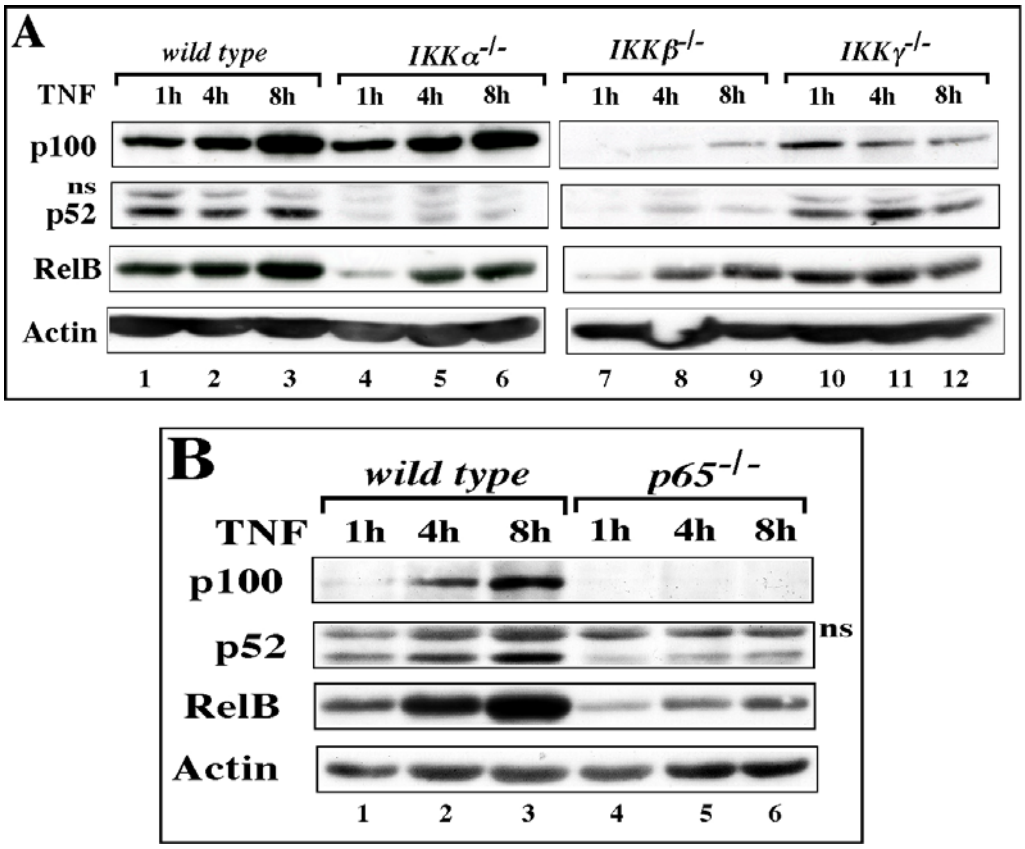

FIGURE 3.21: TNFR mediated p100 upregulation is RelA dependent.
Wild-type and IKK-deficient (**A**) and RelA-deficient fibroblasts (**B**) were stimulated with TNF for 1, 4 and 8 h and whole cell extracts were analysed for p100, p52 and RelB levels by Western blotting. Actin is shown as loading control. ns: non-specific band.

Experiments performed with IKK-deficient fibroblasts revealed that although p100 induction upon TNFR signaling in IKKα-deficient cells is similar to wild-type controls (**Fig. 3.21A**, compare lanes 1-3 versus lanes 4-6), this induction is impaired in IKKγ- (lanes 10-12) and to a greater extent in IKKβ-deficient fibroblasts (lanes 7-9). While TNFR mediated RelB induction was relatively normal in IKKγ-deficient cells, this induction was delayed and reduced in IKKα- and IKKβ-deficient fibroblasts (lanes 4-9). Interestingly, p100 protein levels were almost undetectable in RelA-deficient cells (**Fig. 3.21B**, lanes 4-6), suggesting a RelA dependent feedback mechanism for p100 upregulation downstream of TNFR. Similarly, RelA is also required for full induction of RelB in TNF treated cells (**Fig. 3.21B**, compare lanes 1-3 versus lanes 4-6). RT-PCR analyses showed induction of *relB* and *nfkb2* mRNA upon TNF stimulation (see **Table 3.1**) Thus, this feedback mechanism involves transcriptional activation. Collectively, these results suggest that in TNFR mediated signal transduction cascade, which upregulates p100 and RelB, involves IKKβ and IKKγ subunits and also RelA.

3.4.2 Regulation of RelB by p100 Downstream of TNFR

In almost all the experiments to investigate LTβR signaling in fibroblasts, TNF receptors were triggered by recombinant murine TNF stimulation as control. Interestingly, although RelB strongly accumulated in both cytoplasm and nucleus upon TNF treatment, DNA binding activity by EMSA was almost negligible (see **Fig. 3.15B**). In addition, p100 was not processed but rather accumulated in WCEs (**Fig. 3.21A**) and also in nuclear extracts (see **Figures 3.17A** and **3.22A**). Unlike IκBα, p100 was not previously reported to be a nuclear protein. Therefore cytoplasmic and nuclear extracts used for the experiment shown in **Fig. 3.22A** were also checked with anti-actin and anti-c-Jun Abs by Western blotting for cytoplasmic and nuclear specificity, respectively (data not shown). The results confirmed that p100 precursor is also a nuclear protein. The specific activation of TNFRI by recombinant human TNF also increased total cellular RelB levels comparable to mouse TNF. The increase in total p100 levels were less pronounced though still clearly detectable (**Fig. 3.22B**), suggesting that TNFRII also contributes to p100 induction.

The C-terminal ankyrin repeat domain of p100, also called IκBδ, can function as a potent inhibitor of RelB complexes, in particular of p52-RelB heterodimers (Dobrzanski *et al.*, 1995; Solan *et al.*, 2002). Therefore, a possible explanation for the observed lack of RelB DNA binding in TNF-stimulated fibroblasts is that the accumulated p100 could interact with RelB and inhibit its function. Similar interactions of p100 and p105 with other NF-κB members such as RelA and c-Rel leading to cytoplasmic retention of these proteins were previously reported (Mercurio *et al.*, 1993). In addition, such an interaction of p100 with RelB via its C-terminus was recently shown in human transfected HeLa and 293T cells. RelB preferentially interacts with p100, but not with IκBα, IκBβ, IκBε, nor p105, resulting in its transcriptional repression (Solan *et al.*, 2002). These studies indicate that p100 is a bona fide inhibitor of RelB.

In order to examine whether p100 interacts with RelB also in TNF stimulated mouse fibroblasts, co-immunoprecipitation experiments were performed. Reciprocal experiments using Abs specific for RelB or the C-terminus of p100 showed that endogenous p100 was bound to RelB in TNF-stimulated fibroblast whole cell lysates (**Fig. 3.22C**, second and third panels). Internal positive controls for IP are shown in the first and fourth panel of the figure. However, the outcome of this interaction is not likely to be cytoplasmic retention of RelB as was suggested by previous reports for other members, since TNF treatment in fibroblasts resulted in nuclear RelB accumulation despite abundant p100 and also despite their interaction. Therefore, whether this interaction also takes place in nucleus was addressed by fractionation experiments followed by co-IPs. This interaction was also observed when nuclear fractions were used whereas this interaction was not detected in anti-LTβR mAb stimulated cells (data not shown). Interestingly, while the precipitated RelB was predominantly nuclear in anti-LTβR mAb treated cells, RelB was detected both in cytoplasm and nuclear compartments of TNF stimulated fibroblasts (**Fig. 3.22D**). Collectively, these results indicate that TNFR signaling induced RelB and p100 interaction in both cytoplasmic and nuclear compartments of TNF stimulated mouse fibroblasts.

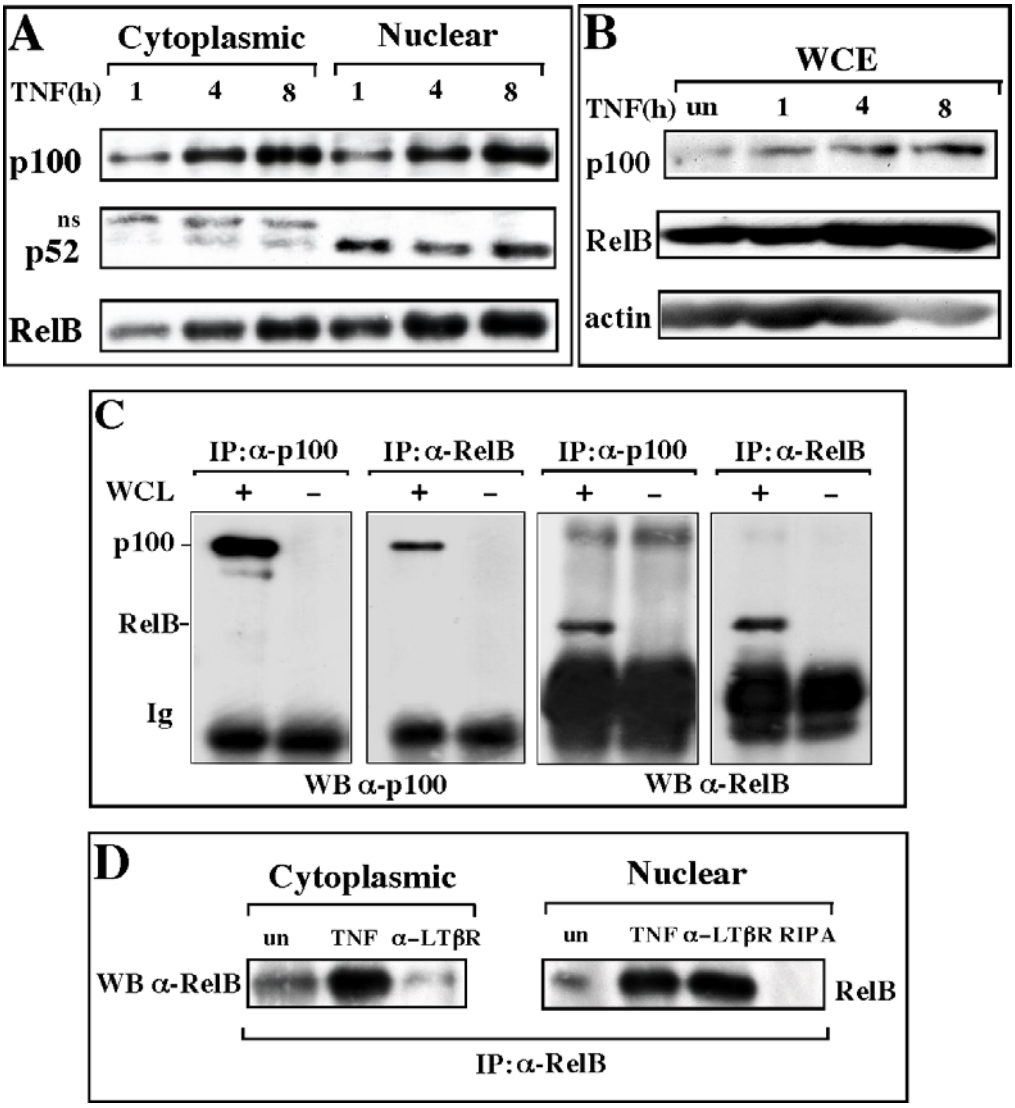

FIGURE 3.22: TNFR induced RelB and p100 interact in mouse fibroblasts
(A) TNF induction results in increased p100 and RelB levels in both cytoplasm and nucleus. Cytoplasmic (50 µg) and nuclear extracts (25 µg) from recombinant mouse TNF (20 ng/ml) treated (1, 4 and 8 h) fibroblasts were analyzed for p100, p52, and RelB levels by Western blotting. ns: non-specific band. **(B)** TNFR1 alone also increased total RelB and p100 levels. WCEs from recombinant human TNF (20 ng/ml) treated (1, 4 and 8 h) fibroblasts were analyzed for p100 and RelB levels by Western blotting. Actin is shown as loading control. (**C**) RelB and p100 interact in TNF-stimulated fibroblasts. Fibroblasts were induced with TNF and cells were lysed under native conditions. Immunoprecipitations (IPs) were carried out with (+) or without (-) whole cell lysates using either p100- or RelB-specific Abs. The precipitated material was separated by SDS-PAGE and analyzed by Western blotting (WB) for p100 and RelB levels. Ig: immunoglobulin. (**D**) Cytoplasmic and nuclear extracts were prepared from unstimulated and TNF or AC.H6 treated fibroblasts and subjected to IP using anti-RelB Abs. Western blotting was performed to detect p100 (not shown) and RelB. RIPA: lysis buffer, denotes no extract.

3.4.3 IκBα and p105 Regulation Downstream of TNFR in Mouse Fibroblasts

Just like the p100 precursor, p105 also has an inhibitory function through its C-terminus conserved among IκB molecules. Since TNFR mediated NF-κB activation involves RelA and can be controlled by IκBα and also p105 (Mercurio *et al.*, 1993), protein levels of p105 and IκBα in TNF stimulated wild-type and IKK-deficient fibroblasts were analysed by Western blotting.

Unlike p100, p105 neither accumulated nor was degraded upon TNF stimulation in wild-type fibroblasts whereas IκBα degradation was clearly observed at four and eight h time points (**Fig. 3.23**, lanes 1-3). Interestingly IκBα degradation was intact in IKKβ-deficient fibroblasts despite the lower levels compared to wild-type (lanes 7-9). This process however, was completely defective in IKKγ-deficient cells (lanes 10-12), which also were impaired in TNFR induced NF-κB activation (see **Fig. 3.16D**). Taken together, TNF induced NF-κB activation involves in fibroblasts, IκBα degradation rather than p105 mediated regulation. Whether these molecules also have regulatory effects on RelB in this system requires further investigations.

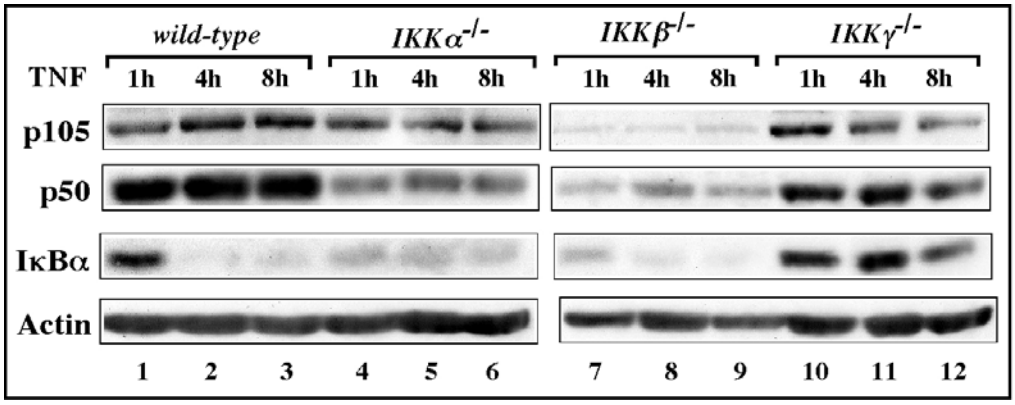

FIGURE 3.23: TNFR triggers IκBα but not p105 degradation.
Wild-type and IKK-deficient fibroblasts were stimulated with TNF for 1, 4 and 8 h and WCE were analysed for p105, p50 and IκBα levels by Western blotting. Actin is shown as loading control.

3.4.4 Neither p50 Nor p52 Overexpression Induces RelB DNA Binding Downstream of TNFR

RelB DNA binding necessitates p50 or p52 as a dimerization partner since RelB does not form homodimers. The results demonstrate that downstream of TNFR, neither p100 nor p105 undergoes induced processing to generate p52 and p50 subunits, respectively. In order to investigate whether the limited availability of free p52 or p50 subunit in TNF treated fibroblasts could be responsible for the lack of observed RelB DNA binding, fibroblasts were transfected with p52 or p50 expression plasmids and DNA binding following TNF stimulation was analysed by EMSA. The result for p50 overexpression is shown in **Fig. 3.24**.

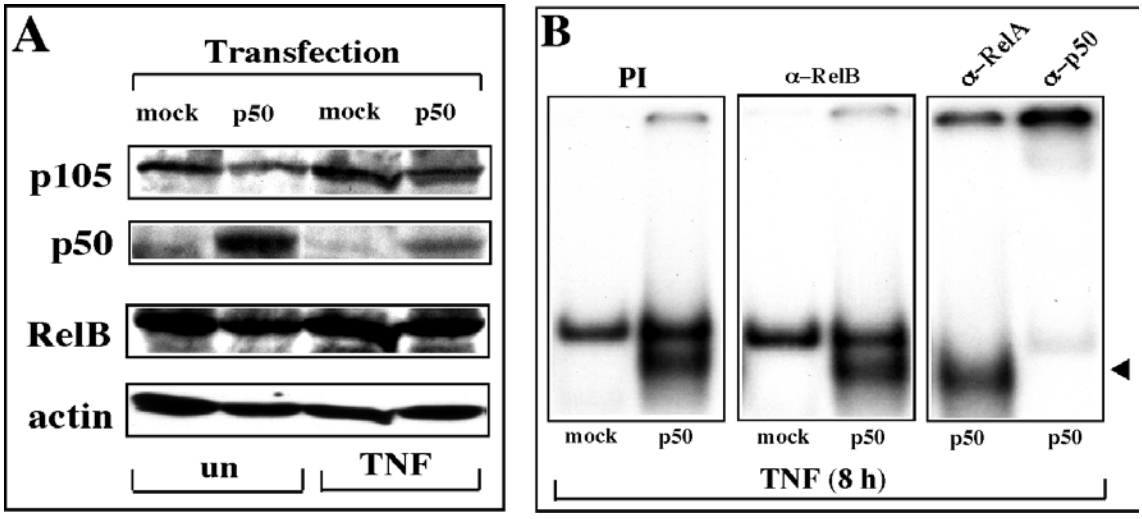

FIGURE 3.24: Overexpression of p50 subunit did not induce RelB DNA binding but triggered p50 homodimers downstream of TNFR.
Wild-type fibroblasts were cotransfected either with empty vector (mock) or p50 expression vector (p50) and β-galactosidase construct. Transfected cells were either left untreated or stimulated with TNF (20 ng/ml) for 8 h. In addition to whole cell and nuclear extract preparation, aliquots of cells were lysed for β-Gal assay to check transfection efficiency. (**A**) Whole cell extracts were analysed by Western blotting for protein levels of p105, p50 and RelB. Actin is shown as loading control. (**B**) Nuclear extracts prepared from TNF induced transfected fibroblasts were assayed by EMSA. Reactions were either incubated with PI or specific Abs against RelB, RelA and p50 subunits. Induced p50 homodimer binding was completely abolished by anti-p50 Abs (arrowhead in the third panel).

Western blot analysis confirmed p50 expression (**Fig. 3.24A**) and both p50 and RelB were also detected in nuclear compartment (not shown). Overexpression of p50 clearly induced a faster migrating complex (**Fig. 3.24B**, PI panel). Anti-RelB Abs did not change the binding indicating that p50-RelB binding was not induced (middle panel). However, while treatment of the extracts with anti-p50 Abs completely abolished this faster complex together with the upper complex to a large extent, anti-RelA Abs

specifically removed the upper complex. This indicates that the observed DNA binding activity under these conditions predominantly consisted of p50-RelA and RelA complexes as slower migrating, and p50 homodimers as faster migrating complexes, the latter being specifically induced by p50 overexpression.

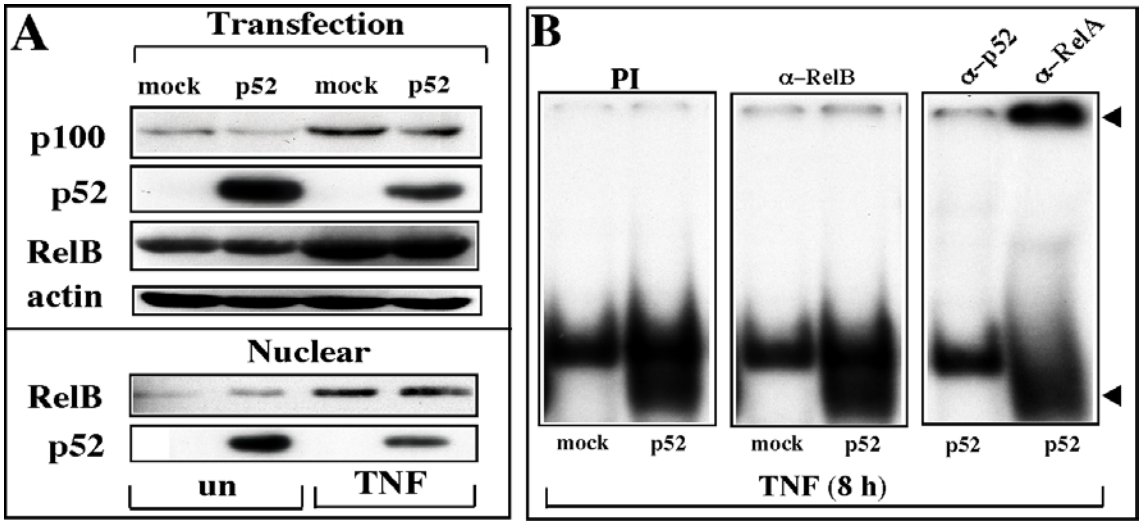

FIGURE 3.25: Overexpression of p52 subunit resulted in p52 homodimer binding downstream of TNFR rather than induction of RelB DNA binding.
Wild-type fibroblasts were cotransfected either with empty vector (mock) or p52 expression vector (p52) and β-galactosidase construct. Transfected cells were either left untreated or stimulated with TNF (20 ng/ml) for 8 h. In addition to whole cell and nuclear extract preparation, aliquots of cells were lysed for β-Gal assay to check transfection efficiency. (**A**) Whole cell and nuclear extracts were analysed by Western blotting for protein levels of p100, p52 and RelB. Actin is shown as loading control. (**B**) Nuclear extracts prepared from TNF induced transfected fibroblasts were assayed by EMSA. Reactions were either incubated with PI or specific Abs against RelB, RelA and p52 subunits. Induced p52 homodimer binding was completely abolished by anti-p52 Abs and upper complex was specifically removed by anti-RelA Abs (arrowheads in the third panel).

Similar experiments were performed to overexpress p52 (**Fig. 3.25**). Western blot analysis confirmed p52 overexpression and RelB upregulation in response to TNF was comparable in mock and p52 transfected cells and total cellular levels of RelB was not altered as a result of transfection (**Fig. 3.25A**, compare mock versus p52). In addition, both p52 and RelB were nuclear (panel **A**, bottom panel) and the difference in p52 protein levels was a result of the difference in transfection efficiency as detected by respective β-Gal values (not shown). Overexpression of p52 also clearly induced a faster migrating complex (**Fig. 3.25B**, PI panel) and overall binding pattern was not changed by anti-RelB Abs (middle panel). However, treatment of the extracts with anti-p52 Abs completely abolished this faster complex by blocking the binding instead of retaining the complexes in the well (upper arrowhead in the third panel). Anti-RelA Abs

specifically removed the upper complex, indicating that the observed DNA binding under these conditions predominantly consisted of RelA complexes (upper), as also detected in mock transfected cells, and p52 homodimers which are induced as a result of p52 overexpression. Taken together, these results demonstrate that the presence of excess p50 or p52 by overexpression did not trigger RelB DNA binding, suggesting that it is not the availability of the DNA binding partner but another mechanism which prevents RelB from binding to DNA in TNF treated fibroblasts.

3.4.5 RelB DNA Binding is Specifically Repressed by the C-terminal Domain of p100 Downstream of TNFR in Mouse Fibroblasts

The TNF induced p100 accumulation and the co-IP experiments suggest a specific inhibition of RelB DNA binding by p100. To address this point, MEFs which lack the p100 precursor C-terminus (*p100*$^{-/-}$), but still expressing p52, were used. In order to test the specificity, MEFs which lack the p105 precursor C-terminus (*p105*$^{-/-}$) while still expressing p50 were also included. Evidence for an *in vivo* inhibitory function of the C-terminus of p100 and p105 comes from the increased constitutive NF-κB activity and the inflammatory phenotype of the respective knockout animals (Ishikawa *et al.*, 1997; Ishikawa *et al.*, 1998).

Wild-type and knockout MEFs were stimulated with TNF and RelB DNA binding was assayed by EMSAs (**Fig. 3.26**). Lack of p100 and p105 in corresponding MEFs was verified by Western blotting and RelB upregulation at protein level upon TNF treatment was not affected in these MEFs (**Fig. 3.26A**). Analysis of NF-κB binding by EMSA did not reveal any RelB DNA binding in wild-type MEFs, as concluded by the anti-RelB Ab treatment, a finding in agreement with previous observations, whereas anti-RelA Ab treatment completely abolished binding of the upper complex. However, considerable RelB binding was detected in extracts from *p100*$^{-/-}$ MEFs (**Fig. 3.26B**, middle panel, lane 2). Quantification revealed an increase of ten-fold for the detected RelB to RelA binding ratio (**Fig. 3.26C**), whereas this ratio decreased four-fold in cells lacking the C-terminus of p105, due to the marked increase in RelA binding (**Fig. 3.26B**, third panel, last lane).

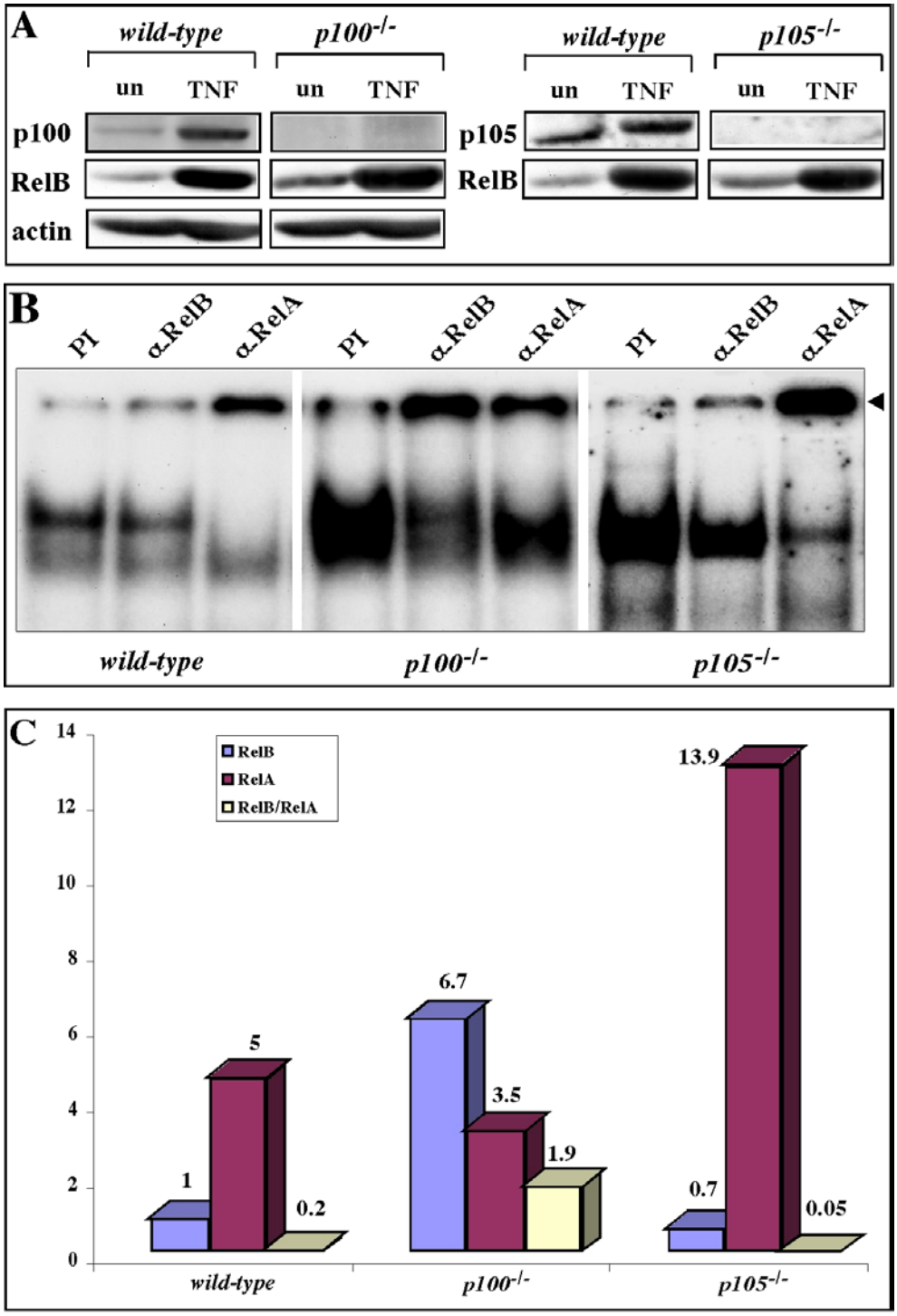

FIGURE 3.26: The C-terminal domain of p100 specifically represses RelB DNA-binding in TNF-induced fibroblasts.
Wild-type, *p100*$^{-/-}$, and *p105*$^{-/-}$ MEFs were either left untreated or stimulated for 8 h and WCEs and nuclear extracts were analyzed for protein levels by Western blotting and NF-κB activity by EMSA, respectively. (**A**) Lack of p100 and p105 expression was verified by Western blotting. TNF induced RelB upregulation in these knockout MEFs was comparable to controls. Actin is shown as loading control. (**B**) Dissection of complexes with specific Abs. (**C**) Quantification of the experiment shown in **B**. The amount of complex retained by the respective Abs in the wells (arrowhead) was quantified, corrected for the signal in samples treated with PI and the amount of RelB DNA-binding in wild-type MEFs was set to one.

Taken together these results clearly demonstrate that it is the C-terminus of p100 which specifically inhibits RelB DNA binding, possibly through a direct interaction with RelB.

Summary

- TNFR does not trigger p100 processing but upregulates p100 in a RelA dependent manner.
- TNFR mediates cytoplasmic and nuclear accumulation of RelB and p100, which interact in both compartments of TNF stimulated fibroblasts.
- Despite marked nuclear accumulation of RelB upon TNF triggerring, DNA binding activity detected is almost negligible.
- TNFR signaling activates the canonical pathway and triggers IκBα degradation, while p105 is not processed.
- Neither overexpression of p50 nor p52 subunit induce RelB DNA binding downstream of TNFR.
- Inhibition of RelB DNA binding activity upon TNF stimulation is mediated by the C-terminus of the p100 precursor.

4 DISCUSSION

Part One: Role of RelB For Spleen Microarchitecture

The histopathological alterations in spleens of RelB-deficient animals start ten days after birth with grade 1 EMH. Marked splenomegaly with two- to eight-fold increase in weight is a consistent phenotype of all *relB*$^{-/-}$ mice at around P20 and thereafter. While the white pulp is reduced, the red pulp dramatically increases as a consequence of increased EMH (Weih *et al.*, 1995). RelB is expressed in PALS, GCs and MZ structures of the splenic white pulp. The defects in the formation of GCs, MZ and FDC networks are not rescued either by the adult BM transplantation experiments or by reconstitution experiments of newborn animals. Taken together these findings suggest requirement of RelB expression in radioresistant stromal cells for the development of GCs and FDC networks in spleen (Weih *et al.*, 2001).

Gene targeting studies in mice revealed important roles for TNF/LT ligand/receptor family members in lymphoid organ development and function. In particular, the similarities in spleen phenotype between knockout lines with hematopoietic defects, such as *tnf*$^{-/-}$, *lt*$\alpha^{-/-}$ and *lt*$\beta^{-/-}$ mice, and mutants with stromal defects, such as *ltbr*$^{-/-}$, *aly/aly*, *nfkb2*$^{-/-}$ and *relB*$^{-/-}$ mice, suggest a network of signaling events (see **Table 1.2**). The production of TNF, LTα, and LTβ by B cells is critical for formation of GCs and FDC networks (Fu *et al.*, 1998; Endres *et al.*, 1999). While LTα and LTβ mRNA levels are reduced, TNF expression is not defective in RelB-deficient spleen. LTβR and LIGHT mRNA levels are increased approximately two-fold. Although the reason is still unclear, a possible compensatory role for the decreased LTα and LTβ levels can not be ruled out since LIGHT also binds to LTβR (Zhai *et al.*, 1998; Weih *et al.*, 2001). Since the hematopoietic compartment in RelB-deficient spleen is also defective, such as MZ B cells, the decreased expression of LTs may be attributed to the improper development of lymphocyte subsets and/or to the inefficient recruitment of these cells to and within the organ.

Important signals for proper development of specialized structures within lymphoid organs are provided by chemokines orchestrating lymphocyte migration. BLC is constitutively expressed by resident stromal cells in lymphoid follicles of all secondary lymphoid organs and attracts B cells via CXCR5 receptor. Similarly, SLC is expressed

by stromal cells within T cell areas of the spleen where RelB is also expressed. ELC expression in T cell areas is provided by macrophages, DCs, and also non-hematopoietic cells. The importance of ELC and SLC for the movement of lymphocytes and DCs to T cell areas of spleen and of BLC to splenic B cell follicles is revealed by CCR7- and CXCR5-deficient mice respectively, Förster *et al*., 1996; Förster *et al*., 1999). BLC seems to have a dual role in follicular compartmentalization of B cells. It not only mediates B cell recruitment, but also induces increased $LT\alpha_1\beta_2$ expression on the recruited cells. $LT\alpha_1\beta_2$ subsequently engages LTβRs on stromal cells, promoting maturation of FDCs and further increase in BLC expression (Ansel *et al*., 2000). Not only BLC but $LT\alpha_1\beta_2$ also mediates SLC and ELC expression (Ngo *et al.*, 1999) and it is possible that this membrane LT mediated chemokine expression requires NF-κB activation (Cyster, 1999). Indeed, BLC expression is markedly reduced in both RelB- and p52-deficient spleen as shown by RT-PCR and Northern analysis. SLC expression is also decreased in *relB*$^{-/-}$ spleen and neither the reduction in BLC nor in SLC levels is restored in *relB*$^{-/-}$ recipients reconstituted with wild-type BM. In contrast, ELC levels are partially restored in these recipients, in agreement with ELC being predominantly produced by hematopoietic cells (Weih *et al.*, 2001). The decrease of SLC expression in RelB-deficient thymus (Tanabe *et al.,* 1997), and of BLC, ELC and SLC mRNA levels in *aly/aly* spleen (Fagarasan *et al.*, 2000), are in agreement with these findings.

Collectively, these results suggest that p52-RelB activation in stromal cells, possibly downstream of TNF and LTαβ and NIK, is responsible for the chemokine-driven positive feedback loop, which mediates proper lymphocyte compartmentalization and structural organization of the spleen.

Part Two: Role of RelB in Peyer's Patch Development

RelB- and p52-deficient adult mice lack PPs while p50-deficient animals have these organs albeit smaller in size and less in number. New insights into PP organogenesis have recently been provided based on immunohistochemical studies of embryonic gut. Three major stages have been defined **(Fig. 1.8)**. First, at E15.5 VCAM-1^+/ICAM-1^+ mesenchymal cells form clusters along the intestine opposite to mesentery. Secondly, at E16.5 IL-7Rα^+CD4^+CD3^- hematoprogenitor cells start to accumulate at these sites along with the establishment of a vascular system with HEV structures. Finally, $CD3^+$ and $B220^+$ mature lymphocytes colonize the developing organ just before birth (Adachi

et al., 1997; Adachi *et al.*, 1998; Yoshida *et al.*, 1999). According to this model, VCAM-1 and ICAM-1 expression is the earliest marker to monitor PP development. Anti-VCAM-1 wholemount immunohistochemistry with intestines from p50-, p52- and RelB-deficient newborns clearly show that the defect in *p52*$^{-/-}$ and *relB*$^{-/-}$ mice resides in the initial step. In these animals, VCAM-1^{+} PP organizing centers do not form, while these structures are present in *p50*$^{-/-}$ mice, suggesting that p52-RelB plays a role in early PP organogenesis. PP anlagen, but no differentiated PPs develop in p52-deficient mice based on the analysis of adult intestines for IL-7Rα expression (Paxian *et al.*, 2002). This IL-7Rα expression, however, may stem from IL7R-α^{+} cells in recently identified isolated lymphoid follicles (ILFs) in mouse small intestine (Hamada *et al.*, 2002). In addition, the presence of these cells is not sufficient for PP development since Jak3-deficient animals also have IL-7Rα^{+} cells but lack VCAM-1^{+} organizing centers in embryos, due to the lack of IL-7 signaling, and developed PPs in adult animals (Adachi *et al.*, 1998). To our knowledge, no mutant has yet been described that has VCAM-1^{+} PP anlagen but lacks PPs.

PP formation is controlled by both LTαβ-LTβR and LTα$_3$/TNF-TNFR1 interactions, with LTβR signaling playing a predominant role. Indeed, Yoshida *et al.* demonstrated IL-7 dependent expression of LTα and LTβ in IL-7Rα^{+} embryonic intestinal cells. This is followed by the interaction with LTβR^{+} cells and expression of not only VCAM-1 and ICAM-1 but also of chemokines BLC and ELC. Further interaction of these hematopoietic LT producers and stromal responders is provided by attracting IL-7Rα^{+} cells, which express the corresponding chemokine receptors CXCR5 and CCR7. As a result of these signaling events, PP developmental programme is initiated in a spatial and temporal manner (Honda *et al.*, 2001). In this study, *relB* and *nfkb2* mRNA expression is shown in embryonic intestine as early as E14.5 and throughout the time window that is critical for PP development. Moreover, RelB protein expression is confined to the developing PP in wild-type animals at E16.5 and E18.5. This RelB expression in embryonic intestine most likely stems from stromal cells, since lymphocytes colonize PP anlagen not before E18. The detected RelB expression in adult PP of wild-type recipients reconstituted with *relB*$^{-/-}$ BM also supports this view and indicates that RelB is expressed by radiation resistant resident stromal cells in adult PPs.

RT-PCR analysis of IL-7, IL-7Rα chain, and LT ligands/receptors expression revealed similar mRNA levels in control and *relB*$^{-/-}$ intestine cells, indicating that RelB is not required for the steady state expression of these genes. LTβR mRNA is detected at E14.5 and expression clearly increased at E16.5 and E18.5, which is in agreement with a recent report **(**Browning and French, 2002**)** showing increased LTβR mRNA expression by *in situ* hybridization experiments in embryonic intestinal epithelium at the same time points. IL-7-induced LTα and LTβ expression in *relB*$^{-/-}$ embryonic intestinal cultures is unaffected. Since IL-7Rα^{+} cells are the only producers of LTα and LTβ at this developmental stage, the conclusion is that these inducers of PP organizing centers are present in *relB*$^{-/-}$ intestine and that the hematopoietic compartment is functional, further supporting a stromal defect downstream of LTβR. However, although LTβ expression is comparable in E16.5 *relB*$^{-/-}$ and *nfkb2*$^{-/-}$ intestine cells, IL-7 induced LTα expression is reduced in *nfkb2*$^{-/-}$ cells. The difference between these two cell types is presently not clear but it may suggest that the p52 subunit could also be functioning in the hematopoietic compartment or that these animals have reduced numbers of IL-7Rα^{+} inducer cells.

RT-PCR experiments to investigate steady state mRNA levels of TNF ligands and receptors, cell adhesion molecules, BLC, and CXCR5 did not reveal significant defect in *relB*$^{-/-}$ intestine cells, with the exception of reduced BLC levels at E18.5. BLC is expressed by LTβR^{+} cells in embryonic intestine (Honda *et al.*, 2001). One interpretation could be that downstream of LTβR, BLC expression is controlled by RelB complexes *in vivo*. In order to support this assumption, RelB-positive intestinal cells should be identified. Interestingly, expression of VCAM-1 and ICAM-1 mRNA is not reduced in *relB*$^{-/-}$ intestine at any time point analyzed although VCAM-1 protein expressing cell clusters are not detected by wholemount immunohistochemistry at E16.5 or P0. RelB may either be involved at the level of protein synthesis or VCAM-1^{+} cells may be defective in cluster formation. Not only RelB but also RelA is activated upon activation of LTβR signaling in fibroblasts and VCAM-1 mRNA induction upon anti-LTβR mAb stimulation is not defective in *relB*$^{-/-}$ MEFs. This data indirectly suggest that VCAM-1 transcriptional activation could be mediated by RelA *in vivo* independent of RelB. Another possible interpretation for the lack of VCAM-1^{+} clusters could be that these cells require RelB and/or p52 for their differentiation *in vivo*.

PPs are suggested to be the major inductive sites for production of sIgA upon class switching thereby not only developing the first line of defense against local pathogens but also inducing immune tolerance. However, treatment of pregnant mice with LTβR antagonistic Ab at E14 and E17 to block LTβR signaling shows that their PP-deficient offspring still have IgA^+ cells in intestinal LP (Yamamoto *et al.*, 2000). This suggests dispensability of PPs and a possible role for mesenteric LN as these animals still retain mesenteric LNs. Moreover, these IgA^+ cells in gut LP are generated from IgM^+ B cells *in situ* upon interaction with LP stromal cells, a process independent of PPs (Fagarasan *et al.*, 2001). These findings collectively suggest the gut LP as a non-structured and self-sufficient lymphoid tissue for IgA production. The molecular mechanism was revealed by Kang *et al.* who showed that LT signaling in LP stromal cells is required irrespective of lymphoid organs and independent of B and T cells. Even though IgA precursor cell numbers are normal, the recruitment of IgA^+ cells to LP is abolished in LTα- and LTβR-deficient mice. The impaired BLC, SLC and MAdCAM-1 expression in small intestine of LTα-deficient mice correlates with this defective migration to LP (Kang *et al.*, 2002).

The analysis of fecal IgA levels in NF-κB mutant animals shows the most dramatic reduction in *relB*$^{-/-}$ mice. B cells from *p50*$^{-/-}$ mice have an intrinsic defect in class switching to IgA (Snapper *et al.*, 1996). However, neither p52- nor RelB-deficient B cells have been reported to have such a defect (Franzoso *et al.,* 1998; Snapper *et al.,* 1996) despite impaired fecal IgA production. In addition, serum IgA concentration in unimmunized *nfkb2*$^{-/-}$ and *relB*$^{-/-}$ mice is normal (Weih *et al*., 1997; Caamaño *et al.,* 1998). Taken together, this reduction seems to be independent of the presence of PPs and is likely to be a B cell defect in p50- and a non cell-autonomous, and rather stromal defect in p52- and RelB- deficient animals. In the light of recent data, it is possible that p52-RelB downstream of LTβR in LP stromal cells regulates IgA production.

Part Three: LTβR and TNFR Signaling in Mouse Embryonic Fibroblasts

Collectively, the defects in spleen microarchitecture and PP organogenesis in RelB-deficient mice strongly suggest the requirement of RelB expression in the stromal compartment of secondary lymphoid organs. Non-lymphoid mouse fibroblasts that express both LTβR and TNFR1 were used as a model system to stimulate these signaling pathways and to study downstream events with the aim of a better understanding of lymphoid organ developmental defects in RelB-deficient mice.

This study demonstrates that TNF induces almost exclusively binding of RelA whereas LTβR signaling stimulates the binding of both RelA and RelB. RelB complexes are detected only after three to four hours of LTβR triggering. LTβR mediated NF-κB activation was also reported for different systems. One common point in most of these studies is that cells were induced for up to one hour (Smith *et al.*, 2001; Yin *et al.*, 2001) or a dissection of the induced NF-κB complexes was performed only for an early time point (Mackay *et al.*, 1996; VanArsdale *et al.*, 1997). Moreover, binding of RelB heterodimers may have been unnoticed due to the preceding induction of RelA.
In four different wild-type fibroblast lines RelA activation is rapid, whereas RelB complexes are induced with slower kinetics and in a *de novo* protein synthesis dependent manner. Dissection experiments demonstrate predominantly p52-RelB activation downstream of LTβR. This activation absolutely requires α and β catalytic subunits of the IKK complex as upstream kinase components while, the regulatory subunit IKKγ is dispensable. To our knowledge, LTβR stimulation in this system is the only NF-κB activator, which does not necessitate IKKγ.

LTβR induced p100 processing results in the generation of p52. This processing correlates with RelB protein induction and with nuclear translocation of RelB and p52 (**Fig. 4.1**). Interestingly, all of these processes are blocked by emetin treatment. Experiments with IKK-deficient cells show that p100 processing is dependent on the IKKα subunit but not on IKKγ, correlating with detectable p52-RelB binding in IKKγ-deficient cells. IKKβ-deficient fibroblasts, however, have intact processing despite very low basal levels of p100, a phenotype similar to RelA-deficient fibroblasts. In addition to low p100 and p52 levels in *IKKβ*$^{-/-}$ cells, RelB protein levels are also significantly reduced, further correlating with the lack of RelB binding. A very interesting question is

whether overexpression of p100 in *IKKβ*$^{-/-}$ cells could restore p52 and RelB levels resulting in detection of p52-RelB binding. Current experiments are aimed to address this point.

As an upstream component, NIK mediates p100 processing in overexpression systems in different human cell lines. In addition, *aly/aly* splenocytes are defective in p100 processing, further suggesting an important role for this kinase in p100 precursor processing(Xiao *et al.*, 2001). However, Senftleben *et al.* clearly demonstrated that overexpression of NIK in IKKα-deficient fibroblasts can not restore processing of p100 and that p100 is a better substrate for IKKα than for NIK *in vitro*, suggesting direct phosphorylation of the p100 precursor by the IKKα subunit. NIK phosphorylates and activates IKKα *in vitro* (Ling *et al.*, 1998). Indeed, this scenario is also supported by demonstrating that p100 processing downstream of LTβR requires IKKα. Additional evidence comes from the lack of p100 processing in IKKα^{AA} B cells, in which two serine residues in the activation loop of IKKα are replaced by alanines rendering IKKα inactive (Senftleben *et al.*, 2001). Therefore, NIK apparently participates in IKKα activation and activated IKKα functions in phosphorylation mediated p100 processing. This prediction is further substantiated by the finding that the *aly* point mutation in NIK disrupts the interaction with IKKα (Matsushima *et al.*, 2001). In addition, NIK mediates the physical association of p100 and β-transducin repeat-containing protein (β-TrCP), thereby inducing polyubiquitination and processing (Fong *et al.*, 2002). This suggests additional functions for NIK in this poorly defined process although the precise role of IKKα in this context is still unclear.

LTβR signaling also induces processing of p105 but not the degradation of IκBα, suggesting that RelA activation downstream of LTβR may be achieved via p105 processing in addition to the canonical pathway. IKKβ-deficient cells have intact p105 processing with low basal levels similar to p100. The lack of processing of p105 in IKKα- and IKKγ-deficient cells also correlates with the lack of RelA activation downstream of LTβR in these cells while this activation is still detectable in IKKβ-deficient fibroblasts. Taken together, the following sequence of events can be suggested downstream of LTβR in mouse fibroblasts (**Fig. 4.1**):

Initially, RelA is activated requiring all subunits of the IKK complex. This is followed by p52-RelB activation as a result of p100 processing through the IKKα and NIK pathway (**Fig. 4.1**, pathway 2), which is prominent after three to four hours of stimulation. Indeed, the defective RelB activation and p100 processing in *aly/aly* fibroblasts was demonstrated by Vallabhapurapu SivaKumar (unpublished observations). This activation results in a positive feedback loop, involving transcriptional activation of RelB and p100 as suggested by reduced levels of these proteins in p52- and RelA-deficient fibroblasts. In addition, p105 processing presumably supports IKKα and IKKγ dependent RelA activation with slower kinetics. (**Fig. 4.1**, pathway 3).

Given the complexity of this signaling pathway leading to the activation of qualitatively and quantitatively different NF-κB complexes, additional experiments were performed to address whether activated RelB complexes are functional. RT-PCR analysis in RelB-deficient fibroblasts shows normal expression of NF-κB members and of some candidate genes implicated in PP development. In addition to RT-PCR, reporter gene assays were performed in transient transfection experiments using an $(NF\text{-}\kappa B)_3$-luciferase reporter construct. This reporter was previously shown to be activated by RelB heterodimers (unpublished observations by Michal Malewicz and Ingmar Scholl). However, these experiments did not reveal a defect in LTβR mediated NF-κB transcriptional activity in RelB-deficient cells. Although LTβR induced NF-κB DNA binding activity in *nik*$^{-/-}$ fibroblasts is normal at one hour time point, transient transfections of an NF-κB-luciferase reporter construct and six to eight hours of anti-LTβR stimulation does not result in NF-κB transcriptional activity. The response to TNF treatment is normal, leading to the conclusion that NIK regulates NF-κB transcriptional activity in a receptor specific manner (Yin *et al.*, 2001). The dispensability for NIK downstream of TNFR, but not of LTβR, in mouse and human fibroblasts was previously reported (Matsushima *et al.*, 2001; Smith *et al.*, 2001). A very important point in the interpretation of these experiments is that LTβR activates different NF-κB members with different kinetics in fibroblasts as shown in this study.

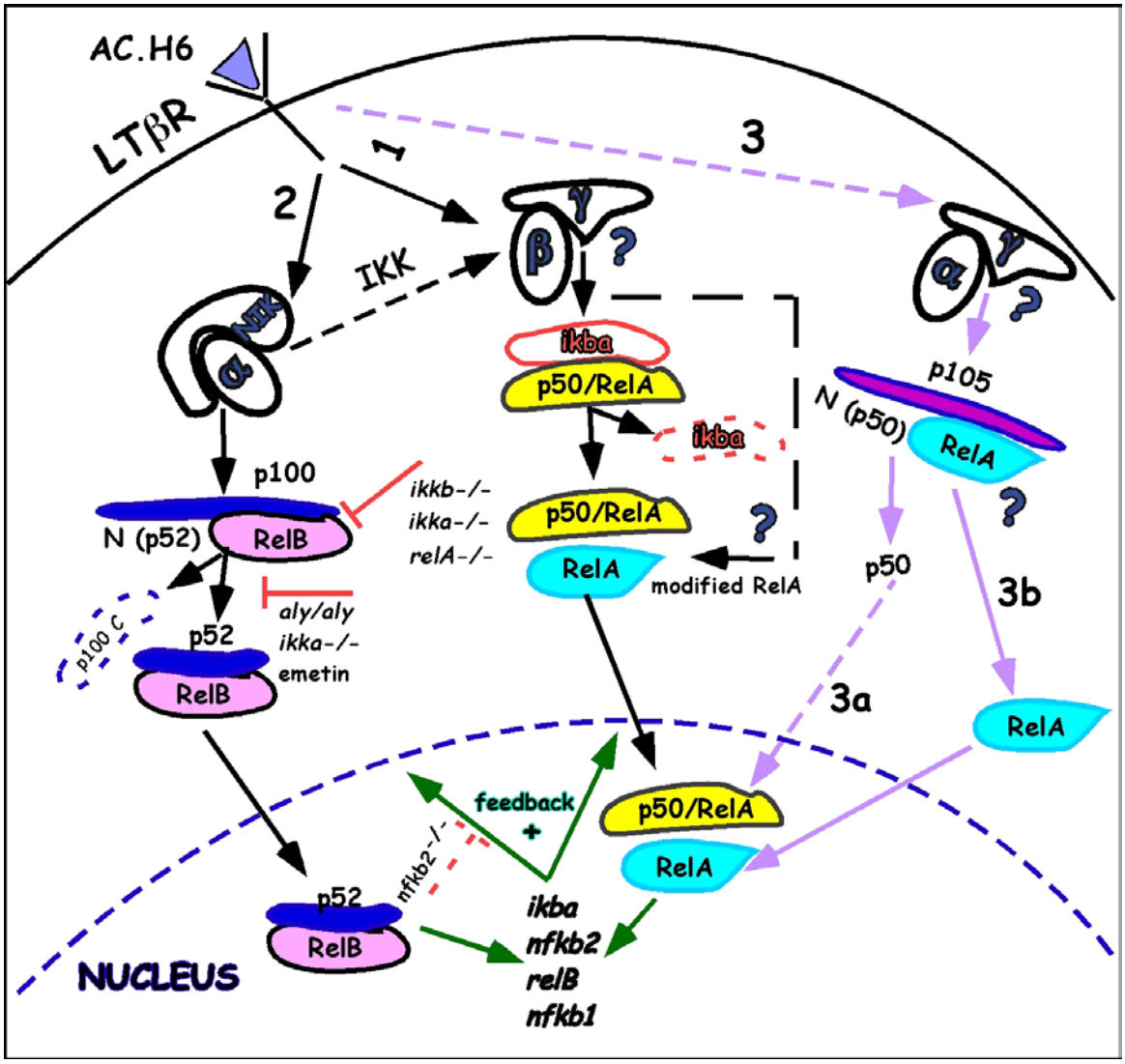

FIGURE 4.1: Model of LTβR-mediated Activation of NF-κB
LTβR triggering initially activates RelA complexes through the canonical pathway involving the IKK complex (**1**). This results in transcriptional activation of *nfkb2* and *relB* and also other family members in a feedback mechanism. In addition, LTβR mediates p100 processing via the NIK-IKKα pathway leading to the activation of p52-RelB (**2**). This process requires *de novo* protein synthesis. IKKα and IKKβ also regulate basal RelB protein levels. LTβR also triggers p105 degradation/processing, which requires IKKα and IKKγ and possibly other factors (**3**). Whether this process takes place co- or post-translationally and generates more p50 (**3a**) is unknown. The exact mechanism of p50-RelA and RelA activation and a possible inhibitory role of p105 on RelA is currently under investigation (**3b**). Collectively, these findings suggest that activation of NF-κB downstream of LTβR involves different pathways resulting in the activation of different NF-κB complexes.

Part Four: TNFR Signaling and Regulation of RelB DNA Binding in Mouse Embryonic Fibroblasts

In wild-type fibroblasts TNFR, unlike LTβR, does not trigger p100 processing but rather its accumulation in both cytoplasm and nucleus. RelB is transcriptionally regulated by NF-κB, particularly RelA. RelB protein levels are induced upon TNF treatment and this RelB induction is significantly reduced in *relA*$^{-/-}$ fibroblasts (Bren *et al.*, 2001 and this study). While IKKα is dispensible for TNF mediated p100 induction, this process requires IKKβ and IKKγ. Another novel finding is that p100 upregulation is completely abolished in RelA-deficient fibroblasts correlating with reduced but detectable p52 protein levels (**Fig. 3.21 B**). The delay in RelB protein level induction in IKKα-, IKKβ-, and RelA-deficient fibroblasts (one hour versus four hours) indicates a RelA-dependent positive feedback loop downstream of IKKα and IKKβ. In TNF induced fibroblasts, IκBα and IKKβ association is mediated by the IKKγ regulatory subunit, resulting in increased IκBα phosphorylation **(**Yamamoto *et al.*, 2001). Given that IκBα phosphorylation is followed by its degradation, the lack of degradation observed in IKKγ-deficient cells (**Fig. 3.23**) is in agreement with the suggested function of the regulatory γ subunit. Whether this degradation defect is a direct consequence of the lack of IKKγ in these cells, will be addressed by reconstitution experiments in which retroviral expression system will be used to express IKKγ. Collectively, these results suggest differential requirements for IKK subunits and a complex network of regulation among NF-κB and IκB family members also downstream of TNFR (see **Fig. 4.2**).

Solan *et al.* recently reported the specific interaction of RelB with the p100 C-terminus resulting in the transcriptional repression of RelB in different human cell lines (Solan *et al.*, 2002). The observations that both p100 and RelB are abundant nuclear proteins in TNF stimulated fibroblasts led to investigate whether RelB DNA binding is inhibited by p100. Similar mechanism in murine cells was not reported before. In this study, it was demonstrated that RelB interacts with p100 in both cytoplasm and nuclear fractions of TNF stimulated murine fibroblasts. Quantitative anti-RelB IP experiments suggest, however, that not all RelB is bound by p100. Whether this interaction is direct or whether additional regulatory mechanisms exist for "free" RelB is not yet clear.

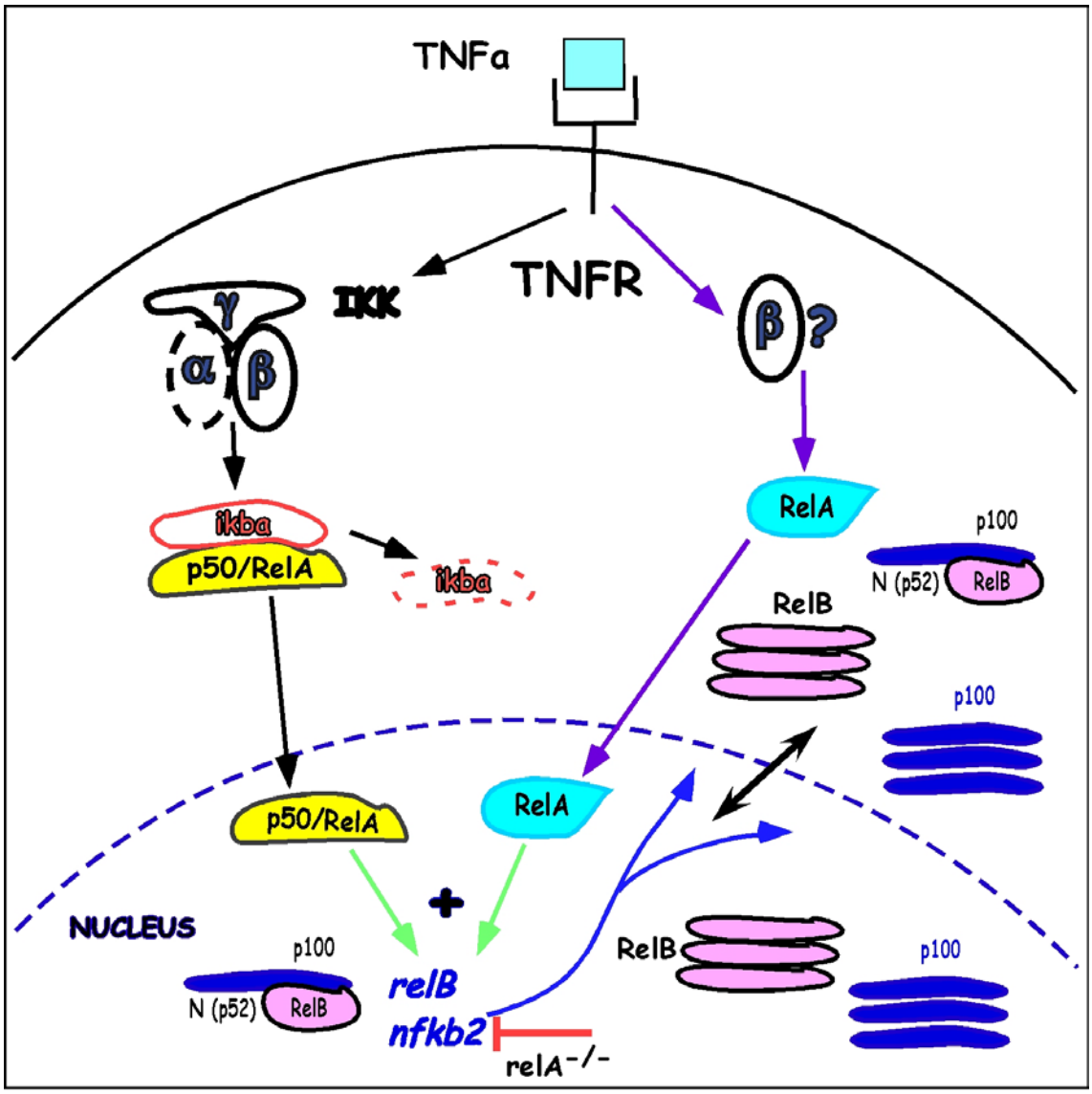

FIGURE 4.2: Model of TNFR-mediated Activation of NF-κB and Regulation of RelB DNA Binding
TNFR triggering activates p50-RelA via IKKβ and IKKγ subunits through IκBα degradation. This pathway upregulates expression of RelB and p100. TNF induced p100 upregulation is severely impaired in IKKβ- and RelA-deficient cells indicating a possible additional pathway leading to RelA activation. RelB and p100 in TNF treated cells and interact both in cytoplasm and nucleus. As a result, RelB is specifically inhibited by the p100 C-terminus.

Modulary phosphorylations are suggested to regulate NF-κB activity and TNF induced phosphorylations were reported for RelA **(**Wang, D., and Baldwin AS. Jr, 1998**)** and c-Rel **(**Martin and Fresno, 2000**).** Such modifications can effect DNA binding and transactivation of NF-κB **(**Schmitz *et al.***,** 2001). Whether RelB undergoes a similar modification is currently unknown. TCR or TPA/ionomycin induces RelB phosphorylation and degradation (Marienfeld *et al.*, 2001). However, a RelB stabilizing modification or a modification which would render RelB incompetent in DNA binding despite its nuclear abundance has not been reported yet.

Another possibility to account for abundant but DNA-unbound RelB in TNF stimulated fibroblasts could be a role in RelA regulation. Preliminary findings with co-IP experiments indicate interaction of RelB and RelA in TNF stimulated fibroblasts (not shown), but further investigations are required to understand the significance of this interaction and the precise function of nuclear RelB *in vivo* downstream of TNFR. Understanding the mechanism(s) of RelB regulation will be interesting since it could well represent a general mechanism. RelB induction upon TNF treatment is not a "mouse fibroblast-specific" but rather a general phenomenon, observed in different cell systems such as U937 cells (Bren *et al.*, 2001), Jurkat and murine S107 plasmocytoma cell lines (Baumann *et al.*, 1998). However in these studies, neither nuclear localization of RelB, nor its DNA binding capability were addressed.

In order to reveal the mechanism of RelB inhibition, initially overexpression experiments were performed to provide excess of the DNA binding partners of RelB, p50 and p52. However, the results clearly demonstrate that the availability of these binding partners is not limiting. Overexpression of p50 or p52 induces p50-p50 and p52-p52 homodimer binding, respectively. These findings are in agreement with the increased NF-κB DNA binding in animals lacking the C-terminus of the p100 and p105 precursors but still expressing p52 and p50, respectively. Analysis of extracts prepared from lymphoid and non-lymphoid tissues from these $p100^{-/-}$ and $p105^{-/-}$ mice show significant increase in NF-κB binding, including p50 and p52 homodimers. The increased inflammatory phenotype of these mice provides additional *in vivo* evidence for the inhibitory/suppressor function of these precursors (Ishikawa *et al.*, 1997; Ishikawa *et al.*, 1998). It is likely that the C-terminus of p100 is the inhibitory factor for

RelB DNA binding in TNF treated cells since experiments performed with TNF stimulated *p100*$^{-/-}$ and *p105*$^{-/-}$ fibroblasts clearly demonstrate the specific inhibitory function of p100. RelB DNA binding increases strongly in *p100*$^{-/-}$ but not in *p105*$^{-/-}$ MEFs. This shows a novel regulatory mechanism of RelB DNA binding activity in fibroblasts. It is interesting to see whether a similar inhibitory mechanism applies to other cell systems in which, RelB is induced in a TNF dependent manner. Previously, a suppressor role for RelB in fibroblasts was suggested due to the increased expression of cytokines and chemokines in RelB-deficient cells after stimulation with LPS and TNF. One mechanism proposed is the regulation of IκBα inhibitor stability by RelB (Xia *et al.*, 1997; Xia *et al.*, 1999). Given the inflammatory phenotype in *relB*$^{-/-}$ mice, it is reasonable to assume a suppressor role for RelB. The inhibitory role of p100 on RelB in wild-type fibroblasts has been demonstrated here at the DNA binding level. What remains to be shown is whether, RelB has an active role in transcriptional activation or repression and whether p100 has any influence in this process.

Collectively, this work provides insights in how related but distinct signaling pathways can activate quantitatively and qualitatively different members of the Rel/NF-κB family with selective requirements for upstream kinase components and through a complex regulatory network within the very same cell type. More importantly, these observations also offer possible *in vivo* operating mechanisms for distinct responses upon inflammatory signals, such as TNF, versus developmental signals, such as LTαβ. Identification of detailed downstream events of LT signaling may provide new molecules essential for lymphoid organ development. One such example is the connection between LTβR-NIK-IKKα-p100 processing and p52-RelB activation in fibroblasts, a signaling pathway which is likely to orchestrate the development of PP and also of other lymphoid organs.

REFERENCES

Adachi, S., Yoshida, H., Honda, K., Maki, K., Saijo, K., Ikuta, K., Saito, T. and Nishikawa, S. I. (1998). Essential role of IL-7 receptor α in the formation of Peyer's patch anlage. *Int. Immunol.* **10**(1): 1-6.

Adachi, S., Yoshida, H., Kataoka, H. and Nishikawa, S. (1997). Three distinctive steps in Peyer's patch formation of murine embryo. *Int. Immunol.* **9**(4): 507-514.

Anderson CN. (2001). Man the barrier! Strategic defences in the intestinal mucosa. *Nature Reviews Immunol.* **1**: 59-67.

Ansel, KM., Ngo, VN., Hyman, PL., Luther, SA., Förster R., Sedgwick, JD., Browning, JL., Lipp, M., and Cyster, JG. (2000). A chemokine-driven positive feedback loop organizes lymphoid follicles. *Nature* **406**: 309-314.

Ansel, KM., and Cyster JG. (2001). Chemokines in lymphopoiesis and lymphoid organ development. *Curr Opin Immunol.* **13**(2): 172-179.

Attar, R. M., Caamaño, J., Carrasco, D., Iotsova, V., Ishikawa, H., Ryseck, R.-P., Weih, F. and Bravo, R. (1997). Genetic approaches to study Rel/NF-κB/IκB function in mice. *Semin. Cancer Biol.* **8**: 93-101.

Baggiolini, M. (1998). Chemokines and leukocyte traffic. *Nature* **392**(6676): 565-568.

Baud, V. and Karin, M. (2001). Signal transduction by tumor necrosis factor and its relatives. *Trends Cell Biol.* **11**(9): 372-377.

Baumann, B., Kistler, B., Kirillov, A., Bergman, Y. and Wirth, T. (1998). The mutant plasmacytoma cell line S107 allows the identification of distinct pathways leading to NF-κB activation. *J. Biol. Chem.* **273**(19): 11448-11455.

Beg, A. A., Sha, W. C., Bronson, R. T., Ghosh, S. and Baltimore, D. (1995). Embryonic lethality and liver degeneration in mice lacking the RelA component of NF-κB. *Nature* 376: 167-169.

Bours, V., Azarenko, V., Dejardin, E. and Siebenlist, U. (1994). Human RelB (I-Rel) functions as a κB site-dependent transactivating member of the family of Rel-related proteins. *Oncogene* **9**(6): 1699-702.

Bours, V., Burd, P. R., Brown, K., Villalobos, J., Park, S., Ryseck, R.-P., Bravo, R., Kelly, K. and Siebenlist, U. (1992). A novel mitogen-inducible gene product related to p50/p105-NF-κB participates in transactivation through a κB site. *Mol. Cell. Biol.* **12**(2): 685-695.

Bren, G. D., Solan, N. J., Miyoshi, H., Pennington, K. N., Pobst, L. J. and Paya, C. V. (2001). Transcription of the RelB gene is regulated by NF-κB. *Oncogene* **20**(53): 7722-7733.

Browning JL., and French LE. (2002). Visualization of Lymphotoxin-β and Lymphotoxin-β receptor expression in mouse embryos. *J. Immunol.* **168**: 5079-5087.

Burkly L., Hession C., Ogata L., Reilly C., Marconi L. A., Olson D., Tizard R., Cate R., and Lo D. (1995). Expression of *rel*B is required for the development of thymic medulla and dendritic cells. *Nature* **373**: 531-536.

Caamaño, J. H., Rizzo, C. A., Durham, S. K., Barton, D. S., Raventos-Suarez, C., Snapper, C. M. and Bravo, R. (1998). Nuclear factor (NF)-κB2 (p100/p52) is required for normal splenic microarchitecture and B cell-mediated immune responses. *J. Exp. Med.* **187**: 185-196.

Carrasco, D., Ryseck, R.-P. and Bravo, R. (1993). Expression of *rel*B transcripts during lymphoid organ development: specific expression in dendritic antigen-presenting cells. *Development* **118**: 1221-1231.

Chaplin, D. D. and Fu, Y.-X. (1998). Cytokine regulation of secondary lymphoid organ development. *Curr. Opin. Immunol.* **10**(3): 289-297.

Crowley, M. T. and Lo, D. (1999). Targeted gene knockouts: insights into dendritic cell biology. Dendritic Cells. M. T. L. a. A. W. Thomson. San Diego, London, Academic Press**:** 579-593.

Cyster, J. G. (1999). Chemokines and cell migration in secondary lymphoid organs. *Science* **286**(5447): 2098-2102.

DiDonato, J. A., Mercurio, F. and Karin, M. (1995). Phosphorylation of IκBα precedes but is not sufficient for its dissociation from NF-κB. *Molecular & Cellular Biology* **15**: 1302-1311.

Dobrzanski, P., Ryseck, R.-P. and Bravo, R. (1993). Both N- and C-terminal domains of RelB are required for full transactivation: role of the N-terminal leucine zipper-like motif. *Mol. Cell. Biol.* **13**: 1572-1582.

Dobrzanski, P., Ryseck, R.-P. and Bravo, R. (1994). Differential interaction of Rel/NF-κB complexes with IκBα determine pools of constitutive and inducible NF-κB activity. *EMBO J.* **13**: 4608-4616.

Dobrzanski, P., Ryseck, R.-P. and Bravo, R. (1995). Specific inhibition of RelB/p52 transcriptional activity by the C-terminal domain of p100. *Oncogene* **10**: 1003-1007.

Endres, R., Alimzhanov, M. B., Plitz, T., Fütterer, A., Kosco-Vilbois, M. H., Nedospasov, S. A., Rajewsky, K. and Pfeffer, K. (1999). Mature follicular dendritic cell networks depend on expression of lymphotoxin β receptor by radioresistant stromal cells and of lymphotoxin β and tumor necrosis factor by B cells. *J. Exp. Med.* **189**(1): 159-168.

Fagarasan S., Kinoshita K., Muramatsu M., Ikuta K., and Honjo T. (2001). *In situ* class switching and differentiation to IgA-producing cells in the gut lamina propria. *Nature.* **413**: 639-643.

Fagarasan, S., Shinkura, R., Kamata, T., Nogaki, F., Ikuta, K., Tashiro, K. and Honjo, T. (2000). Alymphoplasia (*aly*)-type nuclear factor κB-inducing kinase (NIK) causes defects in secondary lymphoid tissue chemokine receptor signaling and homing of peritoneal cells to the gut-associated lymphatic tissue system. *J. Exp. Med.* **191**(9): 1477-1486

Finke D., and Kraehenbuhl JP. (2001). Formation of Peyer's patches. *Curr Opin Genet Dev.* **11**(5): 561-567.

Fong A. and Sun S. C. (2002). Genetic evidence for the essential role of β-transducin repeat-containing protein in the inducible processing of NF-κB2/p100. *J. Biol. Chem.* **277**(25): 22111-22114.

Force W. R., Glass A. A., Benedict C. A., Cheung T. C., Lama J. and Ware, C. F. (2000). Discrete signaling regions in the lymphotoxin-β receptor for tumor necrosis factor receptor-associated factor binding, subcellular localization, and activation of cell death and NF-κB pathways. *J. Biol. Chem.* **275**(15): 11121-11129.

Franzos, G., Carlson L., Poljak L., Shores E. W., Epstein S., Leonardi A., Grinberg A., Tran T., Scharton-Kersten T., Anver M., Love P., Brown K. and Siebenlist U. (1998). Mice deficient in nuclear factor (NF)-κB/p52 present with defects in humoral responses, germinal center reactions, and splenic microarchitecture. *J. Exp. Med.* **187**(2): 147-159.

Fu Y.-X., Huan, G., Wang Y. and Chaplin D. D. (1998). B lymphocytes induce the formation of follicular dendritic cell clusters in a lymphotoxin α-dependent fashion. *J. Exp. Med.* **187**(7): 1009-1018.

Förster R., Mattis A. E., Kremmer E., Wolf E., Brem G. and Lipp M. (1996). A putative chemokine receptor, BLR1, directs B cell migration to defined lymphoid organs and specific anatomic compartments of the spleen. *Cell* **87**(6): 1037-1047.

Förster R., Schubel A., Breitfeld D., Kremmer E., Renner-Müller I., Eckhard W., and Lipp M. (1999). CCR7 coordinates the primary immune response by establishing functional microenvironments in secondary lymphoid organs. *Cell* **99**: 23-33.

Fütterer A., Mink K., Luz A., Kosco-Vilbois M. H. and Pfeffer K. (1998). The lymphotoxin β receptor controls organogenesis and affinity maturation in peripheral lymphoid tissues. *Immunity* **9**(1): 59-70.

Gebert A., Pabst R., and Rothkolter HJ. (1996). M cells in Peyer's patches of the intestine. *Int Rev Cytol.* **167**: 91-159.

Gerondakis S., Grossman, M., Nakamura Y., Pohl T. and Grumon R. (1999). Genetic approaches in mice to understand Rel/NF-κB and IκB function: transgenics and knockouts. *Oncogene* **18**(49): 6888-6895.

Gilmore T. D. (1999). The Rel/NF-κB signal transduction pathway: introduction. *Oncogene* **18**(49): 6842-6844.

Griebe P. J. and Hein W. R. (1996). Expanding the role of Peyer's patches in B-cell ontogeny. *Immunol. Today* **17**(1): 30-39.

Gunn M. D., Kyuwa S., Tam C., Kakiuchi T., Matsuzawa A., Williams L. T. and Nakano H. (1999). Mice lacking expression of secondary lymphoid organ chemokine have defects in lymphocyte homing and dendritic cell localization. *J. Exp. Med.* **189**(3): 451-460.

Gunn M. D., Ngo, V. N., Ansel, K. M., Ekland, E. H., Cyster, J. G. and Williams, L. T. (1998). A B-cell-homing chemokine made in lymphoid follicles activates Burkitt's lymphoma receptor-1. *Nature* **391**(6669): 799-803.

Hamada, H., Hiroi, T., Nishiyama, Y., Takahashi, H., Masunaga, Y., Hachimura, S., Kaminogawa, S., Takahashi-Iwanaga, H., Iwanaga, T., Kiyono, H., Yamamoto, H. and Ishikawa, H. (2002). Identification of multiple isolated lymphoid follicles on the antimesenteric wall of the mouse small intestine. *J. Immunol.* **168**(1): 57-64.

Hashi, H., Yoshida, H., Honda, K., Fraser, S., Kubo, H., Awane, M., Takabayashi, A., Nakano, H., Yamaoka, Y. and Nishikawa, S. (2001). Compartmentalization of Peyer's patch anlagen before lymphocyte entry. *J. Immunol.* **166**(6): 3702-3709.

Hatada, E. N., Krappmann, D. and Scheidereit, C. (2000). NF-κB and the innate immune response. *Curr. Opin. Immunol.* **12**(1): 52-58.

Heissmeyer, V., Krappmann, D., Wulczyn, F. G. and Scheidereit, C. (1999). NF-κB p105 is a target of IκB kinases and controls signal induction of Bcl-3-p50 complexes. *EMBO J.* **18**(17): 4766-4778.

Hess, J., Laumen, H., Muller, K. B. and Wirth, T. (1998). Molecular genetics of the germinal center reaction. *J. Cell. Physiol.* **177**(4): 525-534.

Honda, K., Nakano, H., Yoshida, H., Nishikawa, S., Rennert, P., Ikuta, K., Tamechika, M., Yamaguchi, K., Fukumoto, T., Chiba, T. and Nishikawa, S.-I. (2001). Molecular basis for hematopoietic/mesenchymal interaction during initiation of Peyer's patch organogenesis. *J. Exp. Med.* **193**(5): 621-630.

Ishikawa, H., Carrasco, D., Claudio, E., Ryseck, R-P. and Bravo, R. (1997). Gastric hyperplasia and increased proliferative responses of lymphocytes in mice lacking the COOH-terminal ankyrin domain of NF-κB2. *J. Exp. Med.* **186**: 999-1014.

Ishikawa, H., Claudio, E., Dambach, D., Raventos-Suarez, C., Ryan, C. and Bravo, R. (1998). Chronic inflammation and susceptibility to bacterial infections in mice lacking the polypeptide (p)105 precursor (NF-κB1) but expressing p50. *J. Exp. Med.* **187**(7): 985-996.

Israël, A. (1995). A role for phosphorylation and degradation in the control of NF-κB activity. *Trends Genet.* **11**: 203-205.
Israël, A. (2000). The IKK complex: an integrator of all signals that activate NF-κB? *Trends Cell. Biol.* **10**(4): 129-133.

Kang H-S., Chin RK., Wang Y., Yu P., Wang J., Newell KA., and Fu Y-X. (2002). Signaling via LTβR on the lamina propria stromal cells of the gut is required for IgA production. *Nature Immunol.* **3**(6): 576-582.

Karin, M. (1999). How NF-κB is activated: the role of the IκB kinase (IKK) complex. *Oncogene* **18**(49): 6867-6874.

Karin, M. and Ben-Neriah, Y. (2000a). Phosphorylation meets ubiquitination: the control of NF-κB activity. *Annu. Rev. Immunol.* **18**: 621-663.

Karin, M. and Delhase, M. (2000b). The IκB kinase (IKK) and NF-κB: key elements of proinflammatory signalling. *Semin. Immunol.* **12**(1): 85-98.

Lernbecher, T., Kistler, B. and Wirth, T. (1994). Two distinct mechanisms contribute to the constitutive activation of RelB in lymphoid cells. *EMBO J.* **13**: 4060-4069.
Lin, L., DeMartino, G. N. and Greene, W. C. (1998). Cotranslational biogenesis of NF-κB p50 by the 26S proteasome. *Cell* **92**(6): 819-828.

Ling, L., Cao, Z. and Goeddel, D. V. (1998). NF-κB-inducing kinase activates IKK-α by phosphorylation of Ser-176. *Proc. Natl. Acad. Sci. USA* **95**(7): 3792-3797.

Mackay, F., Majeau, G. R., Hochman, P. S. and Browning, J. L. (1996). Lymphotoxin β receptor triggering induces activation of the nuclear factor κB transcription factor in some cell types. *J. Biol. Chem.* **271**(40): 24934-24938.

Male, D., Cooke, A., Owen, M., Trowsdale, J., and Champion B. (1996). Advanced Immunology. Times Mirror International Publishers Limited. 1.7-1.9.

Marienfeld, R., Berberich-Siebelt, F., Berberich, I., Denk, A., Serfling, E. and Neumann, M. (2001). Signal-specific and phosphorylation-dependent RelB degradation: a potential mechanism of NF-κB control. *Oncogene* **20**(56): 8142-8147.

Martin, AG., and Fresno, M. (2000). TNFα activation of NF-κB requires the phosphorylation of Ser 471 in the transactivation domain of c-Rel. *J. Biol. Chem.* **275**: 24383-24391.

Matheny, HE., Deem, TL., and Cook-Mills, JM. (2000). Lymphocyte migration through monolayers of endothelial cell lines involves VCAM-1 signaling via endothelial cell NADPH oxidase. *J Immunol.* **164**(12): 6550-6559.

Matsumoto, M. (1999). Role of TNF ligand and receptor family in the lymphoid organogenesis defined by gene targeting. *J. Med. Invest.* **46**(3-4): 141-50.

Matsumoto, M., Fu, Y.-X., Molina, H., Huang, G., Kim, J., Thomas, D. A., Nahm, M. H. and Chaplin, D. D. (1997). Distinct roles of lymphotoxin α and the type I tumor

necrosis factor (TNF) receptor in the establishment of follicular dendritic cells from non-bone marrow-derived cells. *J. Exp. Med.* **186**(12): 1997-2004.

Matsushima, A., Kaisho, T., Rennert, P. D., Nakano, H., Kurosawa, K., Uchida, D., Takeda, K., Akira, S. and Matsumoto, M. (2001). Essential role of nuclear factor (NF)-κB-inducing kinase and inhibitor of κB (IκB) kinase α in NF-κB activation through lymphotoxin β receptor, but not through tumor necrosis factor receptor I. *J. Exp. Med.* **193**(5): 631-636.

Mebius, R. E., Rennert, P. and Weissman, I. L. (1997). Developing lymph nodes collect $CD4^+CD3^-$ $LT\beta^+$ cells that can differentiate to APC, NK cells, and follicular cells but not T or B cells. *Immunity* **7**(4): 493-504.

Mebius, RE., Schadee-Eestermans IL., and Weissman IL. (1998). MAdCAM-1 dependent colonization of developing lymph nodes involves a unique subset of $CD4^+CD3^-$ hematolymphoid cells. *Cell Adhes Commun* **6**(2-3): 97-103.

Mercurio, F., DiDonato, J. A., Rosette, C. and Karin, M. (1993). p105 and p98 precursor proteins play an active role in NF-κB-mediated signal transduction. *Genes Dev.* **7**: 705-718.

Murphy, M., Walter, B. N., Pike-Nobile, L., Fanger, N. A., Guyre, P. M., Browning, J. L., Ware, C. F. and Epstein, L. B. (1998). Expression of the lymphotoxin β receptor on follicular stromal cells in human lymphoid tissues. *Cell Death Differ.* 5(6): 497-505.

Nakano, H., Oshima, H., Chung, W., Williams-Abbott, L., Ware, C. F., Yagita, H. and Okumura, K. (1996). TRAF5, an activator of NF-κB and putative signal transducer for the lymphotoxin-β receptor. *J. Biol. Chem.* **271**(25): 14661-14664.

Neutra, MR., Mantis, NJ., and Kraehenbuhl, JP. (2001). Collaboration of epithelial cells with organized mucosal lymphoid tissues. *Nature Immunol.* **2**(11): 1004-1009.

Ngo, V. N., Körner, H., Gunn, M. D., Schmidt, K. N., Riminton, D. S., Cooper, M. D., Browning, J. L., Sedgwick, J. D. and Cyster, J. G. (1999). Lymphotoxin α/β and tumor necrosis factor are required for stromal cell expression of homing chemokines in B and T cell areas of the spleen. *J. Exp. Med.* **189**(2): 403-412.

Nishikawa, S., Honda, K., Hashi, H. and Yoshida, H. (1998). Peyer's patch organogenesis as a programmed inflammation: a hypothetical model. *Cytokine Growth Factor Rev.* **9**(3-4): 213-220.

Pahl, H. L. (1999). Activators and target genes of Rel/NF-κB transcription factors. *Oncogene* **18**(49): 6853-6866.

Pasparakis, M., Alexopoulou, L., Grell, M., Pfizenmaier, K., Bluethmann, H., and Kollias, G. (1997). Peyer's patch organogenesis-cytokines rule, OK?. *Gut* **41**: 707-709.

Paxian, S., Merkle, H., Riemann, M., Wilda, M., Adler, G., Hameister, H., Liptay, S., Pfeffer, K. and Schmid, R. M. (2002). Abnormal organogenesis of Peyer's patches in mice deficient for NF-κB1, NF-κB2, and Bcl-3. *Gastroenterology* **122**(7): 1853-1868.

Perez, P., Lira, S. A. and Bravo, R. (1995). Overexpression of RelA in transgenic mouse thymocytes: specific increase on levels of the inhibitor IκBα. *Mol. Cell. Biol.* **15**: 3523-3530.

Perkins, ND. (2000). The Rel/NF kappa B family: friend or foe. *Trends Biochem Sci.* **25**(9): 434-440.

Poljak, L., Carlson, L., Cunningham, K., Kosco-Vilbois, MH., and Siebenlist, U. (1999). *Distinct* activities of p52/RelB required for proper secondary lymphoid organ microarchitecture: functions enhanced by Bcl-3. *J Immunol* **163**(12): 6581-6588.

Rennert, P. D., James, D., Mackay, F., Browning, J. L. and Hochman, P. S. (1998). Lymph node genesis is induced by signaling through the lymphotoxin β receptor. *Immunity* **9**(1): 71-79.

Ruben, S. M., Klement, J. F., Coleman, T. A., Maher, M., Chen, C.-H. and Rosen, C. A. (1992). I-Rel: a novel *rel*-related protein that inhibits NF-κB transcriptional activity. *Genes Dev.* **6**: 745-760.

Ruddle, NH. Lymphoid neo-organogenesis. Lymphotoxin's role in inflammation and development. *Immunologic Research* **19**(2-3): 119-125.

Roitt, I., Brostoff, J., and Male, D. (1996). Immunology. 4th edition. Mosby. 3.3-3.5.

Ryseck, R.-P., Bull, P., Takamiya, M., Bours, V., Siebenlist, U., Dobrzanski, P. and Bravo, R. (1992). RelB, a new Rel family transcription activator that can interact with p50-NF-κB. *Mol. Cell. Biol.* **12**: 674-684.

Saccani, S., Pantano, S. and Natoli, G. (2002). p38-Dependent marking of inflammatory genes for increased NF-κB recruitment. *Nat. Immunol.* **3**(1): 69-75.

Sambrook, J., and Russell, DW. (2001). Molecular Cloning. A Laboratory Manual. 3rd edition. Cold Spring Harbor Lab Press.

Schmitz ML., Bacher S., and Kracht M. (2001). IκB-independent control of NF-κB activity by modullary phosphorylations. *Trends Biochem Sciences* **26**(3): 187-191.

Sedgwick, J. D., Riminton, D. S., Cyster, J. G. and Körner, H. (2000). Tumor necrosis factor: a master-regulator of leukocyte movement. *Immunol. Today* **21**(3): 110-113.

Senftleben, U., Cao, Y., Xiao, G., Greten, F. R., Krahn, G., Bonizzi, G., Chen, Y., Hu, Y., Fong, A., Sun, S. C. and Karin, M. (2001). Activation by IKKα of a second, evolutionary conserved, NF-κB signaling pathway. *Science* **293**(5534): 1495-1499.

Sha, W. C., Liou, H.-C., Tuomanen, E. I. and Baltimore, D. (1995). Targeted disruption of the p50 subunit of NF-κB leads to multifocal defects in immune responses. *Cell* **80**: 321-330.

Shakhov, AN., and Nedospasov, SA. (2001). Expression profiling in knockout mice: lymphotoxin versus tumor necrosis factor in the maintenance of splenic microarchitecture. *Cytokine and Growth Factor Reviews* **12**: 107-119.

Smith, C., Andreakos, E., Crawley, J. B., Brennan, F. M., Feldmann, M. and Foxwell, B. M. (2001). NF-κB-inducing kinase is dispensable for activation of NF-κB in inflammatory settings but essential for lymphotoxin β receptor activation of NF-κB in primary human fibroblasts. *J. Immunol.* **167**(10): 5895-5903.

Snapper, C. M., Rosas, F. R., Zelazowski, P., Moorman, M. A., Kehry, M. R., Bravo, R. and Weih, F. (1996). B cells lacking RelB are defective in proliferative responses, but undergo normal B cell maturation to Ig secretion and Ig class switching. *J. Exp. Med.* **184**: 1537-1541.

Snapper, C. M., Zelazowski, P., Rosas, F. R., Kehry, M. R., Tian, M., Baltimore, D. and Sha, W. C. (1996). B cells from p50/NF-κB knockout mice have selective defects in proliferation, differentiation, germ-line C_H transcription, and Ig class switching. *J. Immunol.* **156**: 183-191.

Solan, N. J., Miyoshi, H., Carmona, E. M., Bren, G. D. and Paya, C. V. (2002). RelB cellular regulation and transcriptional activity are regulated by p100. *J. Biol. Chem.* **277**(2): 1405-1418.

Suzuki, K., Yamamoto, T. and Inoue, J. (1995). Molecular cloning of cDNA encoding the Xenopus homolog of mammalian RelB. *Nucleic Acids Res* **23**(22): 4664-9.

Tanabe, S., Lu, Z., Luo, Y., Quackenbush, EJ., Berman, MA., Collins-Racie, LA., Mi, S., Reilly, C., Lo, D., Jacobs, KA., and Dorf, ME. (1997). Identification of a new mouse beta-chemokine, thymus-derived chemotactic agent 4, with activity on T lymphocytes and mesangial cells. *J Immunol* **159**(11): 5671-5679.

Tarlinton, D. (1998). Germinal centers: form and function. *Curr Opin Immunol* **10**(3): 245-251.

Tkachuk, M., Bolliger, S., Ryffel, B., Pluschke, G., Banks, T. A., Herren, S., Gisler, R. H. and Kosco-Vilbois, M. H. (1998). Crucial role of tumor necrosis factor receptor 1 expression on nonhematopoietic cells for B cell localization within the splenic white pulp. *J. Exp. Med.* **187**(4): 469-477.

VanArsdale, T. L., VanArsdale, S. L., Force, W. R., Walter, B. N., Mosialos, G., Kieff, E., Reed, J. C. and Ware, C. F. (1997). Lymphotoxin-β receptor signaling complex: role of tumor necrosis factor receptor-associated factor 3 recruitment in cell death and activation of nuclear factor κB. *Proc. Natl. Acad. Sci. USA* **94**(6): 2460-2465.

Wang D., and Baldwin, AS. Jr. (1998). Activation of nuclear factor-κB-dependent transcription by tumor necrosis factor-α is mediated through phosphorylation of RelA/p65 on serine 529. *J. Biol. Chem.* **273**: 29411-29416.

Ware CF, VanArsdale TL, Crowe PD, Browning JL. (1995). The ligands and receptors of the lymphotoxin system. *Curr Top Microbiol Immunol* **198**:175-218.

Weih, D. S., Yilmaz, Z. B. and Weih, F. (2001). Essential role of RelB in germinal center and marginal zone formation and proper expression of homing chemokines. *J. Immunol.* **167**(4): 1909-1919.

Weih, F., Carrasco, D. and Bravo, R. (1994). Constitutive and inducible Rel/NF-κB activities in mouse thymus and spleen. *Oncogene* **9**: 3289-3297.

Weih, F., Carrasco, D., Durham, S. K., Barton, D. S., Rizzo, C. A., Ryseck, R.-P., Lira, S. A. and Bravo, R. (1995). Multiorgan inflammation and hematopoietic abnormalities in mice with a targeted disruption of RelB, a member of the NF-κB/Rel family. *Cell* **80**: 331-340.

Weih, F., Durham, S. K., Barton, D. S., Sha, W. C., Baltimore, D. and Bravo, R. (1996). Both multiorgan inflammation and myeloid hyperplasia in RelB-deficient mice are T cell dependent. *J. Immunol.* **157**: 3974-3979.

Weih, F., Durham, S. K., Barton, D. S., Sha, W. C., Baltimore, D. and Bravo, R. (1997). p50-NF-κB complexes partially compensate for the absence of RelB: severely increased pathology in *p50*$^{-/-}$*relB*$^{-/-}$ double-knockout mice. *J. Exp. Med.* **185**: 1359-1370.

Weih, F., Lira, S. A. and Bravo, R. (1996). Overexpression of RelB in transgenic mice does not affect IκBα levels: differential regulation of RelA and RelB by the inhibitor protein. *Oncogene* **12**: 445-449.

Weih, F., Warr, G., Yang, H. and Bravo, R. (1997). Multifocal defects in immune responses in RelB-deficient mice. *J. Immunol.* **158**: 5211-5218.

Xia, Y., Chen, S., Wang, Y., Mackman, N., Ku, G., Lo, D. and Feng, L. (1999). RelB modulation of IκBα stability as a mechanism of transcription suppression of interleukin-1α (IL-1α), IL-1β, and tumor necrosis factor α in fibroblasts. *Mol. Cell. Biol.* **19**(11): 7688-7696.

Xia, Y., Pauza, M. E., Feng, L. and Lo, D. (1997). RelB regulation of chemokine expression modulates local inflammation. *Am. J. Pathol.* **151**(2): 375-87.

Xiao, G., Harhaj, E. W. and Sun, S.-C. (2001). NF-κB-inducing kinase regulates the processing of NF-κB2 p100. *Mol. Cell* **7**(2): 401-409.

Yamamoto, M., Rennert, P., McGhee, J. R., Kweon, M. N., Yamamoto, S., Dohi, T., Otake, S., Bluethmann, H., Fujihashi, K. and Kiyono, H. (2000). Alternate mucosal immune system: organized Peyer's patches are not required for IgA responses in the gastrointestinal tract. *J. Immunol.* **164**(10): 5184-5191.

Yamamoto Y., Kim D-W., Kwak Y-T., Prajapati S., Verma U., and Gaynor R. (2001). IKKγ/NEMO facilitates the recruitment of the IκB proteins into the IκB kinase complex. *J. Biol. Chem.* **276**(39): 36327-36336.

Yin, L., Wu, L., Wesche, H., Arthur, C. D., White, J. M., Goeddel, D. V. and Schreiber, R. D. (2001). Defective lymphotoxin-β receptor-induced NF-κB transcriptional activity in NIK-deficient mice. *Science* **291**(5511): 2162-2165.

Yoshida, H., Honda, K., Shinkura, R., Adachi, S., Nishikawa, S., Maki, K., Ikuta, K. and Nishikawa, S. I. (1999). IL-7 receptor α^+ $CD3^-$ cells in the embryonic intestine induce the organizing center of Peyer's patches. *Int. Immunol.* **11**(5): 643-655.

Zhai, Y., Guo, R., Hsu, T. L., Yu, G. L., Ni, J., Kwon, B. S., Jiang, G. W., Lu, J., Tan, J., Ugustus, M., Carter, K., Rojas, L., Zhu, F., Lincoln, C., Endress, G., Xing, L., Wang, S., Oh, K. O., Gentz, R., Ruben, S., Lippman, M. E., Hsieh, S. L. and Yang, D. (1998). LIGHT, a novel ligand for lymphotoxin β receptor and TR2/HVEM induces apoptosis and suppresses in vivo tumor formation via gene transfer. *J. Clin. Invest.* **102**(6): 1142-1151.

Acknowledgements

First and foremost, I would like to express my gratitude to Prof. Dr. Peter Herrlich and my adviser Dr. Falk Weih, not only for the opportunity of having done my PhD work here in the Institute of Toxicology and Genetics but also, for the suggestions and support from which I took great benefit to plan my future steps.

I am grateful to Dr. Harald König for reviewing my thesis and for his valuable comments and suggestions, to Dr. Peter Angel and Dr. Axel Schabowski for IKK cells, and for their contribution to this work, to Dr. Susanne Weg-Remers for NIH 3T3 cells and suggestions.

I would like to take this opportunity to thank all the past and the present members of my lab, Lab 112, and histology laboratory; Claudia Stoll, Dr. Feng Guo, Heike Mondzdrak, Ingmar Scholl, Matthew Potts, Monica Pech, Nicholas Zeller, Tanja Herrmann, and SivaKumar Vallabhapurapu. I am thankful to the animal house staff, particularly Norma Howells and Selma Huber for their assistance, to Dr. Wolf Thies and Jörg Katzenberger for their help to solve the endless computer problems, and also to Caroline Balduf, Pawan Gulati, and all the other friends in the institute and in the dojo, especially Stefan Bley, Bugi, and Ike, with whom I shared a smile.

My deepest thanks go to Özlem Karaca, Dr. Tutku Soyer, Dr. Armin Ritzhaupt, Resat Ünal, Michal Malewicz, and particularly to the dear members of the ladies club, Debra S. Weih, Dr. Züleyhan Korali, and Miriam Koch for the exceptional sincere friendship which I know for sure will last forever.

Last but not the least, I am grateful to my dear mother Halime Capki whose intimate love and support I always felt and who makes everything in my life worthwhile, and also to the rest of my family for their never ending trust and care.